U.S.NRC
United States Nuclear Regulatory Commission
Protecting People and the Environment

NUREG/CR-7108
ORNL/TM-2011/509

An Approach for Validating Actinide and Fission Product Burnup Credit Criticality Safety Analyses—Isotopic Composition Predictions

Office of Nuclear Regulatory Research

AVAILABILITY OF REFERENCE MATERIALS IN NRC PUBLICATIONS

NRC Reference Material

As of November 1999, you may electronically access NUREG-series publications and other NRC records at NRC's Public Electronic Reading Room at http://www.nrc.gov/reading-rm.html. Publicly released records include, to name a few, NUREG-series publications; *Federal Register* notices; applicant, licensee, and vendor documents and correspondence; NRC correspondence and internal memoranda; bulletins and information notices; inspection and investigative reports; licensee event reports; and Commission papers and their attachments.

NRC publications in the NUREG series, NRC regulations, and *Title 10, Energy*, in the Code of *Federal Regulations* may also be purchased from one of these two sources.

1. The Superintendent of Documents
   U.S. Government Printing Office
   Mail Stop SSOP
   Washington, DC 20402–0001
   Internet: bookstore.gpo.gov
   Telephone: 202-512-1800
   Fax: 202-512-2250
2. The National Technical Information Service
   Springfield, VA 22161–0002
   www.ntis.gov
   1–800–553–6847 or, locally, 703–605–6000

A single copy of each NRC draft report for comment is available free, to the extent of supply, upon written request as follows:

Address: U.S. Nuclear Regulatory Commission
Office of Administration
Publications Branch
Washington, DC 20555-0001
E-mail: DISTRIBUTION.RESOURCE@NRC.GOV
Facsimile: 301–415–2289

Some publications in the NUREG series that are posted at NRC's Web site address http://www.nrc.gov/reading-rm/doc-collections/nuregs are updated periodically and may differ from the last printed version. Although references to material found on a Web site bear the date the material was accessed, the material available on the date cited may subsequently be removed from the site.

Non-NRC Reference Material

Documents available from public and special technical libraries include all open literature items, such as books, journal articles, and transactions, *Federal Register* notices, Federal and State legislation, and congressional reports. Such documents as theses, dissertations, foreign reports and translations, and non-NRC conference proceedings may be purchased from their sponsoring organization.

Copies of industry codes and standards used in a substantive manner in the NRC regulatory process are maintained at—

The NRC Technical Library
Two White Flint North
11545 Rockville Pike
Rockville, MD 20852–2738

These standards are available in the library for reference use by the public. Codes and standards are usually copyrighted and may be purchased from the originating organization or, if they are American National Standards, from—

American National Standards Institute
11 West 42nd Street
New York, NY 10036–8002
www.ansi.org
212–642–4900

Legally binding regulatory requirements are stated only in laws; NRC regulations; licenses, including technical specifications; or orders, not in NUREG-series publications. The views expressed in contractor-prepared publications in this series are not necessarily those of the NRC.

The NUREG series comprises (1) technical and administrative reports and books prepared by the staff (NUREG–XXXX) or agency contractors (NUREG/CR–XXXX), (2) proceedings of conferences (NUREG/CP–XXXX), (3) reports resulting from international agreements (NUREG/IA–XXXX), (4) brochures (NUREG/BR–XXXX), and (5) compilations of legal decisions and orders of the Commission and Atomic and Safety Licensing Boards and of Directors' decisions under Section 2.206 of NRC's regulations (NUREG–0750).

U.S.NRC
United States Nuclear Regulatory Commission
Protecting People and the Environment

NUREG/CR-7108
ORNL/TM-2011/509

An Approach for Validating Actinide and Fission Product Burnup Credit Criticality Safety Analyses—Isotopic Composition Predictions

Manuscript Completed: December 2011
Date Published: April 2012

Prepared by
G. Radulescu
I. C. Gauld
G. Ilas
J. C. Wagner

Oak Ridge National Laboratory
Managed by UT-Battelle, LLC
Oak Ridge, TN 37831-6170

Don Algama, NRC Project Manager

Prepared for
Division of Systems Analysis
Office of Nuclear Regulatory Research
U.S. Nuclear Regulatory Commission
Washington, DC 20555-0001

NRC Job Code V6005

Office of Nuclear Regulatory Research

ABSTRACT

Taking credit for the reduced reactivity of spent nuclear fuel in criticality analyses is referred to as burnup credit. Criticality safety evaluations employing burnup credit require validation of the depletion and criticality calculation methods and computer codes with available measurement data. To address the issues of burnup credit criticality validation, the U.S. Nuclear Regulatory Commission initiated a project with Oak Ridge National Laboratory to (1) develop and establish a validation approach for commercial spent nuclear fuel criticality safety evaluations based on best-available data and methods and (2) apply the approach on representative spent nuclear fuel storage and transport systems and conditions to demonstrate its usage and applicability, as well as to provide reference bias and bias uncertainty results. This report describes an approach for establishing depletion code bias and bias uncertainty in terms of a reactivity difference based on comparison of measured and calculated nuclide concentrations.

TABLE OF CONTENTS

Section **Page**

ABSTRACT iii
LIST OF FIGURES vii
LIST OF TABLES ix
EXECUTIVE SUMMARY xi
ACKNOWLEDGMENTS xiii
LIST OF ACRONYMS AND UNITS xv
1. INTRODUCTION 1
2. OVERVIEW OF BURNUP CREDIT ANALYSIS 3
3. ISOTOPIC VALIDATION DATA 7
3.1 NUCLIDES IMPORTANT TO BURNUP CREDIT 7
3.2 PWR ISOTOPIC VALIDATION DATA 9
3.3 BWR ISOTOPIC VALIDATION DATA 12
4. COMPUTER CODES AND NUCLEAR DATA 15
5. SAFETY ANALYSIS MODELS 17
5.1 PWR ASSEMBLY MODEL 17
5.2 PWR SFP STORAGE RACK MODELS 17
5.3 PWR SNF CASK MODEL 18
5.4 LOADING CURVES FOR PWR SNF 19
5.5 BWR ASSEMBLY MODEL 20
5.6 BWR SFP STORAGE RACK MODEL 21
6. CALCULATION OF BIAS AND BIAS UNCERTAINTY IN k_{eff} 23
6.1 MONTE CARLO UNCERTAINTY SAMPLING METHOD 23
6.1.1 Calculation of Bias and Bias Uncertainty in Calculated Nuclide Concentrations ... 24
6.1.2 Statistical Analysis of the Measured-to-Calculated Concentration Ratio Values ... 25
6.1.2.1 Analysis of Trends 26
6.1.2.2 Normality Test Results 28
6.1.2.3 Correlations among Nuclide Concentration Uncertainties 28
6.1.3 Isotopic Bias and Bias Uncertainty Values 29
6.1.4 Nuclide Concentrations for k_{eff} Calculations 32
6.1.5 Validation of the Assumption for Data Normality 33

TABLE OF CONTENTS
(Continued)

Section **Page**

6.1.6 Convergence of the Monte Carlo k_{eff} Bias Uncertainty Estimate 34
6.2 DIRECT-DIFFERENCE METHOD 36
7. BIAS AND BIAS UNCERTAINTY IN k_{eff} RESULTS 43
7.1 PWR SNF ANALYSIS MODELS 43
7.2 BWR SFP STORAGE RACK MODEL 47
7.3 PARAMETRIC ANALYSIS 47
8. CONCLUSIONS 53
9. REFERENCES 55
APPENDIX A. k_{eff} UNCERTAINTY ANALYSIS USING CROSS-SECTION SENSITIVITY/UNCERTAINTY ANALYSES A-1
A.1 Relative Importance of Individual Nuclides to Fuel Reactivity A-2
A.2 Non-normal Distributions for Measured-to-Calculated Concentration Ratio A-3
A.3 Analysis of k_{eff} Bias and Bias Uncertainty Components A-7
A.4 Importance of Decay-Time Corrections for the Direct-Difference Method A-11
APPENDIX B. ISOTOPIC VALIDATION DATA CORRELATIONS B-1
APPENDIX C. REFERENCE SPENT FUEL NUCLIDE CONCENTRATIONS C-1

LIST OF FIGURES

Figure **Page**

Figure 2.1 Overview of the burnup credit validation process 5

Figure 3.1 Atom density as a function of decay time for burnup credit nuclides exhibiting density variations after fuel discharge. 9

Figure 3.2 Enrichment and burnup values of the measured PWR fuel samples compared to loading curves for a representative PWR SFP storage rack model. 11

Figure 5.1 Horizontal cross section of the representative PWR SFP storage rack cell representation 18

Figure 5.2 Cutaway view of the GBC-32 cask model showing bottom half with a quarter of the model removed 19

Figure 5.3 Loading curves for PWR SNF in cask and pool storage rack configurations. 20

Figure 5.4 Horizontal cross section of the BWR SFP storage rack cell representation. 21

Figure 6.1 Measured-to-calculated concentration ratio versus fuel sample burnup for (a) ^{235}U; (b) ^{239}Pu. 27

Figure 6.2 Illustration of the Monte Carlo estimates. 35

Figure 6.3 Linear regression analysis of the Δk_{eff} results illustrating the bias and the margin for uncertainty represented by the one-sided tolerance limit at a 95% probability, 95% confidence level [95% tolerance limit (TL)] for the unpoisoned SFP storage rack 41

Figure 7.1 k_{eff} bias uncertainty for the representative PWR SFP storage rack model 44

Figure 7.2 k_{eff} bias uncertainty for the PWR SNF cask model 46

Figure 7.3 Variation of bias uncertainty in k_{eff} with parameters important to criticality analyses for (a) 10-, (b) 25-, and (c) 40-GWd/MTU assembly average burnup 51

Figure A.1 Sensitivity coefficients (absolute values) shown on a logarithmic scale for burnup credit actinide and fission product nuclides in the representative PWR SFP rack model at 3-day cooling time A-2

Figure A.2 Sensitivity coefficients (absolute values) shown on a logarithmic scale for burnup credit actinide and fission product nuclides in the PWR SNF cask (GBC-32) model at 5-year cooling time A-3

Figure A.3 Histogram of the M/C concentration ratio values for ^{235}U within the burnup interval 15 to 40 GWd/MTU. A-4

Figure A.4 Histogram plot for $\Delta k_{eff_{^{235}U}}$ values based on actual M/C concentration ratio values for ^{235}U within the burnup range 15 to 40 GWd/MTU A-6

Figure A.5 Individual nuclide contributions to k_{eff} bias uncertainty for the representative PWR SFP storage rack model and 10-GWd/MTU assembly average burnup A-7

LIST OF FIGURES
(Continued)

Figure **Page**

Figure A.6 Individual nuclide contributions to k_{eff} bias uncertainty for the representative PWR SFP storage rack model and 40-GWd/MTU assembly average burnup. ... A-8

Figure A.7 Individual nuclide contributions to k_{eff} bias uncertainty for the PWR SNF cask model and 10-GWd/MTU assembly average burnup A-8

Figure A.8 Individual nuclide contributions to k_{eff} bias uncertainty for the PWR SNF cask model and 40-GWd/MTU assembly average burnup A-8

Figure A.9 Individual nuclide contributions to k_{eff} bias uncertainty for the unpoisoned PWR SFP storage rack model and 40-GWd/MTU assembly average burnup. .. A-9

Figure A.10 Illustration of k_{eff} bias components using (a) ENDF/B-VII nuclear data; (b) ENDF/B-V nuclear data A-10

LIST OF TABLES

Table **Page**

Table 3.1 Actinide and fission product nuclides important to burnup credit criticality analyses 8

Table 3.2 Initial enrichment and burnup values for the measured PWR fuel samples..... 11

Table 3.3 Initial enrichment and burnup values for the measured BWR fuel samples..... 13

Table 6.1 Isotopic bias and bias uncertainty values for PWR SNF compositions..... 30

Table 6.2 Isotopic bias and bias uncertainty values for BWR SNF compositions..... 31

Table 6.3 Unpoisoned PWR SFP storage rack Δk_{eff} obtained with measured and calculated nuclide concentrations 39

Table 7.1 k_{eff} bias and k_{eff} bias uncertainty for the representative PWR SFP storage rack model..... 44

Table 7.2 k_{eff} bias and k_{eff} bias uncertainty for the unpoisoned PWR SFP storage rack model using burnup credit actinide and fission product nuclides 45

Table 7.3 k_{eff} bias and k_{eff} bias uncertainty for the representative PWR SNF cask model..... 45

Table 7.4 k_{eff} bias and k_{eff} bias uncertainty for the BWR SFP storage rack model 47

Table 7.5 Model parameters addressed in the sensitivity analysis..... 48

Table 7.6 k_{eff} bias and k_{eff} bias uncertainty as a function of sensitivity parameter 50

Table A.1 k_{eff} bias due to the bias in calculated ^{235}U concentration based on measurement data from fuel samples within the burnup range 15 to 40 GWd/MTU A-5

Table A.2 k_{eff} bias calculations using fuel sample and analysis model compositions A-13

Table B.1 Correlations at the 0.5 significance level for the isotopic validation data applicable to the burnup range 40 to 60 GWd/MTU..... B-3

Table C.1 Reference nuclide concentrations (g/gU initial)..... C-2

EXECUTIVE SUMMARY

One of the most significant remaining challenges associated with expanded implementation of burnup credit is the validation of depletion and criticality computer codes used in the safety evaluation—in particular, the availability and use of applicable experimental data to support validation, especially for fission products. This report presents an approach for determining bias and bias uncertainty in the effective neutron multiplication factor (k_{eff}) that results from biases and bias uncertainties in the calculated nuclide concentrations. The validation approach described in this report is independent of the depletion and criticality computational methods being used and of the choice of the safety analysis models.

The depletion validation approach has the following characteristics: (1) calculated nuclide concentrations are compared to available measurements of nuclide concentrations obtained by destructive radiochemical assay (RCA) to determine isotopic biases and bias uncertainties in the calculated nuclide concentrations, and (2) the isotopic biases and bias uncertainties are applied to the fuel compositions of representative safety analysis models to determine reference values for bias and bias uncertainty in k_{eff} by the use of the Monte Carlo uncertainty sampling method. The Monte Carlo uncertainty sampling method represents the effects of nuclide concentration uncertainty on k_{eff} values by sampling nuclide concentrations from uncertainty distributions developed from measurement data. The direct-difference method was used in a limited manner to provide a check of the validation results obtained from the Monte Carlo uncertainty sampling method. The direct-difference method applies measured nuclide concentrations directly in the safety analysis model to calculate a k_{eff} value, which then is compared with the k_{eff} value for the safety analysis model that uses calculated nuclide concentrations.

The SCALE 6.1 code system and the ENDF/B-VII nuclear data were used to obtain reference k_{eff} bias and bias uncertainty results for representative safety analysis models, which include a pressurized water reactor (PWR) spent fuel pool (SFP) storage rack model, a boiling water reactor (BWR) SFP storage rack model, and a spent nuclear fuel (SNF) cask model. The fuel compositions for these models consist of 28 actinide and fission product nuclides that are important to fuel reactivity (i.e., nuclides with large neutron fission cross sections and nuclides with large neutron absorption cross sections) and have sufficient experimental data for use in depletion code validations. The RCA data for isotopic bias and bias uncertainty calculations include measured nuclide concentration values for 100 PWR fuel samples with initial enrichments varying from 2.453 to 4.657 wt % ^{235}U and burnup varying from 7 to 60 GWd/MTU and 32 BWR fuel samples with initial enrichments varying from 2.54 to 3.91 wt % ^{235}U and burnup varying from 14.4 to 44.0 GWd/MTU. Depletion validation results are provided for PWR fuel assembly average burnup values up to 60 GWd/MTU and for a BWR fuel assembly at peak reactivity.

The calculated k_{eff} bias and bias uncertainty values are similar for the representative PWR SFP storage rack and SNF cask models. For the assembly average burnup range 5 to 40 GWd/MTU, the k_{eff} bias is approximately 0.004 and the k_{eff} bias uncertainty is approximately 0.016. For an assembly average burnup range of 40 to 60 GWd/MTU, the estimated k_{eff} bias and k_{eff} bias uncertainty values gradually increase to 0.010 and 0.030, respectively. The results show that the PWR nuclide concentrations calculated with the SCALE 6.1 code system and the ENDF/B-VII nuclear cross-section data produce a small positive k_{eff} bias (i.e., slight overprediction of k_{eff}) with a significantly larger associated uncertainty value. The k_{eff} bias uncertainty is primarily due

to bias uncertainties associated with actinide nuclide concentrations. The uncertainties in the calculated ^{235}U and ^{239}Pu concentrations contribute approximately 90 to 95% of the k_{eff} bias uncertainty. The k_{eff} bias uncertainty due to the bias uncertainties in the calculated fission product concentrations is small (<3% of the k_{eff} bias uncertainty). The calculated k_{eff} bias and k_{eff} bias uncertainty values for BWR SNF are approximately 0.002 and 0.032, respectively.

Sensitivity of bias and bias uncertainty in k_{eff} to parameters important to PWR SFP criticality safety analyses was evaluated considering variations in fuel assembly design, fuel irradiation conditions, rack design, soluble boron concentration, fuel cooling time, axial representation of fuel burnup in the safety analysis model, and nuclear data (ENDF/B-V only). The assembly average burnup values considered in the parametric study are 10, 25, and 40 GWd/MTU. The calculated k_{eff} bias uncertainty values exhibit a small variability as a function of the sensitivity parameter and assembly average burnup. Based on the ENDF/B-VII calculations, the average values of k_{eff} bias uncertainty are 0.015, 0.016, and 0.017 for the assembly average burnup values of 10, 25, and 40 GWd/MTU, respectively. The largest variations from the representative SFP safety analysis model were obtained for the unpoisoned (i.e., 0-g/cm^2 ^{10}B areal density in the Boral panels) PWR SFP analysis model. For this analysis model, the k_{eff} bias uncertainty is approximately 0.019 for the burnup range 10 to 40 GWd/MTU. The k_{eff} bias for all the evaluated cases using the ENDF/B-VII nuclear data is approximately 0.004. The k_{eff} bias values in the case of the ENDF/B-V nuclear data are negative and vary with assembly average burnup from -0.0001 (10 GWd/MTU) to -0.004 (40 GWd/MTU).

The bias and bias uncertainty values estimated from the direct-difference method for a single application model are comparable with, but smaller than, the values obtained by the Monte Carlo uncertainty sampling method. Although not definitive, the comparison provides increased confidence in the Monte Carlo approach for uncertainty propagation. For depletion code validations using the direct-difference method, recommendations are provided concerning use of surrogate (i.e., substitute) data for nuclides with very few measurement data and appropriate decay-time adjustments for measured nuclide concentrations.

ACKNOWLEDGMENTS

This work was performed under contract with the Office of Nuclear Regulatory Research, U.S. Nuclear Regulatory Commission (NRC). The authors acknowledge useful review comments and suggestions provided by D. Algama, the NRC Project Manager; K. A. L. Wood of the Office of Nuclear Reactor Regulation; M. Aissa and R. Y. Lee of the Office of Nuclear Research; M. Rahimi, A. B. Barto, and Z. Li of the Office of Nuclear Material Safety and Safeguards; and C. N. Van Wert and A. Patel of the Office of New Reactors. The authors would like to thank J. M. Scaglione and W. J. Marshall for their peer review of this document and H. Turpin for her careful editing of the final report.

LIST OF ACRONYMS AND UNITS

2-D	two dimensional
ANSI/ANS	American National Standards Institute, Inc./American Nuclear Society
ARIANE	Actinide Research in a Nuclear Element
B&W	Babcock & Wilcox
BWR	boiling water reactor
CFR	*Code of Federal Regulations*
ENDF	Evaluated Nuclear Data File
GBC	generic burnup credit cask
GE	General Electric
GKN II	Gemeinschaftskernkraftwerk Unit II in Neckarwestheim/Neckar
GWd/MTU	gigawatt-day per metric ton of uranium (unit of fuel burnup)
k_{eff}	effective neutron multiplication factor
ISG	interim staff guidance
LCE	laboratory critical experiments
M/C	measured-to-calculated
MALIBU	radiochemical analysis of MOX and UOX LWR fuels irradiated to high burnup
MOX	mixed oxide
MTU	metric ton of uranium
NRC	U.S. Nuclear Regulatory Commission
PWR	pressurized water reactor
OFA	optimized fuel assembly
RCA	radiochemical assay
REBUS	Reactivity Tests for a Direct Evaluation of the Burnup Credit on Selected Irradiated LWR Fuel Bundles
ROP	range of parameters
SFP	spent fuel pool
SNF	spent nuclear fuel
$T_{1/2}$	half-life
TL	tolerance limit
TMI	Three Mile Island
W	Westinghouse
WABA	wet annular burnable absorber

1. INTRODUCTION

One of the most significant challenges associated with implementing burnup credit is the validation of the depletion and criticality computer codes used in the safety evaluation—in particular, the availability and application of experimental data to support computer code validation. The expanded use of burnup credit in the United States for dry storage casks and transportation packages, hereafter referred to as casks, has been constrained by the availability of experimental fission product data to support computer code validation (Ref. 1). Historically, uncertainty in the fuel depletion calculation for burnup credit in spent fuel pools has been based on engineering judgment (Ref. 2) in lieu of validation with experimental data. To address the issues of burnup credit criticality validation, the U.S. Nuclear Regulatory Commission (NRC) initiated a project with Oak Ridge National Laboratory to (1) develop and establish a validation approach for burnup credit commercial spent nuclear fuel (SNF) system criticality safety evaluations based on best-available data and methods and (2) apply the approach on representative SNF storage and transport configurations and conditions to demonstrate its usage and applicability, as well as to provide reference k_{eff} bias and bias uncertainty results.

The purpose of this report is to describe an approach for establishing depletion code bias and bias uncertainty in terms of a reactivity difference (i.e., Δk_{eff}). Validation of criticality calculations is addressed in a companion report (Ref. 3). The main characteristics of the depletion validation approach are as follows: (1) calculated nuclide concentrations are compared to available measurements of nuclide concentrations from destructive radiochemical assay (RCA) to determine isotopic biases and bias uncertainties in the calculated nuclide concentrations, and (2) the isotopic biases and bias uncertainties are applied to the fuel compositions of representative safety analysis models to determine reference values for bias and bias uncertainty in k_{eff} by the use of the Monte Carlo uncertainty sampling method.

Several methods for isotopic depletion code validation have been previously developed, as detailed in NUREG/CR-6811 (Ref. 4). The current validation study expands on two of these methods, the Monte Carlo uncertainty sampling method and the direct-difference method, in great detail. The Monte Carlo uncertainty sampling method represents the effects of nuclide concentration uncertainty on k_{eff} values by sampling isotopic concentrations from uncertainty distributions developed from experimental data. This method is used in this depletion validation study to calculate reference results of k_{eff} bias and bias uncertainty for representative safety analysis models. The direct-difference method applies measured nuclide concentrations directly in the safety analysis model to calculate a k_{eff} value, which then is compared with the k_{eff} value for the safety analysis model with calculated nuclide concentrations. This method is primarily used in this validation study to analyze the importance of establishing surrogate (i.e., substitute) data for nuclides with very few measurement data and performing decay-time adjustments for measured nuclide concentrations.

The depletion validation approach described in this report is independent of the depletion and criticality computational methods being used and of the choice of the safety analysis models. Application of the depletion validation approach is demonstrated for representative SNF storage pool and cask configurations/conditions. Reference results for bias and bias uncertainty in k_{eff} due to biases and bias uncertainties in calculated nuclide concentrations are obtained with SCALE 6.1 (Ref. 5) and the *Evaluated Nuclear Data File/B Version VII.0* (ENDF/B-VII) nuclear cross-section data (Ref. 6).

This document is organized as follows: Section 2 presents an overview of a generic burnup credit analysis methodology identifying the main components of the depletion and criticality validation methodologies documented in this report and in the companion report (Ref. 3), respectively. The RCA data used in the depletion validation are presented in Sect. 3. Section 4 describes the computational methods and nuclear data used to demonstrate application of the depletion validation approach. Representative analysis models for pressurized water reactor (PWR) and boiling water reactor (BWR) SNF burnup credit applications are described in Sect. 5. Implementation details for the Monte Carlo uncertainty sampling and direct-difference methods are provided in Sect. 6. Section 7 presents k_{eff} bias and bias uncertainty results based on SCALE 6.1. Results are provided for representative analysis models as well as for variants of those models. Conclusions are provided in Sect. 8. The appendices of this document describe various calculations in support of the depletion validation approach.

2. OVERVIEW OF BURNUP CREDIT ANALYSIS

Criticality safety analyses are performed to demonstrate that a proposed fuel storage or transport configuration meets the applicable requirements of Title 10, *Code of Federal Regulations* (CFR), Parts 50, 52, 70, 71, and 72 (Ref. 7). A general overview of the process for implementing burnup credit for SNF criticality safety analyses is outlined in Figure 2.1. The process includes development of safety analysis models considering a range of parameters important to criticality safety and isotopic and criticality validation analyses to demonstrate that the proposed configuration will meet the maximum k_{eff} limits specified in the applicable requirements and guidance. The methods of analysis used to determine the burnup credit nuclide compositions are validated through comparisons to measurement data. The depletion validation provided in this report addresses items (5) through (7) in Figure 2.1. The criticality validation (Ref. 3) addresses items (8) through (15) in Figure 2.1. For the sake of facilitating this discussion with a common terminology, the terms from ANSI/ANS-8.27 (Ref. 8) are being used in a slightly modified format as presented in Eq. (1).

The depletion validation approach consists of two consecutive calculation steps: (1) calculated and measured nuclide concentrations for fuel samples are compared to determine biases and bias uncertainties associated with calculated nuclide concentrations, and (2) depletion code bias and bias uncertainty are established in terms of a reactivity difference (i.e., Δk_{eff}). This latter step is referred to as "propagation" of isotopic composition uncertainties to k_{eff} in Figure 2.1, item 6. Throughout this document, the average change in k_{eff} from biases in the calculated nuclide concentrations is referred to as "k_{eff} bias," and the variance of the change in k_{eff} at a 95% probability, 95% confidence level, resulting from bias uncertainties in calculated nuclide concentrations is referred to as "k_{eff} bias uncertainty." Consistent with the approach in NUREG/CR-6698 (Ref. 9), a bias that reduces the calculated value of k_{eff} is not considered in Eq. (1).

The criteria for establishing subcriticality with credit for the reactivity decrease due to fuel burnup is that the calculated multiplication factor k_p plus allowances for biases and uncertainties shall be equal to or less than an established, allowable neutron multiplication factor; that is,

$$k_p + \Delta k_p + \beta_i + \Delta k_i + \beta + \Delta k_\beta + \Delta k_x + \Delta k_m \leq k_{limit}, \quad (1)$$

where

k_p is the calculated multiplication factor of the model for the system being evaluated;

Δk_p is an allowance for
- statistical or convergence uncertainties, or both, in the determination of k_p,
- material and fabrication tolerances,
- uncertainties due to geometric or material representation limitations of the models used in the determination of k_p;

β_i is the bias in k_p due to depletion code bias in the calculated nuclide concentrations;

Δk_i is the bias uncertainty in k_p due to depletion code bias uncertainty in the calculated nuclide concentrations;

β is the bias that results from using a particular calculation method and nuclear cross-section data to calculate the benchmark criticality experiments;

Δk_β is the criticality bias uncertainty, which includes

- statistical or convergence uncertainties, or both, in the computation of β,
- uncertainties in the benchmark criticality experiments,
- uncertainty in the bias resulting from application of the linear least-squares fitting technique to the critical experiment results,
- tolerance interval multiplier to yield a single-sided 95% probability and 95% confidence level;

Δk_x is a supplement to β and Δk_β that may be included to provide an allowance for the bias and uncertainty from nuclide cross-section data that might not be adequately accounted for in the benchmark criticality experiments used for calculating β;

Δk_m is a margin for unknown uncertainties deemed to be adequate to ensure subcriticality of the physical system being modeled (this term is typically referred to as an administrative margin);

k_{limit} is the upper limit on the k_{eff} value for which the system is considered.

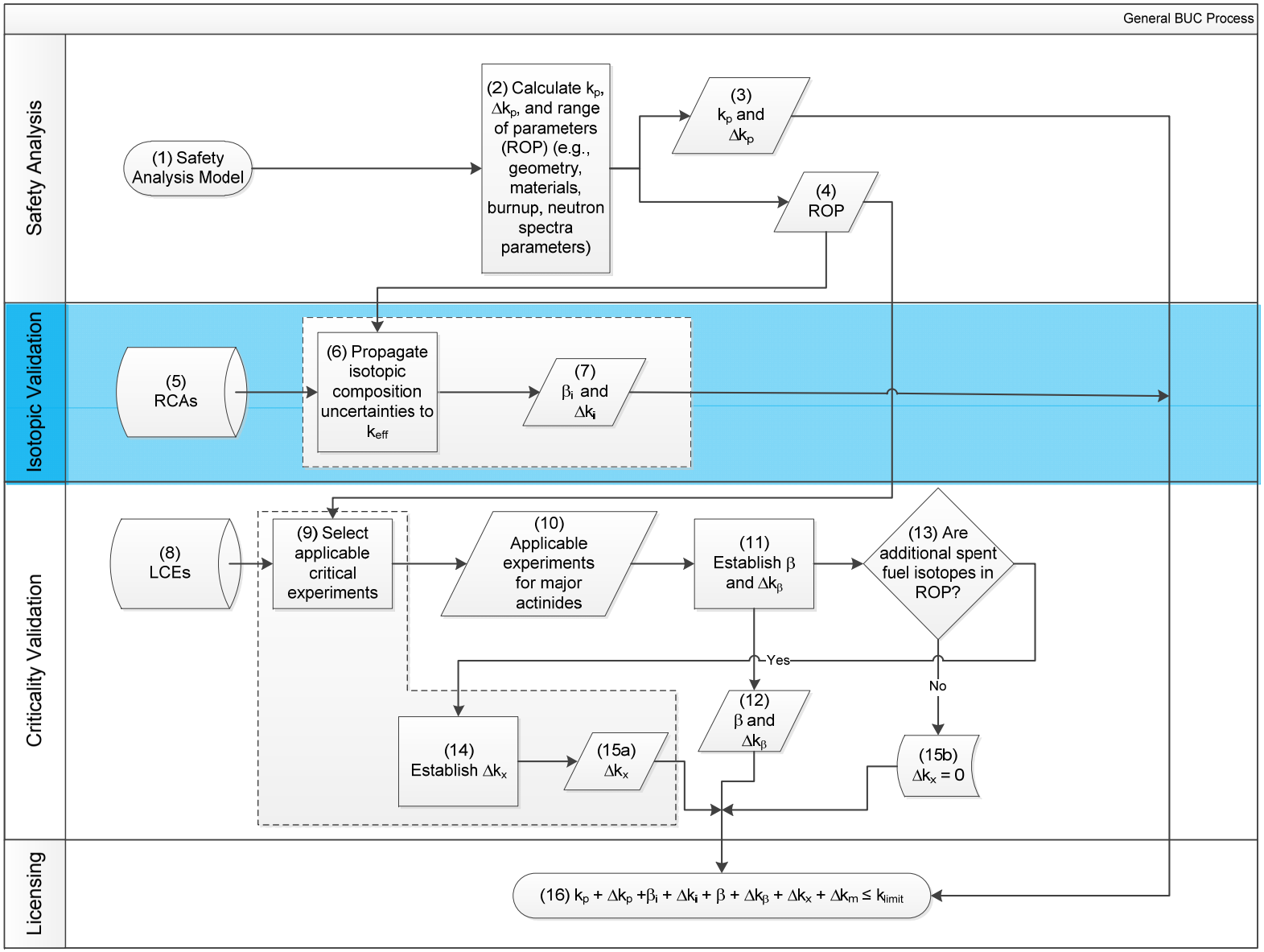

Figure 2.1 Overview of the burnup credit validation process

3. ISOTOPIC VALIDATION DATA

An approach accepted by the international nuclear engineering community for use in depletion code validations is based on comparing calculated nuclide concentrations with measured nuclide concentrations from destructive radiochemical assay of fuel samples (Refs. 8, 10, 11, 12, 13). A fuel sample is a small portion of an irradiated fuel rod (e.g., a pellet segment or a few adjacent pellets cut from a fuel rod). A small number of assembly-average measurements also exist (e.g., measurements for five Obrigheim full-length reprocessed fuel assemblies as described in Ref. 14). To obtain measurements of nuclide concentrations, SNF samples are destructively examined with radiochemical analysis methods that involve a series of complex analytical techniques for sample preparation and isotopic and elemental measurements. Measurement error is dependent on the measurement instruments and radiochemical procedures, and can range from <1% for the major uranium and plutonium isotopes when using state-of-the-art radiochemical analysis methods (Ref. 15), to more than 5% when using less precise methods (Ref. 16). Measurement data for uranium and plutonium nuclides exist for each measured fuel sample. However, measurement data for additional burnup credit nuclides vary depending on the experimental programs. Modern measurement programs, such as ARIANE, MALIBU, REBUS, and ENUSA (Refs. 17, 18, 19), dedicated to radiochemical analysis of high-burnup PWR and BWR fuel samples, provide thorough isotopic characterization and include multi-laboratory cross checks.

Inherent components of the biases and bias uncertainties associated with the calculated nuclide concentrations determined from comparisons to RCA data include biases and uncertainties related to the radiochemical assay data, the measurement techniques, the ability to model the sample depletion environments, the nuclear cross-section data used, and the intrinsic uncertainties and approximations used in the numerical solutions. The objective of depletion code validation is to establish a predictable relationship between calculated nuclide concentrations and reality. For depletion code validations, local depletion conditions for a measured fuel sample or assembly-average depletion conditions for a measured fuel assembly must be modeled as accurately as possible to avoid introducing additional inaccuracy in the validation result.

The RCA data evaluations described in Refs. 20 and 21 are based on a review of primary experimental references; hence, these references provide a database that can be used for validating computational predictions of SNF isotopic compositions. Burnup credit nuclides with available RCA data are described in Sect. 3.1. The PWR and BWR RCA data used in this report to determine biases and bias uncertainties in the calculated nuclide concentrations are presented in Sects. 3.2 and 3.3, respectively.

3.1 NUCLIDES IMPORTANT TO BURNUP CREDIT

Nuclide concentrations in commercial SNF and corresponding fuel reactivity vary depending on fuel design, depletion parameters, and cooling time. The reactivity of a discharged commercial SNF assembly reaches a maximum value at approximately 3 days after fuel discharge, when short-lived fission product nuclides with significant neutron absorption cross sections (e.g., ^{135}Xe) and their precursors are mostly decayed. The reactivity then decreases with increasing cooling time until approximately 100 years after fuel discharge, primarily a result of the decay of the fissile nuclide ^{241}Pu ($T_{1/2}$ = 14.4 years) to ^{241}Am (neutron absorber) and of the formation of ^{155}Gd (a strong neutron absorber) from the beta decay of ^{155}Eu ($T_{1/2}$ = 4.75 years) (Ref. 22).

The depletion validation presented in this report considers SNF compositions consisting of 12 actinide and 16 fission product nuclides selected on the basis of their importance to fuel reactivity (i.e., nuclides with large neutron fission cross sections and nuclides with large neutron absorption cross sections) and on the basis of availability of sufficient experimental data for use in depletion code validations. The 28 nuclides, referred to hereafter as burnup credit nuclides, are presented in Table 3.1. The burnup credit nuclides have been identified in previous studies (Refs. 23 and 24) as the nuclides with the most significant effects on k_{eff} for SNF cask burnup credit applications. The 28 nuclides or subsets of those nuclides are the ones commonly considered in fuel compositions for burnup credit criticality safety analyses that base validation of calculated nuclide concentrations on comparisons to available RCA data (Refs. 13, 25, 26). Except for ^{151}Sm ($T_{1/2}$ = 90 years), ^{238}Pu ($T_{1/2}$ = 87.7 years), ^{241}Pu ($T_{1/2}$ = 14.4 years), and ^{241}Am ($T_{1/2}$ = 432.7 years), the burnup credit nuclides are either very long-lived or stable. The concentrations of nuclides such as ^{147}Sm, ^{149}Sm, ^{151}Eu, ^{155}Gd, ^{234}U, ^{239}Pu, ^{237}Np, and ^{241}Am increase after fuel discharge as a result of the decay of their precursors. Figure 3.1 shows atom density variation as a function of decay time for nuclides exhibiting density variations after fuel discharge. Concentration values for ^{147}Sm, ^{151}Eu, ^{155}Gd, and ^{241}Am, typically measured at cooling times greater than 5 years, contain significant contributions from the radioactive decay of precursors ^{147}Pm, ^{151}Sm, ^{155}Eu, and ^{241}Pu, respectively. Note that ^{239}Pu atom density slightly increases a short time after fuel discharge as a result of ^{239}Np ($T_{1/2}$ = 2.355 day) decay; however, ^{239}Pu is not shown in the graph as a nuclide with varying atom density after fuel discharge.

Table 3.1 Actinide and fission product nuclides important to burnup credit criticality analyses

^{234}U	^{235}U	^{236}U	^{238}U	^{237}Np	^{238}Pu
^{239}Pu	^{240}Pu	^{241}Pu	^{242}Pu	^{241}Am	^{243}Am
^{95}Mo	^{99}Tc	^{101}Ru	^{103}Rh	^{109}Ag	^{133}Cs
^{143}Nd	^{145}Nd	^{147}Sm	^{149}Sm	^{150}Sm	^{151}Sm
^{152}Sm	^{151}Eu	^{153}Eu	^{155}Gd	–	–

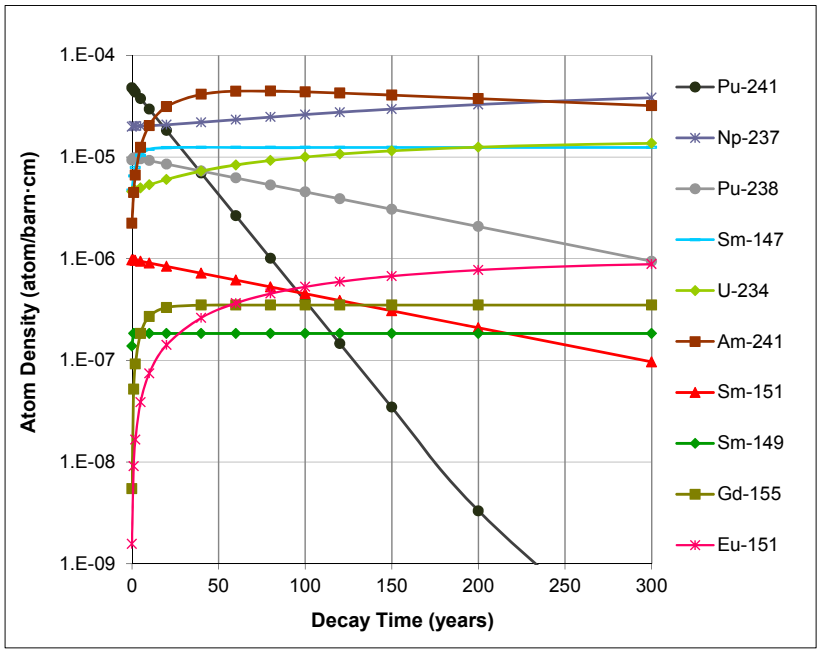

Figure 3.1 Atom density as a function of decay time for burnup credit nuclides exhibiting density variations after fuel discharge. Atom density values are shown for a Westinghouse 17×17 optimized fuel assembly of 4.7 wt % ^{235}U initial enrichment and 40 GWd/MTU burnup.

3.2 PWR ISOTOPIC VALIDATION DATA

The isotopic validation data used in this report for PWR SNF include RCA data for 100 PWR fuel samples with initial enrichments varying from 2.453 to 4.657 wt % ^{235}U and burnup varying from 7 to 60 GWd/MTU obtained from low-, moderate-, and high-burnup fuel assemblies irradiated in the following nine PWRs: Trino Vercellese, Kernkraftwerk Obrigheim, Turkey Point Unit 3, H. B. Robinson Unit 2, Calvert Cliffs Unit 1, Three Mile Island (TMI) Unit 1, Takahama Unit 3, Gösgen, and GKN II. The 100 PWR fuel samples were selected from the 118 PWR fuel samples evaluated in Ref. 20 as explained further in this section.

Three Gösgen fuel samples with burnup values ranging from 47.2 to 70.4 GWd/MTU from the MALIBU program were excluded from the isotopic validation data set because the results of the MALIBU program are proprietary information (Ref. 18) and therefore not publicly available at this time. Twelve measured PWR fuel samples obtained from the peripheral rods of Obrigheim assemblies BE124 and BE210 were irradiated in a core containing both UO_2 and mixed oxide (MOX) assembly types (Ref. 27). Information concerning the locations and the characteristics of the MOX assemblies was unavailable (Ref. 20); therefore, significant uncertainty exists regarding the type of fuel assembly adjacent to the measured rods. Hence, the Obrigheim samples from assembly peripheral rods were not used in this evaluation. Takahama fuel samples SF95-1, SF96-1, and SF97-1 were excluded because of their proximity to the end of the active fuel region. These samples were obtained from locations near the extreme ends of the fuel rods (<20 cm) where the neutron flux gradient varies significantly over short lengths. The depletion calculation method used to demonstrate the validation approach (see Sect. 4) uses a two-dimensional representation of the depletion environment, so the effects of the strong

gradient would not be accounted for accurately in the depletion calculations. Therefore, these samples were omitted for the purpose of this study.

The number of samples and the ranges of initial enrichment and final burnup of the PWR fuel samples providing measurement data for each burnup credit nuclide are presented in Table 3.2. Measured concentrations for the ^{235}U, ^{238}U, ^{239}Pu, ^{240}Pu, and ^{241}Pu nuclides are available for all PWR fuel samples. However, there are significantly fewer fuel samples providing RCA data for fission product nuclides. A comparison of the enrichment and burnup values of the 100 PWR fuel samples to loading curves developed for a representative spent fuel pool (SFP) storage rack model (see Sect. 5.2) is shown in Figure 3.2. The graph identifies the initial enrichment and final burnup of the fuel samples providing measurement data for actinide sets, partial fission product sets, and for the full set of actinide and fission product (28) nuclides considered in fuel compositions for this depletion validation (see Table 3.1). Only two Gösgen fuel samples provide measured concentrations for all 28 burnup credit nuclides. The TMI, Takahama, and some of the Calvert Cliffs fuel samples provide measurement data for most of the 16 burnup credit fission product nuclides.

The range of applicability of the initial enrichments and final burnups of the measured PWR fuel samples is presented in Table 3.2. For measured actinide concentrations, fuel sample initial enrichment ranges from approximately 2.5 to 4.7 wt % ^{235}U, and final burnup ranges from approximately 10 to 60 GWd/MTU. For most of the measured fission product nuclides, fuel sample initial enrichment ranges from approximately 2.5 to 4.7 wt % ^{235}U, and final burnup ranges from approximately 20 to 60 GWd/MTU. Measurement data for fission product nuclides such as ^{95}Mo, ^{101}Ru, ^{103}Rh, and ^{133}Cs have a burnup range of applicability from approximately 30 to 60 GWd/MTU; the ^{109}Ag measurement data has a burnup range of applicability from approximately 45 to 60 GWd/MTU. In this depletion validation, the PWR RCA data is used to calculate bias and bias uncertainty in k_{eff} for fuel assemblies with an axial burnup profile (see Sect. 5.1) and average burnup up to 60 GWd/MTU (see Sect. 7.1).

For a PWR application model (see Sect. 5) with the 60 GWd/MTU assembly average burnup value, the applied axial burnup profile resulted in a maximum burnup value of approximately 66.5 GWd/MTU. Therefore, for this assembly average burnup value, the area of applicability of the RCA data was expanded to burnup values up to 66.5 GWd/MTU. The impact on k_{eff} bias uncertainty of extending the area of applicability of the RCA data to higher burnup values was evaluated with PWR RCA data that includes the MALIBU proprietary data for three Gösgen fuel samples having burnup values from 47.2 to 70.4 GWd/MTU. This validation data set was used to calculate the k_{eff} bias uncertainty value for a SFP storage rack model (see Sect. 5.2) with an assembly average burnup of 60 GWd/MTU, which was then compared to the k_{eff} bias uncertainty value for this model obtained from applying isotopic bias uncertainties based on the measurement data for the 100 PWR fuel samples with burnup values up to 60 GWd/MTU. The two k_{eff} bias uncertainty values differed by approximately 1%. Therefore, expanding the area of applicability of the RCA data to higher burnup values is justified because the impact on k_{eff} bias uncertainty is small.

Measured nuclide concentrations for burnup credit nuclides have been reported either at the time of fuel discharge or at the actual measurement time depending on the measurement program (see Ref. 20). The measurement data reported for discharged compositions include decay time corrections for nuclides exhibiting concentration variation as a function of the decay time (see Figure 3.1) that have been performed by the experimental programs. Note that ^{239}Pu measurement data reported for discharged compositions includes a very small contribution from ^{239}Np ($T_{1/2}$ = 2.355 day) decay (Ref. 28). Applicability of measured data for nuclides with varying

concentrations as a function of decay time is limited to the reported time relative to fuel discharge. For the direct-difference method, which uses measurement nuclide concentrations directly in k_{eff} calculations, decay-time corrections may be necessary to extend the area of applicability of the measurement data for nuclides exhibiting variation with cooling time to the cooling time of the criticality safety analysis (see Sect. 6.2).

Table 3.2 Initial enrichment and burnup values for the measured PWR fuel samples

Nuclide	No. of samples	Enrichment range (wt % ^{235}U)	Burnup range (GWd/MTU)	Nuclide	No. of samples	Enrichment range (wt % ^{235}U)	Burnup range (GWd/MTU)
^{234}U	63	2.453–4.657	7.2–59.7	^{101}Ru	15	3.5–4.1	31.1–59.7
^{235}U	100	2.453–4.657	7.2–59.7	^{103}Rh	16	2.453–4.1	31.1–59.7
^{236}U	85	2.453–4.657	12.9–59.7	^{109}Ag	14	3.5–4.1	44.8–59.7
^{238}U	100	2.453–4.657	7.2–59.7	^{133}Cs	7	3.038– 4.1	27.4–59.7
^{237}Np	44	2.453–4.657	16.0–59.7	^{143}Nd	44	2.453–4.657	16.0–59.7
^{238}Pu	85	2.453–4.657	12.9–59.7	^{145}Nd	44	2.453–4.657	16.0–59.7
^{239}Pu	100	2.453–4.657	7.2–59.7	^{147}Sm	32	2.453–4.657	23.7–59.7
^{240}Pu	100	2.453–4.657	7.2–59.7	^{149}Sm	28	3.5–4.657	23.7–59.7
^{241}Pu	100	2.453–4.657	7.2–59.7	^{150}Sm	32	2.453–4.657	23.7–59.7
^{242}Pu	99	2.453–4.657	7.2–59.7	^{151}Sm	32	2.453–4.657	23.7–59.7
^{241}Am	47	2.453–4.657	17.1–59.7	^{152}Sm	32	2.453–4.657	23.7–59.7
^{243}Am	48	2.63–4.657	17.1–59.7	^{151}Eu	21	3.5–4.657	23.7–59.7
^{95}Mo	15	3.5–4.1	31.1–59.7	^{153}Eu	27	2.453–4.657	23.7–59.7
^{99}Tc	25	2.453–4.1	16.0–59.7	^{155}Gd	27	2.453–4.657	23.7–59.7

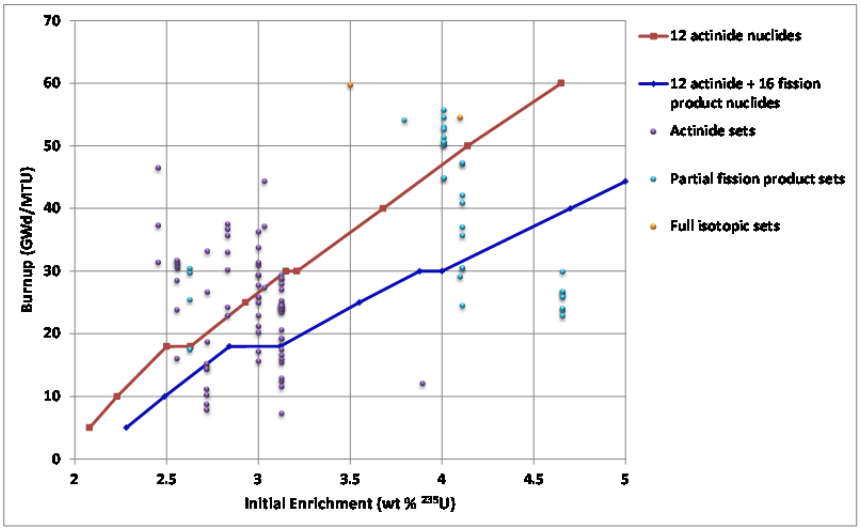

Figure 3.2 Enrichment and burnup values of the measured PWR fuel samples compared to loading curves for a representative PWR SFP storage rack model

3.3 BWR ISOTOPIC VALIDATION DATA

The biases and bias uncertainties associated with calculated nuclide concentrations in BWR SNF were based on comparisons to measured nuclide concentrations for 32 BWR fuel samples obtained from fuel assemblies consisting of 8×8, 7×7, and 6×6 pin lattices from the Fukushima Daini Unit 2, Cooper, and Gundremmingen-A reactors, respectively. Therefore, the BWR assay data is limited in its range of applicability since modern BWR assembly designs are significantly more complex. More extensive BWR isotopic assay data from modern assembly designs (i.e., 10×10 lattice) exists but was not available for inclusion in this analysis. The initial fuel enrichment for the measured samples varies from 2.54 to 3.91 wt % ^{235}U, and the burnup varies from 14.4 to 44.0 GWd/MTU.

Measurement data for the 12 burnup credit actinide nuclides and for eight of the 16 burnup credit fission product nuclides were available for use in the depletion validation. The number of samples and the ranges of initial enrichment and final burnup values of the BWR fuel samples providing measurement data for each burnup credit nuclide are presented in Table 3.3.

As described in Ref. 21, void fraction values corresponding to the fuel sample locations were unavailable for some of the measured BWR fuel samples considered in this validation study. For those BWR fuel samples, representative void fraction values were derived based on actual reported void fraction distributions from other similar assemblies at different average assembly powers. Consequently, the calculated nuclide concentrations for the BWR fuel samples include an uncertainty component due to approximate moderator density values used in the depletion calculations.

Table 3.3 Initial enrichment and burnup values for the measured BWR fuel samples

Nuclide	No. of samples	Enrichment range (wt % ^{235}U)	Burnup range (GWd/MTU)	Nuclide	No. of samples	Enrichment range (wt % ^{235}U)	Burnup range (GWd/MTU)
^{234}U	21	2.93–3.91	16.7–44	^{99}Tc	6	2.93	17.8–33.9
^{235}U	32	2.54–3.91	14.4–44	^{143}Nd	14	3.41–3.91	16.7–44
^{236}U	32	2.54–3.91	14.4–44	^{145}Nd	14	3.41–3.91	16.7–44
^{238}U	32	2.54–3.91	14.4–44	^{147}Sm	11	3.41–3.91	16.7–44
^{237}Np	20	2.93–3.91	16.7–44	^{149}Sm	11	3.41–3.91	16.7–44
^{238}Pu	32	2.54–3.91	14.4–44	^{150}Sm	11	3.41–3.91	16.7–44
^{239}Pu	32	2.54–3.91	14.4–44	^{151}Sm	11	3.41–3.91	16.7–44
^{240}Pu	32	2.54–3.91	14.4–44	^{152}Sm	11	3.41–3.91	16.7–44
^{241}Pu	32	2.54–3.91	14.4–44	–	–	–	–
^{242}Pu	32	2.54–3.91	14.4–44	–	–	–	–
^{241}Am	20	2.93–3.91	16.7–44	–	–	–	–
^{243}Am	14	3.41–3.91	27.2–44	–	–	–	–

4. COMPUTER CODES AND NUCLEAR DATA

This section describes the various computer codes and nuclear data used to perform the calculations described throughout this report.

SCALE 6.1 (Ref. 5) and the ENDF/B-VII nuclear data were selected in this study to obtain reference k_{eff} bias and bias uncertainty values for representative SFP storage rack and SNF cask configurations. SCALE 6.1 is the most recent release version of the SCALE code system developed at Oak Ridge National Laboratory. This computer code has been distributed for more than 30 years through the Radiation Safety Information Computational Center and the Nuclear Energy Agency Data Bank under license agreement. SCALE has been used for safety analysis and design by regulators, licensees, and research institutions around the world. This code is accepted by the NRC for criticality safety applications (Ref. 29). SCALE 6.1 was selected because it has multiple unique capabilities (Ref. 30) relevant to depletion and criticality code validations as briefly described in this section. SCALE 6.1 provides both depletion and criticality analysis capabilities within a common system.

SCALE 6.1 contains improved capabilities relevant to the current burnup credit calculations, including improved resonance self-shielding methodologies for cross-section processing and an improved ENDF/B-VII nuclear cross-section library for transport calculations. The ENDF/B-VII cross-section data yield significantly more accurate calculated eigenvalues than those obtained with the previous nuclear data version for a wide range of critical experiments, including moderated, low-enriched uranium fuel rod lattice configurations, and for unmoderated, bare or reflected, critical benchmark assemblies (Refs. 31 and 32). Improvements have also been observed in isotopic predictions using SCALE and the ENDF/B-VII cross-section data (Ref. 33).

The SCALE 6.1 capabilities used in the report include automated sequences to produce problem-dependent multigroup cross-section data (Ref. 34) and analysis sequences for Monte Carlo neutron transport (CSAS5 and CSAS6) (Ref. 35), fuel depletion (TRITON) (Ref. 36), isotopic decay (ORIGEN-S) (Ref. 37), burnup-credit criticality safety (STARBUCS) (Ref. 38), and cross-section sensitivity and uncertainty (TSUNAMI) (Ref. 39) calculations. Unless otherwise noted, the 238-group cross-section library based on the ENDF/B-VII.0 nuclear data and the resonance cross-section methodology employing CENTRM (Ref. 34) were used in the various SCALE 6.1 calculations in support of this depletion validation study.

The TRITON two-dimensional (2-D) depletion sequence (Ref. 5, Sect. T01) was used to perform depletion calculations. TRITON has the capability of simulating the depletion of multiple mixtures in a fuel assembly model, which allows a detailed representation of the local flux distribution for a specific fuel rod in the assembly. Within the TRITON 2-D depletion calculation sequence, ORIGEN-S (Ref. 5, Sect. F07) is used to perform depletion and decay calculations, and NEWT (Ref. 5, Sect. F21) is used to perform 2-D discrete ordinates transport calculations.

The STARBUCS sequence was used to determine burnup-dependent nuclide concentrations for PWR criticality calculations (see Sect. 5.1) and to generate loading curves for the PWR safety analysis models (see Sect. 5.4). STARBUCS enables modeling of the phenomena important to burnup credit and allows analysts to investigate the impact on criticality safety of various assumptions related to the burnup credit calculation methodology. The STARBUCS sequence provides a burnup credit loading curve search capability in addition to its initial capability of performing criticality safety analyses employing burnup credit. This capability may be used to determine the combination of assembly initial enrichment and burnup values that result in a

user-specified k_{eff} value. STARBUCS uses the ORIGEN-ARP method, described in Section D01 of Ref. 5, to rapidly generate fuel compositions as a function of fuel mixture initial enrichment and burnup. ORIGEN-ARP libraries for the STARBUCS calculations were obtained by performing TRITON depletion calculations for the PWR assembly types used in the safety analysis models and for a range of fuel initial enrichment (e.g., 1 to 5 wt % ^{235}U) and assembly average burnup (e.g., 0 to 80 GWd/MTU) values.

TSUNAMI-3D was used to determine sensitivity coefficients for individual burnup credit nuclides in support of the sensitivity/uncertainty analyses presented in this report. TSUNAMI-3D is the SCALE analysis sequence dedicated to computing the sensitivity of k_{eff} to energy-dependent cross-section data for each reaction of each nuclide in a system model using linear perturbation theory as described in Sections C09 and F22 of Ref. 5. The sensitivity of k_{eff} to total cross section, integrated over energy, is referred to as the sensitivity coefficient. Sensitivity coefficient values may also be obtained by performing direct perturbation calculations that employ variations of nuclide atom density resulting in small k_{eff} variations that are consistent with the linear-perturbation approximation.

KENO V.a (Ref. 5, Sect. F11) is the Monte Carlo transport criticality code used within the CSAS5 (Ref. 5, Sect. C05), STARBUCS, and TSUNAMI sequences to calculate the k_{eff} values of the PWR safety analysis models. KENO VI is the Monte Carlo transport criticality code used within the CSAS6 (Ref. 5, Sect. C06) sequence to calculate k_{eff} values for the BWR safety analysis model.

5. SAFETY ANALYSIS MODELS

To assess the impact of nuclide concentration uncertainties on k_{eff} for realistic storage configurations and to provide reference k_{eff} bias and bias uncertainty values, representative safety analysis models were developed for SFP storage rack and SNF cask configurations. The characteristics of a PWR SFP storage rack model, a PWR SNF cask model, and a BWR SFP storage rack model are described in this section. The sensitivity of bias and bias uncertainty in k_{eff} to a range of parameters important to criticality safety analysis (e.g., SFP storage rack design, fuel assembly type, burnup, cooling time, axial burnup representation, boron concentration, and nuclear data) was also evaluated (see Sect. 7.3).

5.1 PWR ASSEMBLY MODEL

The fuel assembly type selected for use in the PWR SFP storage rack and SNF cask models was the Westinghouse (W) 17×17 optimized fuel assembly (OFA). This assembly type is one of the assembly types used in previous burnup credit studies (Ref. 40) performed in support of ISG-8 Rev. 2 (Ref. 1). The fuel rods were represented in the model with 18 axial zones; the burnup values for the axial zones were based on burnup-dependent axial burnup profiles, which have been demonstrated to be conservative with respect to criticality (Refs. 41 and 42). Axially varying burnup-dependent nuclide concentrations were generated with reactor operating parameters for depletion calculations that increase discharge reactivity (Ref. 23), including the use of (1) wet annular burnable absorber (WABA) rod insertion in each of the 24 guide tube locations throughout the irradiation time period; (2) higher fuel and moderator temperatures (1100 K and 610 K, respectively) than typical values; (3) decreased moderator density (0.63 g/cm^3); and (4) a constant soluble boron concentration of 1000 ppm throughout the irradiation time period.

5.2 PWR SFP STORAGE RACK MODELS

The PWR SFP storage rack model is represented as a laterally infinite array of loaded fuel storage cells reflected on the top and bottom by 30 cm of full-density water. Each storage cell is a stainless steel box having an internal dimension of 22.352 cm (8.8 in.) and a wall thickness of 0.292 cm (0.115 in.). One 0.203-cm-thick (0.080-in.-thick) Boral® panel with a ^{10}B areal density of 0.020 g/cm^2 was modeled between each storage cell. The center-to-center spacing for this model is 23.139 cm (9.110 in.). The poison panels were modeled to the same axial length as the active fuel. The PWR fuel used in the safety analysis model is the W 17×17 OFA described in Sect. 5.1. The PWR fuel assembly was modeled as centered in the storage cell. A horizontal cross-section view of the PWR SFP storage rack cell model is shown in Figure 5.1. This PWR SFP storage rack configuration is referred to as the “representative” SFP storage rack model.

As shown in Sect. 5.4, the representative SFP storage rack configuration uses fuel assemblies with high initial enrichment relative to burnup so that the maximum burnup value corresponding to 5 wt % ^{235}U initial enrichment is 44.33 GWd/MTU. To obtain k_{eff} bias and bias uncertainty results for assemblies of higher burnup values, a second PWR SFP storage rack configuration was considered. This configuration differs from the representative SFP storage rack model in that it utilizes unpoisoned panels; this configuration is referred to as the “unpoisoned” SFP storage rack model.

The cooling time used to generate burnup-dependent nuclide concentrations for the PWR SFP storage rack models was 3 days. This cooling time approximately corresponds to maximum SNF reactivity, which results from the decay of short-lived fission product nuclides with significant neutron absorption cross sections. The burnup-dependent nuclide concentrations were determined so that the k_{eff} value of the PWR SFP storage rack models without soluble boron is 0.99. This value was based on the requirements of 10 CFR 50.68[b](4) (if credit is taken for soluble boron and the system is flooded with unborated water) and an assumed allowance for biases and uncertainties of 1%.

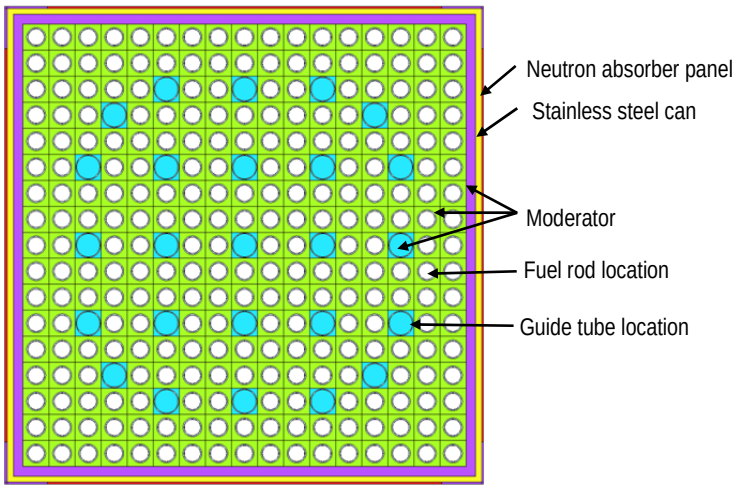

Figure 5.1 Horizontal cross section of the representative PWR SFP storage rack cell representation

5.3 PWR SNF CASK MODEL

The representative safety analysis model for a PWR SNF cask is a generic high-capacity cask design, referred to as a GBC-32 cask, which has been developed in Ref. 43 as a reference configuration for burnup credit studies. The generic cask, which can accommodate 32 PWR assemblies, uses Boral panels containing ^{10}B as a fixed neutron poison dispersed uniformly with a ^{10}B areal density of 0.0225 g/cm^2. The PWR fuel used in the safety analysis model is the W 17×17 OFA described in Sect. 5.1. A cutaway view of the GBC-32 cask model showing the bottom half with a quarter of the model removed is illustrated in Figure 5.2. The cooling time used to generate burnup-dependent nuclide concentrations for the representative PWR SNF cask was 5 years. The burnup-dependent nuclide concentrations for the GBC-32 cask model were determined so that the k_{eff} value was 0.94. The model k_{eff} value was determined by applying an assumed allowance for biases and uncertainties of 0.01 to the recommended k_{eff} value of 0.95 for cask criticality safety analyses (Refs. 29, 44, 45).

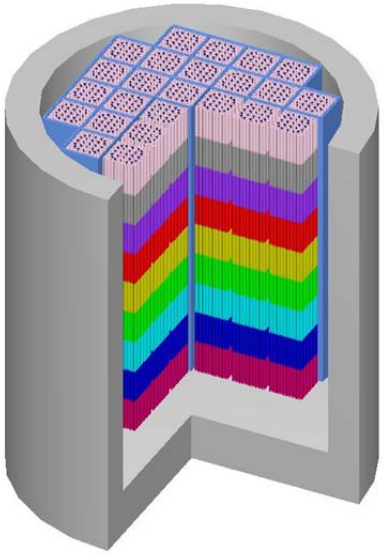

Figure 5.2 Cutaway view of the GBC-32 cask model showing bottom half with a quarter of the model removed. The different colors in the fuel region represent varying axial burnup zones.

5.4 LOADING CURVES FOR PWR SNF

For validation purposes only, loading curves were developed for the PWR SFP storage rack and SNF cask models with the k_{eff} values of 0.99 and 0.94, respectively, for fuel compositions consisting of the 12 burnup credit actinide nuclides and for the 28 burnup credit actinide and fission product nuclides (see Table 3.1). The effects of including the 16 fission product nuclides in actinide-only compositions on loading curves for the representative SNF configurations are illustrated in Figure 5.3, where the loading curves are shown superimposed over the 2002 PWR SNF assembly inventory (Ref. 46).

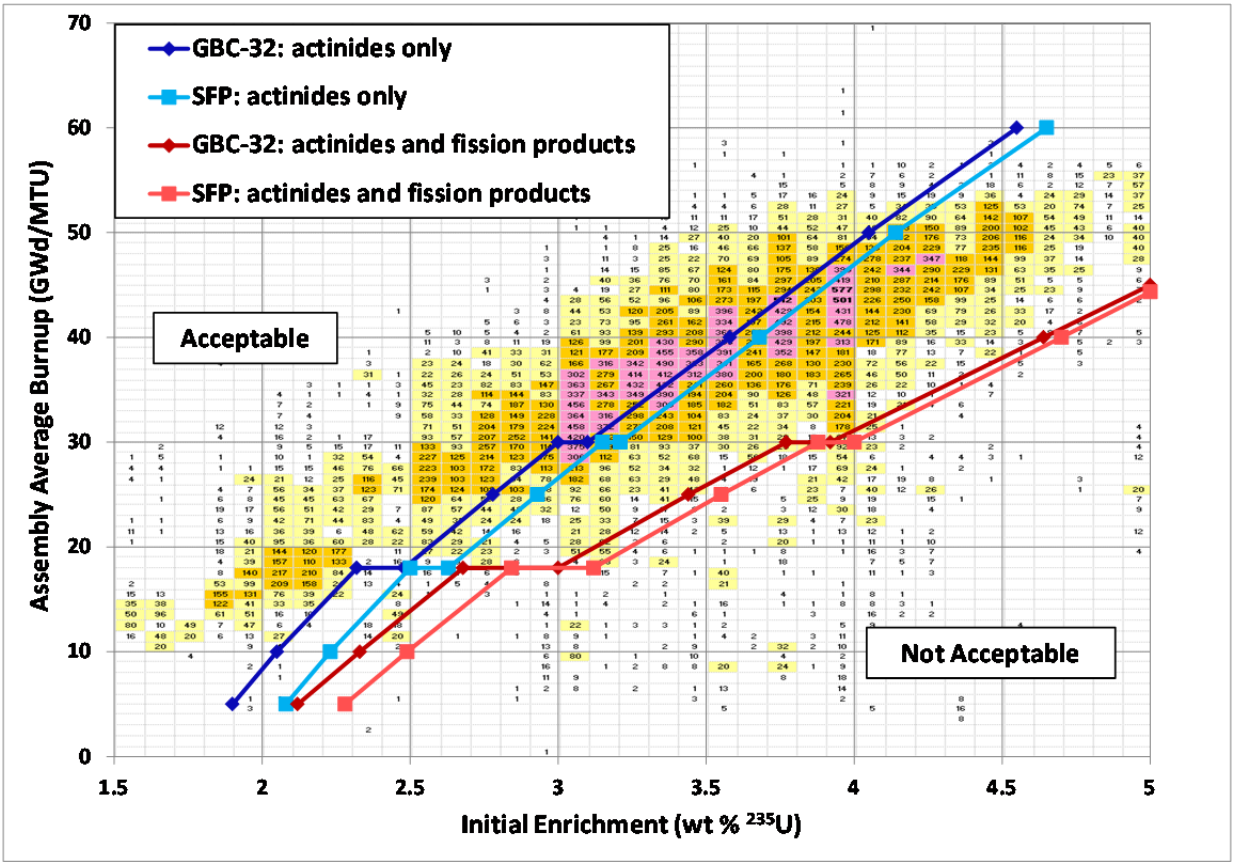

Figure 5.3 Loading curves for PWR SNF in cask and pool storage rack configurations. Loading curves developed for the representative PWR SFP storage rack and SNF cask models correspond to the k_{eff} values of 0.99 and 0.94, respectively. The horizontal segments of the loading curves were caused by changes in the fuel axial burnup profiles at 18 and 30 GWd/MTU. The color-coded numbers shown on the graph represent the numbers of PWR assemblies with certain initial enrichment and final burnup; yellow, burnt orange, and pink identify a number of assemblies in the range 20 to 99, 100 to 299, and greater than 300, respectively.

5.5 BWR ASSEMBLY MODEL

A BWR assembly model was developed using the approach commonly employed in criticality safety evaluations for the wet storage of BWR SNF in a high-density fuel storage rack (Ref. 47). The model for a BWR fuel assembly was a generic 10×10-8 assembly design with eight fuel rods containing gadolinium oxide (Gd_2O_3) and two water rods that displaced eight fuel rods. Unlike the approach employed for the PWR burnup credit criticality analysis, which uses a range of enrichment and burnup values based on the loading curve, the BWR analysis uses fuel compositions corresponding to the assembly peak reactivity. A 5 wt % ^{235}U initial enrichment of the UO_2 fuel was used to account for the highest anticipated fuel enrichment. The Gd_2O_3 content in UO_2 was 3 wt %. The BWR SFP application assumed a 3 day post-irradiation decay period.

The reactivity of a fuel assembly in the BWR reactor core initially increases with burnup as a result of the depletion of gadolinium (burnable poison) until it reaches a peak value. The peak reactivity value is reached when the burnable poison is mostly depleted. Then the reactivity of the fuel assembly decreases with burnup until the fuel assembly is removed from the reactor. For the representative model, the assembly peak reactivity occurred at approximately 11 GWd/MTU.

5.6 BWR SFP STORAGE RACK MODEL

The BWR SFP storage rack was modeled as an infinite array of loaded fuel storage cells. Each storage cell is a stainless steel box having an internal dimension of 15.063 cm (5.93 in.) and a wall thickness of 0.18 cm (0.070 in.). One 0.203-cm-thick (0.080-in.-thick) Boral plate with a ^{10}B areal density of 0.020 g/cm^2 was modeled between each storage cell. The center-to-center spacing for this model is 17.063 cm (6.72 in.). The BWR fuel assembly was modeled as centered in the storage cell with reflective boundary conditions used axially and radially. The assembly axial burnup representation is uniform. A horizontal cross section of the unit cell of the BWR SFP rack model is illustrated in Figure 5.4. The k_{inf} value of the BWR SFP storage rack model is 0.94. This value was based on the requirements of 10 CFR 50.68[b](4) (if no credit is taken for soluble boron and the system is flooded with unborated water) and an assumed allowance for biases and uncertainties of 0.01.

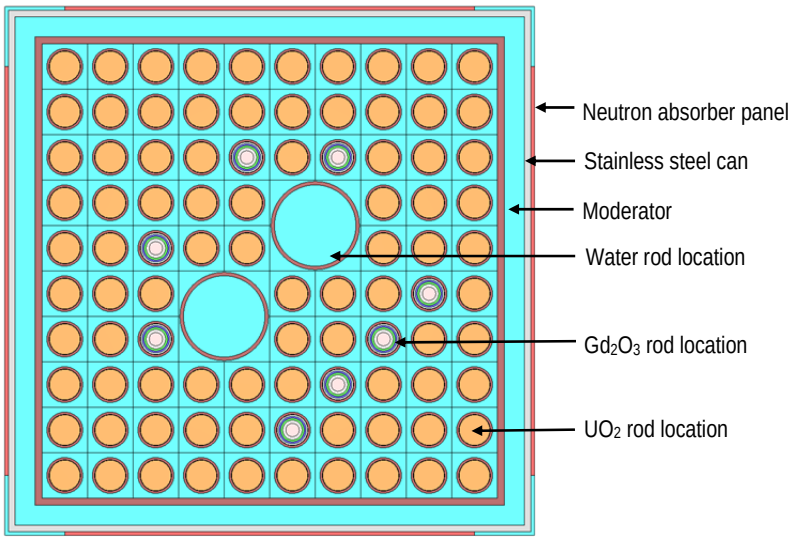

Figure 5.4 Horizontal cross section of the BWR SFP storage rack cell representation

6. CALCULATION OF BIAS AND BIAS UNCERTAINTY IN k_{eff}

Two different methods are used in this validation study: the Monte Carlo uncertainty sampling method (Sect. 6.1) and the direct-difference method (Sect. 6.2). These methods were selected on the basis of an evaluation of existing depletion validation methods (Refs. 4, 25, 48). The characteristics of the methods and their implementation for the current validation study are described in this section.

6.1 MONTE CARLO UNCERTAINTY SAMPLING METHOD

The Monte Carlo uncertainty sampling method is often used in simulating uncertainties in physical systems with many coupled degrees of freedom as well as in modeling phenomena with significant uncertainty in inputs (Refs. 49, 50, 51). In this depletion validation study, the method is used to represent the effects of nuclide concentration uncertainty on k_{eff} values by sampling isotopic concentrations from uncertainty distributions developed from experimental data. The Monte Carlo uncertainty sampling method requires determination of biases and bias uncertainties in the calculated nuclide concentrations. Implementation of the Monte Carlo uncertainty sampling method uses a normal or a uniform probability distribution (Sect. 6.1.1), depending on the number of available measurements for each burnup credit nuclide, as the mathematical model for expected isotopic concentration uncertainty variation, and independent sampling from the uncertainty distributions of individual nuclides. This implementation of the method requires analysis of the assumptions concerning normality and independence of the isotopic uncertainty data to determine the impact of those assumptions on the depletion validation results.

The following calculations and analyses were performed:

- calculation of bias and bias uncertainty in calculated nuclide concentrations (Sects. 6.1.1 and 6.1.3);
- statistical analysis of the measured-to-calculated (M/C) concentration ratio values (Sect. 6.1.2), including
  - analysis of trends,
  - normality tests, and
  - correlation coefficient calculations;
- calculation of isotopic bias and bias uncertainty (Sect. 6.1.3);
- calculation of nuclide concentration values for use in k_{eff} calculations (Sect. 6.1.4);
- validation of the normality assumption for bias uncertainty in calculated nuclide concentrations (Sect. 6.1.5); and
- convergence of the Monte Carlo k_{eff} bias uncertainty estimate (Sect. 6.1.6).

6.1.1 Calculation of Bias and Bias Uncertainty in Calculated Nuclide Concentrations

The measured-to-calculated nuclide concentration ratio, X_n^j, is calculated with Eq. (2),

$$X_n^j = M_n^j / C_n^j, \tag{2}$$

where

n = a burnup credit nuclide,
j = the index of a measured fuel sample in the series of N_n evaluated fuel samples,
M_n^j = the measured concentration of nuclide n in the evaluated fuel sample j,
C_n^j = the calculated concentration of nuclide n in the evaluated fuel sample j.

The sample mean $\overline{X}_n$ and sample standard deviation s_n of the X_n^j values are calculated with Eqs. (3) and (4), respectively,

$$\overline{X}_n = \sum_{j=1}^{N_n} X_n^j / N_n, \tag{3}$$

$$s_n = \sqrt{\sum_{j=1}^{N_n} (X_n^j - \overline{X}_n)^2 \Big/ (N_n - 1)}, \tag{4}$$

where

X_n^j = M/C concentration ratio defined by Eq. (2);
N_n = the number of evaluated fuel samples.

A normal distribution is characterized by the mean value and the standard deviation. Sample mean and sample standard deviation calculated with Eqs. (3) and (4), respectively, are only approximations of the true mean and standard deviation of nuclide concentration uncertainties because the calculations use a limited number of fuel samples. To bound the uncertainty in a sample standard deviation value because a limited number of measurement data was used, tolerance intervals are used in place of confidence intervals in the sampling procedure. Tolerance intervals have been introduced as a means to account for uncertainty due to sample size (Ref. 52). A statistical tolerance interval defines the limits within which a stated proportion of a population is expected to lie, based on a sample that was measured from this population. In this analysis, a tolerance interval is determined with tolerance limit factors for the normal distribution, which depend on the sample size, the specified proportion of the population within the bounds, and the specified certainty. Note that the magnitude of a tolerance-limit factor increases as the sample size decreases and that a tolerance interval for isotopic uncertainty determined as described further in this section is significantly larger than a confidence interval for nuclides with a small number of measurements.

The Monte Carlo uncertainty sampling method uses a normal or a uniform probability distribution, depending on the number of available measurements for each burnup credit nuclide, as the mathematical model for expected isotopic concentration uncertainty variation (Sect. 6.1.4). A normal distribution is used if more than 10 measurement data are available for a nuclide. For nuclides with fewer than 10 measured concentration values (i.e., ^{133}Cs and ^{99}Tc for PWR and BWR fuel, respectively), it is not appropriate to represent the uncertainty with a

normal distribution. Therefore, a uniform distribution model is used because this model enables conservative sampling of a larger uncertainty range than a normal distribution.

The two-sided tolerance-limit factor, denoted as tf_2^n, for the normal distribution corresponding to the sample size, 95% certainty, and 68.3% of the population, is applied as an adjustment factor as shown in Eq. (5) to determine a bounding value for one-sigma isotopic uncertainty based on more than 10 measurement data. This adjustment is made to account for uncertainty due to limited sample size. For example, the two-sided tolerance-limit factor values applied vary from 1.174 (69 samples) to 1.664 (11 samples) (Ref. 53). The 68.3% probability level is used because the tolerance-limit factor is applied as an adjustment factor to the one-sigma sample standard deviation. The adjusted one-sigma sample standard deviation is then used to define the sampling distribution. Hence, a normal distribution of mean $\overline{X}_n$ and variance σ_n determined as shown in Eqs. (3) and (5), respectively, is used as the mathematical model of uncertainty in the calculated nuclide concentrations for a nuclide *n* with more than 10 measurement data. If fewer than 10 measurement data are available to determine sample mean and standard deviation values, the one-sided tolerance-limit factor for the normal distribution corresponding to the sample size, 95% certainty, and 95% of the population, denoted as tf_1^n, is used as an adjustment factor as shown in Eq. (5) to determine a uniform sampling interval. For example, the one-sided tolerance limit factor values applied for six and seven samples are 3.711 and 3.399 (Ref. 54), respectively. A uniform distribution is characterized by the lower and upper limits within which a random variable falls. Hence, a uniform distribution of parameters $-\sigma_n$ and σ_n is used as the mathematical model of uncertainty in the calculated nuclide concentrations for nuclides with fewer than 10 measurement data,

$$\sigma_n = \begin{cases} s_n \cdot tf_2^n, & \text{if } N_n \geq 10 \text{ ,} \\ s_n \cdot tf_1^n, & \text{otherwise .} \end{cases} \tag{5}$$

The sample mean, $\overline{X}_n$, and sample standard deviation adjusted to account for uncertainties related to sample size, σ_n, determined as shown in Eqs. (3) and (5), respectively, are hereafter referred to as isotopic bias and isotopic bias uncertainty, respectively.

6.1.2 Statistical Analysis of the Measured-to-Calculated Concentration Ratio Values

Prior to developing probability distribution functions for nuclide concentration uncertainties, a statistical evaluation of the M/C concentration ratio values is required. A trending analysis (Sect. 6.1.2.1) was performed to identify M/C concentration ratio values exhibiting variations with sample burnup. The trending analysis was performed by applying the test described in Ref. 55, which is designed to evaluate the statistical significance of the slope resulting from a linear regression model. The Shapiro-Wilk normality test was applied to the M/C concentration ratio values for individual burnup credit nuclides to identify non-normal data sets (Sect. 6.1.2.2). The degree of correlation (dependence) among nuclide composition uncertainties was determined on the basis of correlation coefficient calculations (Sect. 6.1.2.3).

6.1.2.1 Analysis of Trends

For the PWR isotopic composition evaluations, a trending analysis identified a dependence of the M/C concentration ratio values on sample burnup for the major actinide nuclides ^{235}U, ^{236}U, ^{238}U, ^{239}Pu, ^{240}Pu, and ^{241}Pu. The isotopic bias for these nuclides varies as a function of sample burnup. In addition, the variance of the M/C concentration ratio values within the burnup range 40 to 60 GWd/MTU is significantly larger than that of the M/C concentration ratio values within the burnup range 5 to 40 GWd/MTU. Dependence of the M/C concentration ratio values on the initial enrichment of the PWR fuel samples was not identified for any of the burnup credit nuclides. The observed dependencies on sample burnup were considered in calculating isotopic bias and bias uncertainty values for burnup intervals, as explained further in this section.

A stepwise function was used to define constant isotopic bias and constant isotopic bias uncertainty within defined burnup intervals and to avoid a regression analysis. The burnup interval 5 to 60 GWd/MTU was divided into two or three subintervals so that the isotopic bias as well as the isotopic bias uncertainty are constant (i.e., do not exhibit a dependence on burnup) within each individual burnup subinterval. For nuclides with a large number of measurements that cover a wide range of fuel burnup values, including major actinide nuclides ^{235}U, ^{238}U, ^{239}Pu, ^{240}Pu, ^{241}Pu, and ^{242}Pu, isotopic bias and bias uncertainty values were determined for three burnup subintervals: 5 to 15 GWd/MTU, 15 to 40 GWd/MTU, and 40 to 60 GWd/MTU. Two different sets of isotopic bias and bias uncertainty values applicable to burnup values below and above 40 GWd/MTU were determined for the actinide nuclides ^{234}U, ^{236}U, ^{237}Np, ^{238}Pu, ^{241}Am, and ^{243}Am. A single set of isotopic bias and bias uncertainty values was determined for each burnup credit fission product nuclide since a smaller number of measurement data were available (e.g., from 7 for ^{133}Cs and up to 44 for ^{143}Nd and ^{145}Nd). The M/C concentration ratio values for ^{235}U and ^{239}Pu are shown in Figure 6.1(a) and Figure 6.1(b), respectively. The figures illustrate the approach of subdividing the burnup interval 5 to 60 GWd/MTU to calculate isotopic bias and bias uncertainty values.

In the case of the BWR isotopic data evaluations, the isotopic bias and bias uncertainty values were based on the entire set of available BWR RCA data since dependencies on fuel sample initial enrichment and final burnup were not identified for any of the burnup credit nuclides with measured concentrations.

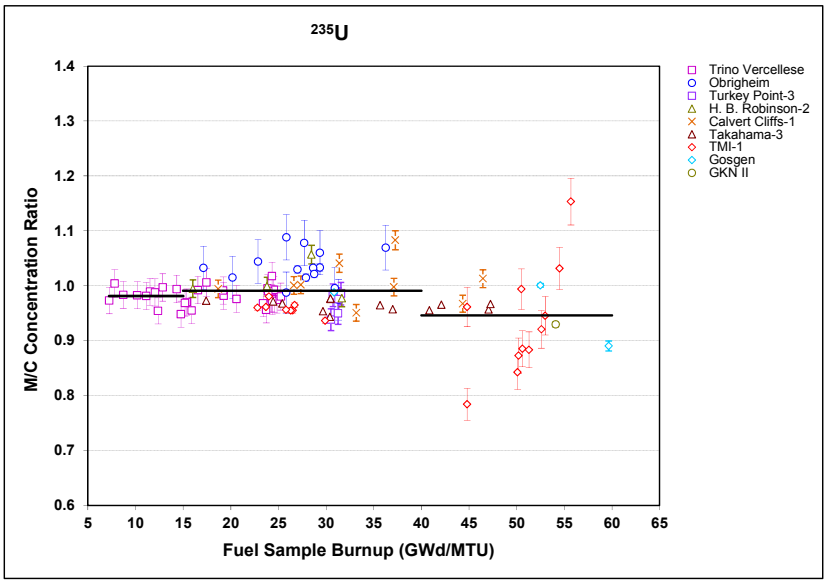

(a)

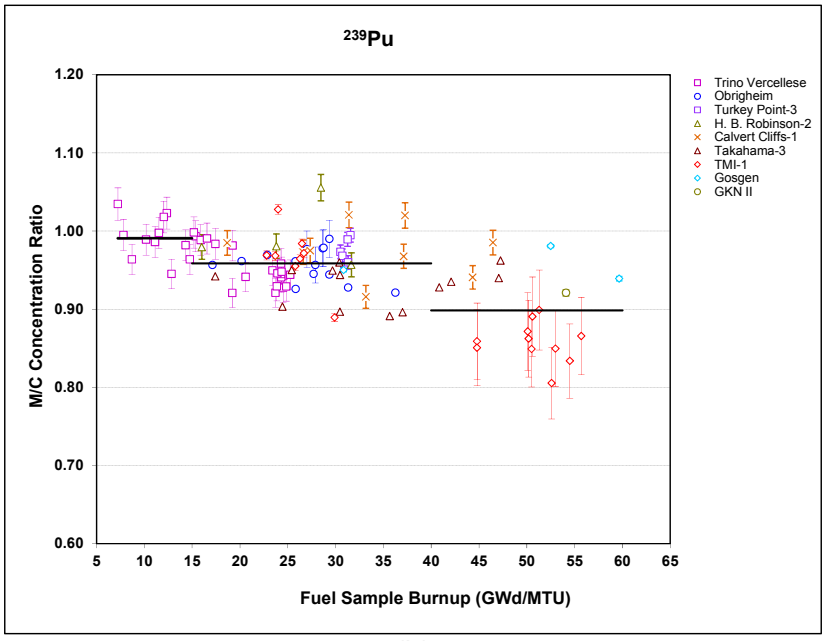

(b)

Figure 6.1 Measured-to-calculated concentration ratio versus fuel sample burnup for (a) ^{235}U; (b) ^{239}Pu. The error bars in the graph represent the reported one sigma measurement errors; very small measurement errors (0.1%) are not visible on the graph.

6.1.2.2 Normality Test Results

Data normality was assessed with the Shapiro-Wilk normality test at the 0.05 significance level (Ref. 56). The PWR M/C concentration ratio values for ^{235}U within the burnup interval 15 to 40 GWd/MTU did not approach a normal distribution. Other nuclides with non-normal PWR M/C concentration ratio values are ^{238}U, ^{237}Np, ^{241}Am, ^{147}Sm, ^{150}Sm, ^{151}Sm, ^{151}Eu, and ^{155}Gd.

In the case of the BWR isotopic composition data evaluations, the M/C concentration ratio values for nuclides with minor importance to fuel reactivity such as ^{236}U, ^{143}Nd, and ^{147}Sm were identified as non-normal data sets.

The impact on k_{eff} bias uncertainty of using a normal distribution probability function to sample nuclide concentration uncertainties for these nuclides is analyzed in Sect. 6.1.5.

6.1.2.3 Correlations among Nuclide Concentration Uncertainties

The independence of variables is an assumption used in the current implementation of the Monte Carlo uncertainty sampling method. Complex multivariate statistical analyses (Refs. 57 and 58), which attempt to establish mathematical relationships between variables considered relevant to the problem being studied, require detailed understanding of both the calculational and experimental uncertainties and correlations. This analysis evaluated the degree of correlations (dependence) based on Pearson correlation coefficient (Ref. 53) calculations. An example of correlation coefficient values for the burnup range 40 to 60 GWd/MTU is presented in Appendix B.

Correlations between the M/C concentration ratio values for ^{235}U and ^{239}Pu were evaluated because these two nuclides are the main contributors to k_{eff} bias uncertainty. The uncertainties in the calculated ^{235}U and ^{239}Pu concentrations contribute approximately 90% to 95% of the k_{eff} bias uncertainty [see Eq. (8)] for the SFP storage rack and SNF cask models analyzed in this report, as demonstrated in Sect. A.3. A negative correlation between the ^{235}U and ^{239}Pu M/C concentration ratio values may exist because of biases associated with measured fuel sample burnup values or because of depletion code biases. Correlations between the isotopic validation data for ^{235}U and ^{239}Pu were determined to be insignificant at the 0.05 significance level throughout the burnup range 5 to 60 GWd/MTU based on correlation coefficient calculations. Statistically significant correlations were identified for the Pu isotopes; the effects of positive ^{239}Pu and ^{241}Pu correlations need to be considered for fuel assemblies with high burnup and relatively low initial enrichment for the burnup (refer to the fuel initial enrichment and burnup values in Table 7.2), such as the nuclide concentrations in the unpoisoned SFP storage rack model (see Sect. 5.2). For these assemblies, the uncertainties in the calculated Pu concentrations dominate k_{eff} bias uncertainty (see Sect. A.3, Figure A.9). The contribution of the bias uncertainty in the calculated ^{241}Pu concentration to k_{eff} bias uncertainty is <1% and ~5% for the representative models and for the unpoisoned rack model, respectively. In this analysis, as described in Appendix B, to account for additional uncertainty due to neglected positive correlations in the validation data for ^{239}Pu and ^{241}Pu, the contribution to k_{eff} bias uncertainty of the bias uncertainty in the prediction of ^{241}Pu was doubled in the calculation of total k_{eff} bias uncertainty. For the unpoisoned SFP storage rack model with 40-GWd/MTU assembly average burnup, this resulted in a 0.001 Δk_{eff} effect, which is small compared to the k_{eff} bias uncertainty value of 0.018 (~5%). For the representative SFP and cask analysis models, existing correlations are considered to have negligible impact on the calculated k_{eff} bias uncertainty values because the k_{eff} bias uncertainty is dominated by ^{235}U and ^{239}Pu concentration prediction

uncertainties; all other nuclides have a relatively small (<1.3%) or negligible contributions to k_{eff} bias uncertainty.

6.1.3 Isotopic Bias and Bias Uncertainty Values

Isotopic bias and bias uncertainty values for PWR and BWR SNF, along with their corresponding burnup range of applicability, are presented in Table 6.1 and Table 6.2, respectively. The isotopic bias and bias uncertainty values were determined with Eqs. (3) and (5), respectively, where the nuclide concentration values for measured nuclides in fuel samples were calculated with SCALE 6.1 and the ENDF/B-VII nuclear data (see Sect. 4).

The isotopic bias and bias uncertainty values were used as parameters for the distribution models in the Monte Carlo uncertainty sampling procedure (see Sect. 6.1.4).

The area of applicability of the isotopic bias and bias uncertainty values is based on fuel samples with the enrichment and burnup values as shown in Table 3.2 and Table 3.3 for the PWR and BWR fuel samples, respectively. The area of applicability of the isotopic bias and bias uncertainty values for fission products, typically measured for mid- and high-burnup samples, is extended to low burnup values. This extension of the area of applicability has insignificant impact on the accuracy of the calculated k_{eff} bias uncertainty values because (1) the relative importance of fission products to fuel reactivity for low-burnup assemblies is small (see Sect. A.1); and (2) the total contribution to k_{eff} bias uncertainty of the bias uncertainties associated with the calculated fission product concentrations is very small (e.g., <3%, as demonstrated in Sect. A.3) for the analysis models.

Table 6.1 Isotopic bias and bias uncertainty values for PWR SNF compositions

Burnup range	5 < Burnup [a] ≤ 15 GWd/MTU			15 < Burnup ≤ 40 GWd/MTU			40 < Burnup ≤ 60 GWd/MTU		
Nuclide	No. of samples	Isotopic bias	Isotopic bias uncertainty [b]	No. of samples	Isotopic bias	Isotopic bias uncertainty	No. of samples	Isotopic bias	Isotopic bias uncertainty
^{235}U	11	0.9814	0.0284	69	0.9907	0.0416	20	0.9459	0.1096
^{238}U	11	0.9990	0.0063	69	1.0017	0.0042	20	1.0020	0.0021
^{239}Pu	11	0.9906	0.0453	69	0.9587	0.0375	20	0.8984	0.0727
^{240}Pu	11	1.0155	0.0700	69	0.9801	0.0317	20	0.8981	0.0810
^{241}Pu	11	1.0648	0.1103	69	1.0108	0.0514	20	0.9833	0.0839
^{242}Pu	10	1.1029	0.1905	69	1.0647	0.0783	20	1.0636	0.0852

Burnup range	5 < Burnup ≤ 40 GWd/MTU			40 < Burnup ≤ 60 GWd/MTU		
Nuclide	No. of samples	Isotopic bias	Isotopic bias uncertainty	No. of samples	Isotopic bias	Isotopic bias uncertainty
^{234}U	43	0.9119	0.1749	20	0.9114	0.1077
^{236}U	65	1.0249	0.0445	20	0.9862	0.0303
^{237}Np	25	0.9905	0.2429	19	1.0011	0.1072
^{238}Pu	65	1.1500	0.0923	20	1.1375	0.2331
^{241}Am	27	0.9312	0.2077	20	0.9947	0.3224
^{243}Am	30	0.9998	0.2269	18	0.9216	0.2124

Burnup range	5 < Burnup ≤ 60 GWd/MTU		
Nuclide	No. of samples	Isotopic bias	Isotopic bias uncertainty
^{95}Mo	15	1.0002	0.0745
^{99}Tc	25	0.9400	0.2030
^{101}Ru	15	0.9726	0.1152
^{103}Rh	16	0.9021	0.0894
^{109}Ag	14	0.5546	0.2694
^{133}Cs [c]	7	0.9810	0.0680
^{143}Nd	44	0.9779	0.0526
^{145}Nd	44	0.9978	0.0291
^{147}Sm	32	0.9379	0.0967
^{149}Sm	28	0.9634	0.0995
^{150}Sm	32	0.9656	0.0663
^{151}Sm	32	0.9961	0.0782
^{152}Sm	32	0.9736	0.0427
^{151}Eu	21	1.4721	0.7644
^{153}Eu	27	0.9967	0.0480
^{155}Gd	27	1.2556	0.3391

[a]Either axial zone burnup or assembly average burnup.
[b]One-sigma uncertainty value.
[c]Uniform distribution within the interval defined by bias ± bias uncertainty (i.e., 0.9130 to 1.0410) was assumed.

Table 6.2 Isotopic bias and bias uncertainty values for BWR SNF compositions

Nuclide	No. of samples	Isotopic bias	Isotopic bias uncertainty [a]
^{234}U	20	0.9648	0.0508
^{235}U	32	1.0027	0.0726
^{236}U	32	1.0315	0.0295
^{238}U	32	1.0046	0.0096
^{237}Np	20	1.0334	0.1596
^{238}Pu	32	1.0866	0.1121
^{239}Pu	32	0.9768	0.0561
^{240}Pu	32	0.9944	0.0394
^{241}Pu	32	1.0042	0.0613
^{242}Pu	32	1.0342	0.0796
^{241}Am	20	0.8985	0.1244
^{243}Am	14	0.9506	0.1056
^{99}Tc [b]	6	0.8761	0.1013
^{143}Nd	14	1.0012	0.0353
^{145}Nd	14	1.0102	0.0364
^{147}Sm	11	1.0494	0.0541
^{149}Sm	11	1.0607	0.2255
^{150}Sm	11	1.0355	0.0397
^{151}Sm	11	1.0687	0.0858
^{152}Sm	11	1.0389	0.0524

[a]One-sigma uncertainty value.
[b]Uniform distribution within 0.7748 to 0.9774 was assumed for ^{99}Tc.

6.1.4 Nuclide Concentrations for k_{eff} Calculations

In the Monte Carlo uncertainty sampling procedure, a normal distribution model is used to determine isotopic bias and bias uncertainty values if more than 10 measured concentration values are available for a nuclide. For nuclides with fewer than 10 measured concentration values (i.e., ^{133}Cs and ^{99}Tc for PWR and BWR fuel, respectively), it is not appropriate to use a normal distribution to represent the uncertainty. Therefore, a uniform distribution model is used because this model enables conservative sampling of a larger uncertainty range than a normal distribution.

The calculated nuclide concentrations in each burnup-dependent fuel mixture of the safety analysis model are adjusted as shown in Eq. (6) for burnup-dependent isotopic bias and bias uncertainty. Random numbers drawn from either the standard normal distribution (i.e., the normal distribution with the distribution mean of zero and standard deviation of unity) or from the uniform distribution of parameters –1 and +1 are used as shown in Eq. (6) to simulate nuclide concentration variations within the range of uncertainty,

$$c_{n,b}^{k} = \begin{cases} c_{n,b} \cdot (\bar{X}_n^b + \sigma_n^b \cdot R_n^k\big|_{normal}), & \text{if } N_n \geq 10 \\ c_{n,b} \cdot (\bar{X}_n^b + \sigma_n^b \cdot R_n^k\big|_{uniform}), & \text{otherwise} \end{cases}, \tag{6}$$

where

n = credited nuclide in SNF compositions;
k = the index of a criticality calculation;
$c_{n,b}^{k}$ = concentration of nuclide n in a fuel mixture of burnup b for criticality calculation k adjusted for isotopic bias and bias uncertainty;
$c_{n,b}$ = calculated concentration of nuclide n in a fuel mixture of burnup b;
$\bar{X}_n^b$ = isotopic bias (see Sect. 6.1.3) corresponding to the burnup b of the fuel mixture;
σ_n^b = isotopic bias uncertainty (see Sect. 6.1.3) corresponding to the burnup b of the fuel mixture;
$R_n^k\big|_{normal}$ = random number sampled from the standard normal distribution (i.e., the normal distribution with the distribution mean of zero and standard deviation of unity). Random numbers from the standard normal distribution have the following characteristics: 68.3% of the population falls between ±1, 95.5% of the population falls between ±2, and 99.7% of the population falls between ±3 (Ref. 53);
$R_n^k\big|_{uniform}$ = random number sampled from the uniform distribution ranging from -1 to 1.

Sampling from the standard normal distribution was performed by the method described in Ref. 59. Note that Eq. (6) may result in negative nuclide concentration values for nuclides with very large isotopic bias uncertainty values, as in the case of the isotopic bias uncertainty for ^{151}Eu (see Table 6.1). In the implementation of the Monte Carlo uncertainty sampling method, negative nuclide concentration values resulting from application of Eq. (6) were set to zero.

The k_{eff} values from a statistically significant number (Sect. 6.1.6) of Monte Carlo calculations approach a normal distribution with the mean and standard deviation given by Eqs. (7) and (8), respectively,

$$\bar{k}_{eff} = \sum_{i=1}^{N_C} k_{eff}^{i} / N_C \ , \tag{7}$$

$$\sigma_{k_{eff}} = \sqrt{\sum_{i=1}^{N_C} (k_{eff}^{i} - \bar{k}_{eff})^2 \Big/ (N_C - 1)} \ , \tag{8}$$

where

$\bar{k}_{eff}$ = sample mean of the k_{eff} values from the Monte Carlo calculations;
N_C = number of calculated k_{eff} values;
k_{eff}^{i} = k_{eff} value for criticality calculation i in the series of N_C criticality calculations;
$\sigma_{k_{eff}}$ = sample standard deviation of the k_{eff} values from the Monte Carlo simulations.

The series shown in Eq. (7) converges to the k_{eff} value obtained by adjusting the calculated nuclide concentrations for isotopic bias only. The difference between the reference value, $k_{eff\text{-}REF}$, (i.e., k_{eff} for the calculated nuclide concentrations with no adjustments) and $\bar{k}_{eff}$ represents the bias in the application k_{eff} resulting from isotopic bias,

$$k_{eff} \text{ bias} = k_{eff-REF} - \bar{k}_{eff} . \tag{9}$$

Bias uncertainty in k_{eff} at a 95% probability, 95% confidence level is calculated with Eq. (10),

$$k_{eff} \text{ bias uncertainty} = \sigma_{k_{eff}} \times tf_1^{N_C} \ , \tag{10}$$

where $\sigma_{k_{eff}}$ is determined with Eq. (8) and $tf_1^{N_C}$ is the one-sided tolerance-limit factor for the normal distribution corresponding to the number of calculated k_{eff} values (N_c), at a 95% probability, 95% confidence level.

The bias and bias uncertainty in k_{eff} resulting from biases and bias uncertainties in the calculated nuclide concentrations, i.e., $\beta_i + \Delta k_i$ in Eq. (1), is determined with Eq. (11),

$$\beta_i + \Delta k_i = \begin{cases} (\bar{k}_{eff} - k_{eff-REF}) + \sigma_{k_{eff}} \times tf_1^{N_C} & \text{if } \bar{k}_{eff} > k_{eff-REF}, \\ \sigma_{k_{eff}} \times tf_1^{N_C}, \text{ otherwise.} \end{cases} \tag{11}$$

6.1.5 Validation of the Assumption for Data Normality

As indicated in Sect. 6.1.2.2, the PWR M/C concentration ratio values for ^{235}U within the burnup interval 15 to 40 GWd/MTU did not pass the normality test. Since ^{235}U is a very important nuclide to fuel reactivity, a sensitivity/uncertainty analysis using the actual M/C concentration

ratio values for ^{235}U in place of the normal distribution model was performed in Sect. A.2 to evaluate the impact of assuming a normal distribution. The analysis determined the k_{eff} bias uncertainty, including all burnup credit nuclides, to be 0.0152, which is slightly less than 0.0168, calculated on the basis of a normal distribution with mean and standard deviation of 0.9907 and 0.0416, respectively (see Table 6.1), for this burnup range. For this case, a normal distribution can be used because the k_{eff} bias uncertainty value obtained from the normal distribution in place of the actual distribution is slightly conservative (i.e., larger uncertainty).

Other nuclides for which PWR M/C concentration ratio values did not pass a normality test, such as ^{238}U, ^{237}Np, ^{241}Am, ^{147}Sm, ^{150}Sm, ^{151}Sm, ^{151}Eu, and ^{155}Gd, have either negligible or relatively small individual contributions (<0.5%) to k_{eff} bias uncertainty (see Section A.3). The individual contributions to k_{eff} bias uncertainty of the nuclides with non-normal BWR M/C concentration ratio values (i.e., ^{236}U, ^{143}Nd, and ^{147}Sm) were evaluated and found to be negligible. Therefore, the impact of the sampling distribution model on the k_{eff} bias uncertainty values is negligible for these nuclides. Hence, sampling from a normal distribution is adequate.

6.1.6 Convergence of the Monte Carlo k_{eff} Bias Uncertainty Estimate

The Monte Carlo uncertainty sampling method is computationally intensive because a significant number of fuel composition simulations are necessary to ensure that the underlying probability distributions are adequately sampled and that the Monte Carlo estimates of $\bar{k}_{eff}$ [see Eq. (7)] and $\sigma_{k_{eff}}$ [see Eq. (8)] have reached convergence. Convergence is considered achieved when $\bar{k}_{eff}$ and $\sigma_{k_{eff}}$ values change insignificantly (e.g., within ±0.0005) with additional simulation.

The impact of the statistical estimates on the accuracy of using 250 simulations was further analyzed for the representative PWR SFP rack model and the 40-GWd/MTU assembly average burnup using a total of 2500 k_{eff} simulations. The sample standard deviation of the k_{eff} values was 0.0083 based on 2500 simulations, varied from 0.0078 to 0.0086 based on five batches of 500 simulations, and varied from 0.0078 to 0.0088 based on 10 batches of 250 simulations. Based on this study, the sample standard deviation of the k_{eff} values based on 250 k_{eff} calculations is determined within ±0.0005. For the Monte Carlo uncertainty sampling method, 250 criticality calculations are considered sufficient to ensure that the k_{eff} bias uncertainty estimate is determined with significant accuracy.

The results for k_{eff} bias uncertainty were obtained from the use of either 250 or 500 k_{eff} calculations. The graph in Figure 6.2 shows the k_{eff} values from a Monte Carlo simulation for 500 k_{eff} calculations, the sample mean, $\bar{k}_{eff}$, the upper limit of the 95%/95% tolerance interval, and the bias and bias uncertainty in k_{eff}, $\beta_i + \Delta k_i$ [see Eq. (11)], for the representative PWR SFP storage rack model with a 40-GWd/MTU assembly average burnup. The simulated k_{eff} values passed the Shapiro-Wilk normality test at the 0.05 level.

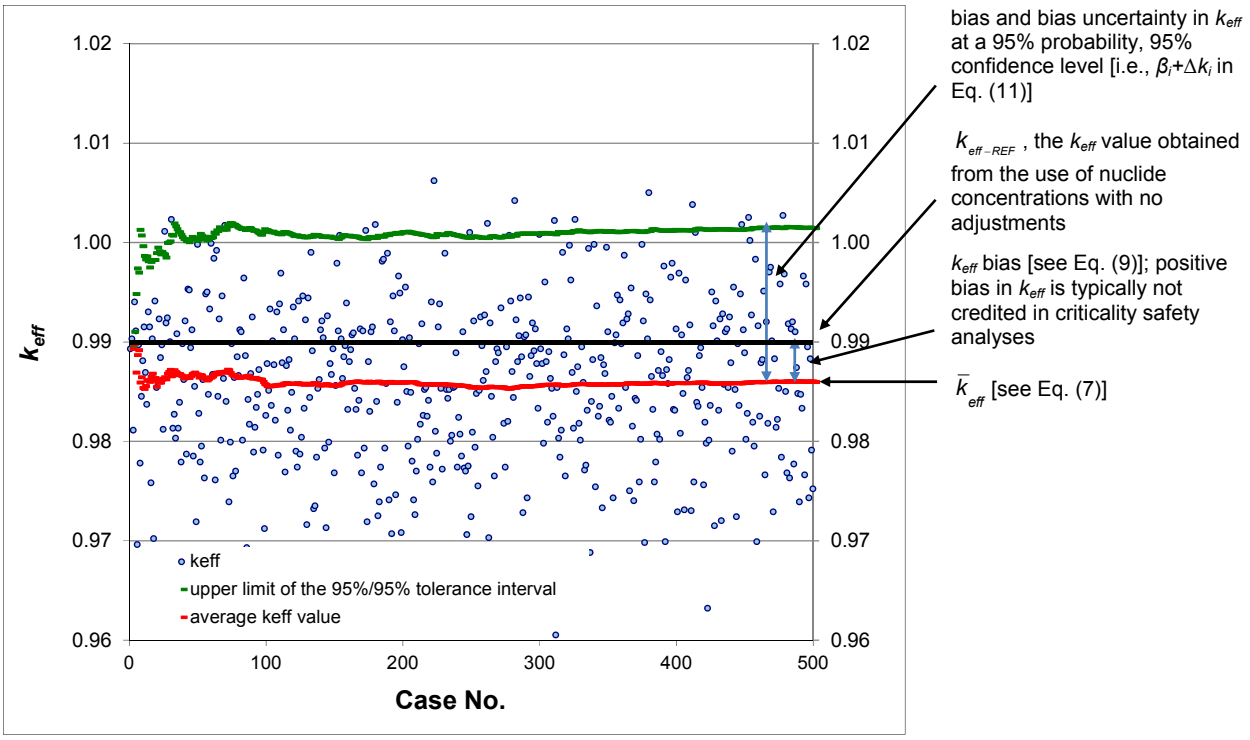

Figure 6.2 Illustration of the Monte Carlo estimates

6.2 DIRECT-DIFFERENCE METHOD

The bias and bias uncertainty in criticality calculations resulting from the bias and bias uncertainty in the computed nuclide concentrations may be assessed by a method that compares k_{eff} values obtained with calculated nuclide concentrations, k_{eff}^{c}, to k_{eff} values obtained with measured nuclide concentrations, k_{eff}^{m}. The difference in the values,

$$\Delta k_{eff} = k_{eff}^{c} - k_{eff}^{m}, \tag{12}$$

is a direct measure of the k_{eff} bias associated with the calculated SNF concentrations. Given a sufficient set of measurements for fuel compositions that are representative of the application, multiple k_{eff} calculations can be performed to generate a distribution of Δk_{eff} values that can then be statistically evaluated to determine average k_{eff} bias and bias uncertainty associated with the calculated nuclide concentrations. This method is sometimes referred to as the "direct difference" uncertainty analysis method. The method has the advantage of not requiring an evaluation of uncertainties associated with individual nuclide concentrations. Nuclide concentration uncertainties are propagated directly to the k_{eff} value, without a requirement to quantify individual nuclide uncertainties, trends, or correlations between different nuclides (i.e., covariance). The direct-difference approach used in this report is similar to that described in Ref. 4 except for the use of surrogate (i.e., substitute) data in place of missing measurement data and decay-time corrections for measurement data.

The experimental data evaluated for this analysis included the 100 PWR SNF samples listed in Table 6.3. Depletion calculations were performed with the best available information on fuel design and reactor operating conditions for the SNF samples to obtain the calculated nuclide concentrations. An immediate challenge for the direct-difference method is that measurements are generally available for only a subset of the 28 actinide and fission product nuclides used in the burnup credit analysis. Measurement data for major uranium and plutonium nuclides exist for each measured fuel sample. However, measurement data for additional burnup credit nuclides vary depending on the experimental programs. Surrogate data were developed for nuclides without measurements to avoid introducing potential bias in the Δk_{eff} results caused by using samples with different credited nuclides (corresponding to the measured nuclides) and to provide a consistent basis for comparing the results for different SNF samples. These surrogate data are presented in Appendix C, Table C.1.

The surrogate data were based on measurement results from other samples for which nuclide measurements were available. Calculated nuclide concentrations adjusted for the mean measured-to-calculated concentration ratio obtained from other similar samples (see Table 6.1) were used as surrogate data for nuclides without measurements. For example, measurements of ^{103}Rh were available for only 16 of the evaluated samples. Based on these samples, the calculation bias was determined to be 0.9021 (see Table 6.1); that is, ^{103}Rh is overpredicted, on average, by about 10%. Surrogate data for samples without ^{103}Rh measurements were therefore derived by multiplying the calculated ^{103}Rh concentration by the bias, effectively reducing the calculated content by about 10% and correcting for known computational bias. This procedure ensures that the bias attributed to each nuclide is accounted for in the k_{eff} calculations, but it does not include the uncertainties (variance) associated with the surrogate data (i.e., the uncertainty in the nuclide bias). An analysis of uncertainties in Sect. A.3 of this report demonstrated that k_{eff} bias uncertainty is dominated by the major uranium and plutonium

isotopes for which measurement data are available in all samples considered. Hence, the approach of using average bias values to derive surrogate measurement data is justified.

The impact on k_{eff}^{m} of applying the calculated fission product bias values to lower burnup values, particularly for nuclides with relatively few available measurements, are further analyzed with sensitivity coefficients that represent the relative change in k_{eff} caused by a change in the nuclide concentration [see Appendix A, Eq. (A-1)]. Additional uncertainties in the nuclide M/C concentration ratio values may be introduced by extrapolating the results beyond the range of the measurement data. For example, measurements for the fission product nuclides ^{95}Mo, ^{101}Ru, ^{103}Rh, and ^{133}Cs were not available in samples with a burnup less than approximately 30 GWd/MTU, and ^{109}Ag measurements were not available below approximately 45 GWd/MTU. The error in the calculated nuclide concentrations attributed to nuclear cross section data has been evaluated previously as a function of burnup of the fuel (Ref. 60). The results in Ref. 60 show that the relative error in the calculated nuclide contents increases as a function of burnup for the fission products listed above. Therefore, the bias (i.e., over prediction or under prediction by a code) derived using measurements for high burnup fuels are expected to be bounding for applications at lower burnup values. The maximum standard error in the k_{eff} bias caused by extrapolation of data, estimated with sensitivity coefficients [Eq. (A-1)] for these five fission products without extensive measurements for low burnup fuels, is determined to be less than 0.04%.

The relative error in the average M/C concentration ratio value is represented by the confidence interval of the mean, calculated using the standard deviation of the M/C concentration ratio distributions and the number of samples (obtained from Table 6.1). The impact on k_{eff}^{m} caused by uncertainties in the average M/C concentration ratio values was estimated using sensitivity coefficients [Eq. (A-1)]. The maximum standard error in the k_{eff} values for the representative SFP storage rack model was found to be approximately 0.06%. This value is derived assuming surrogate data are applied for all 16 fission product nuclides and the actinide nuclides ^{234}U, ^{236}U, ^{237}Np, ^{238}Pu, ^{241}Am, and ^{243}Am, considered in the burnup credit analysis. Therefore, it is concluded that the potential bias associated with the use of surrogate data in this analysis is minor.

Another consideration in the application of measured data is the decay time of the measurements. Several burnup credit nuclides have time-dependent concentrations due to decay and in-growth from decay precursors. Burnup credit nuclides exhibiting the largest changes include ^{241}Pu, ^{241}Am, ^{147}Sm, ^{151}Eu, and ^{155}Gd (see Sect. 3.1). Note that the measurement laboratories commonly use the decay schemes and nuclide half-lives to analytically adjust the measurement results to a common reference date for convenience. The measurement nuclide concentrations must correspond to the decay time considered for the application model to ensure that representative k_{eff} bias uncertainty values are obtained. For example, an application model involving SNF with a cooling time of 3 days will include relatively low concentrations of ^{241}Am, ^{155}Gd, and ^{151}Eu, as these nuclides are generated predominantly by the decay of parent nuclides after discharge (i.e., ^{241}Pu, ^{155}Eu, and ^{151}Sm, respectively). Therefore, these nuclides will not contribute significantly to the k_{eff} bias uncertainty for this model. However, SNF compositions measured several years after discharge will include larger concentrations of these nuclides than would be present at 3 days. It is important to consider the effect of decay time between the application model and measurement data to ensure that representative k_{eff} bias uncertainty values are obtained (see Sect. A.4).

Measured concentrations for nuclides that vary with the decay time must be adjusted according to analytical decay equations, to account for differences between the time of measurement and a reference time corresponding to the application. Nuclides that vary with time according to their half-lives, such as ^{151}Sm, can be adjusted with only their decay constant. The adjustment of nuclides that are produced by the decay of other nuclides, such as ^{151}Eu, must account for both decay of the nuclide and decay of precursor nuclides; in this case, the production of ^{151}Eu from the decay of ^{151}Sm. For a general case of radionuclide *B* with a decay precursor *A*, e.g., *A* → *B* → *C*, the content of nuclide *B* at the measurement time *t* is:

$$N_B = N_A^0 \frac{\lambda_A}{\lambda_B - \lambda_A}\left(e^{-\lambda_A t} - e^{-\lambda_B t}\right) + N_B^0 e^{-\lambda_B t}, \tag{13}$$

where N_B is the content of nuclide *B* at the measurement time *t*, N_A^0 is the content of precursor nuclide *A* in the discharged fuel composition (i.e., zero time), N_B^0 is the content of nuclide *B* in the discharged fuel composition (i.e., at zero time), and λ_A and λ_B are the decay constants for nuclides *A* and *B*, respectively. In experiments where measurements of a decay precursor are not reported, precluding the adjustment of the measured nuclide concentrations, the calculations should consider the effect on the derived bias and uncertainties of differences between the nuclide concentrations at the time of measurement and the application.

As an illustrative example of the approach, the SNF samples listed in Table 6.3 were applied to an uncertainty analysis for the unpoisoned SFP storage rack model evaluated for a cooling time of 3 days after the fuel was discharged from the reactor. The nuclides ^{241}Am, ^{155}Gd, and ^{151}Eu were excluded from the k_{eff} calculations (measured and calculated nuclide contents) because of their low concentrations at the time of interest. Other nuclides are either stable or exhibit relatively small changes in their concentration between the time of measurement and the time of application (see Sect. 3.1) and therefore do not require corrections.

The k_{eff} values for the application model using the measured nuclide concentrations and the calculated nuclide concentrations as well as the Δk_{eff} values are listed in Table 6.3. Statistical analysis of the Δk_{eff} values for all samples with a burnup less than 45 GWd/MTU was performed with a linear regression model to calculate the fit and the one-sided 95% upper prediction limit (tolerance limit). The analysis was performed with the linear regression model in the OriginPro 8.1 software (copyright OriginLab Corporation). Statistical analysis of the data yields a small burnup-dependent bias (~ 0.002) in k_{eff} and a one-sided tolerance limit (uncertainty) of 0.013 at a 95% probability, 95% confidence level, when burnup is used as the trending parameter (Figure 6.3). The bias and bias uncertainty values estimated from the direct-difference calculations for this single application model are comparable with, but smaller than, the values obtained by the Monte Carlo uncertainty sampling method presented in Sect. 7 (Table 7.2). This comparison provides some limited evidence that the two different methods can produce similar results, thereby providing limited reassurance in the Monte Carlo approach for uncertainty propagation. However, further work with the direct-difference method, including additional comparisons and fully addressing the considerations described below, is needed prior to drawing firm conclusions.

Table 6.3 Unpoisoned PWR SFP storage rack Δk_{eff} obtained with measured and calculated nuclide concentrations

Reactor	Assembly	Sample ID	Enrichment (wt % ^{235}U)	Burnup (GWd/MTU)	k_{eff}^{c} [a]	k_{eff}^{m} [b]	Δk_{eff} [c]
Calvert Cliffs	BT03	NBD107-GG	2.453	37.27	0.8027	0.8178	-0.0150
Calvert Cliffs	BT03	NBD107-MM	2.453	31.40	0.8495	0.8661	-0.0166
Calvert Cliffs	BT03	NBD107-Q	2.453	46.46	0.7574	0.7629	-0.0056
Calvert Cliffs	D047	MKP109-CC	3.038	37.12	0.9207	0.9174	0.0033
Calvert Cliffs	D047	MKP109-LL	3.038	27.35	1.0047	1.0037	0.0010
Calvert Cliffs	D047	MKP109-P	3.038	44.34	0.8782	0.8647	0.0135
Calvert Cliffs	D101	MLA098-BB	2.72	26.62	0.9719	0.9700	0.0019
Calvert Cliffs	D101	MLA098-JJ	2.72	18.68	1.0477	1.0469	0.0008
Calvert Cliffs	D101	MLA098-P	2.72	33.17	0.9227	0.9033	0.0195
H.B. Robinson	B05	N9BN	2.561	23.81	0.9632	0.9638	-0.0006
H.B. Robinson	B05	N9BS	2.561	16.02	1.0465	1.0470	-0.0005
H.B. Robinson	B05	N9CD	2.561	31.66	0.9053	0.8994	0.0059
H.B. Robinson	B05	N9CJ	2.561	28.47	0.9333	0.9569	-0.0236
Obrigheim	BE124	E3P1	3.0	20.18	1.0612	1.0608	0.0004
Obrigheim	BE124	E3P2	3.0	29.35	0.9782	0.9809	-0.0027
Obrigheim	BE124	E3P3	3.0	36.26	0.9341	0.9276	0.0065
Obrigheim	BE124	E3P4	3.0	30.92	0.9794	0.9736	0.0058
Obrigheim	BE124	E3P5	3.0	22.86	1.0451	1.0518	-0.0067
Obrigheim	BE124	G7P1	3.0	17.13	1.1005	1.1050	-0.0045
Obrigheim	BE124	G7P2	3.0	25.83	1.0233	1.0291	-0.0058
Obrigheim	BE124	G7P3	3.0	31.32	0.9872	0.9724	0.0148
Obrigheim	BE124	G7P4	3.0	27.71	1.0193	1.0251	-0.0058
Obrigheim	BE124	G7P5	3.0	25.81	1.0341	1.0294	0.0047
Obrigheim	BE168	-	3.13	29.35	1.0032	1.0124	-0.0092
Obrigheim	BE170	-	3.13	27.01	1.0231	1.0301	-0.0070
Obrigheim	BE171	-	3.13	28.74	1.0087	1.0164	-0.0077
Obrigheim	BE172	-	3.13	27.89	1.0147	1.0160	-0.0013
Obrigheim	BE176	-	3.13	28.78	1.0076	1.0140	-0.0064
Takahama	NT3G23	SF95-2	4.11	24.46	1.1705	1.1596	0.0109
Takahama	NT3G23	SF95-3	4.11	35.68	1.0987	1.0853	0.0134
Takahama	NT3G23	SF95-4	4.11	37.01	1.0824	1.0682	0.0142
Takahama	NT3G23	SF95-5	4.11	30.45	1.1197	1.1087	0.0110
Takahama	NT3G23	SF96-2	2.63	17.43	1.1259	1.1205	0.0054
Takahama	NT3G23	SF96-3	2.63	29.69	1.0301	1.0391	-0.0090
Takahama	NT3G23	SF96-4	2.63	30.41	1.0147	1.0239	-0.0092
Takahama	NT3G23	SF96-5	2.63	25.42	1.0478	1.0515	-0.0037
Takahama	NT3G24	SF97-2	4.11	30.48	1.1161	1.1105	0.0056
Takahama	NT3G24	SF97-3	4.11	42.10	1.0369	1.0301	0.0068
Takahama	NT3G24	SF97-4	4.11	47.07	0.9948	0.9876	0.0072
Takahama	NT3G24	SF97-5	4.11	47.26	0.9839	0.9825	0.0014
Takahama	NT3G24	SF97-6	4.11	40.85	1.0280	1.0170	0.0110
TMI-1	NJ05YU	A1B	4.013	44.80	0.9878	0.9676	0.0202
TMI-1	NJ05YU	A2	4.013	50.60	0.9577	0.9294	0.0283
TMI-1	NJ05YU	B1B	4.013	54.50	0.9353	0.9199	0.0154
TMI-1	NJ05YU	B2	4.013	50.10	0.9644	0.9295	0.0349
TMI-1	NJ05YU	B3J	4.013	53.00	0.9375	0.9149	0.0226
TMI-1	NJ05YU	C1	4.013	50.20	0.9729	0.9430	0.0299
TMI-1	NJ05YU	C2B	4.013	52.60	0.9497	0.9160	0.0337
TMI-1	NJ05YU	C3	4.013	51.30	0.9599	0.9432	0.0167
TMI-1	NJ05YU	D1A2	4.013	55.70	0.9363	0.9446	-0.0083
TMI-1	NJ05YU	D1A4	4.013	50.50	0.9695	0.9551	0.0144
TMI-1	NJ05YU	D2	4.013	44.80	1.0109	0.9639	0.0470
TMI-1	NJ070G	O12S4	4.657	23.54	1.1975	1.1906	0.0069
TMI-1	NJ070G	O12S5	4.657	26.26	1.1824	1.1752	0.0072
TMI-1	NJ070G	O12S6	4.657	24.09	1.1997	1.1996	0.0001
TMI-1	NJ070G	O13S7	4.657	23.21	1.1998	1.1930	0.0068
TMI-1	NJ070G	O13S8	4.657	26.10	1.1837	1.1748	0.0089
TMI-1	NJ070G	O1S1	4.657	25.53	1.1817	1.1729	0.0088
TMI-1	NJ070G	O1S2	4.657	29.92	1.1554	1.1359	0.0195
TMI-1	NJ070G	O1S3	4.657	26.84	1.1798	1.1725	0.0073

Table 6.3 Unpoisoned PWR SFP storage rack k_{eff} obtained with measured and calculated nuclide concentrations (continued)

Reactor	Assembly	Sample ID	Enrichment (wt % ^{235}U)	Burnup (GWd/MTU)	k_{eff}^{c} [a]	k_{eff}^{m} [b]	Δk_{eff} [c]
Trino Vercellese	032	E11P1	3.13	7.24	1.2240	1.2204	0.0036
Trino Vercellese	032	E11P4	3.13	15.38	1.1616	1.1581	0.0035
Trino Vercellese	032	E11P7	3.13	15.90	1.1560	1.1492	0.0068
Trino Vercellese	032	E11P9	3.13	11.53	1.1875	1.1871	0.0004
Trino Vercellese	032	H9P4	3.13	16.56	1.1468	1.1478	-0.0010
Trino Vercellese	032	H9P7	3.13	17.45	1.1393	1.1420	-0.0027
Trino Vercellese	032	H9P9	3.13	12.37	1.1766	1.1744	0.0022
Trino Vercellese	049	J8P1	2.719	8.71	1.1696	1.1654	0.0042
Trino Vercellese	049	J8P4	2.719	14.77	1.1205	1.1094	0.0111
Trino Vercellese	049	J8P7	2.719	15.49	1.1147	1.1115	0.0032
Trino Vercellese	049	J8P9	2.719	11.13	1.1465	1.1427	0.0038
Trino Vercellese	049	L5P1	2.719	14.16	1.1799	1.1826	-0.0027
Trino Vercellese	049	L5P4	2.719	14.49	1.1307	1.1306	0.0001
Trino Vercellese	049	L5P9	2.719	10.18	1.1588	1.1559	0.0029
Trino Vercellese	104	M11P7	3.897	12.04	1.2452	1.2452	0.0000
Trino Vercellese	069	E11P1	3.13	12.86	1.1816	1.1785	0.0031
Trino Vercellese	069	E11P2	3.13	20.60	1.1295	1.1215	0.0080
Trino Vercellese	069	E11P4	3.13	23.72	1.1087	1.0938	0.0149
Trino Vercellese	069	E11P5	3.13	24.52	1.1024	1.0914	0.0110
Trino Vercellese	069	E11P7	3.13	24.30	1.1014	1.0947	0.0067
Trino Vercellese	069	E11P8	3.13	23.41	1.1062	1.0979	0.0083
Trino Vercellese	069	E11P9	3.13	19.25	1.1325	1.1298	0.0027
Trino Vercellese	069	E5P4	3.13	23.87	1.1074	1.1004	0.0070
Trino Vercellese	069	E5P7	3.13	24.68	1.0997	1.0914	0.0083
Trino Vercellese	069	E5P9	3.13	19.21	1.1325	1.1249	0.0076
Trino Vercellese	069	J9P4	3.13	24.85	1.0948	1.0845	0.0103
Trino Vercellese	069	J9P7	3.13	25.26	1.0884	1.0805	0.0079
Trino Vercellese	069	L11P4	3.13	23.93	1.1069	1.1011	0.0058
Trino Vercellese	069	L11P7	3.13	24.36	1.1008	1.0926	0.0082
Trino Vercellese	069	L5P4	3.13	24.33	1.1045	1.1031	0.0014
Trino Vercellese	069	L5P7	3.13	24.31	1.1008	1.1008	0.0000
Turkey Point	D01	G10	2.556	30.51	0.9309	0.9283	0.0026
Turkey Point	D01	G9	2.556	30.72	0.9294	0.9321	-0.0027
Turkey Point	D01	H9	2.556	31.56	0.9215	0.9303	-0.0089
Turkey Point	D04	G10	2.556	31.31	0.9247	0.9254	-0.0007
Turkey Point	D04	G9	2.556	31.26	0.9254	0.9304	-0.0050
GKN-II	419	M11	3.8	54.00	0.9244	0.9076	0.0168
Gösgen	1240	GU1	3.5	60.70	0.8269	0.8098	0.0171
Gösgen	1701	GU3	4.1	53.20	0.9385	0.9533	-0.0148
Gösgen	1701	GU4	4.1	31.10	1.0894	1.0813	0.0081

[a] k_{eff} value obtained with calculated nuclide concentrations.
[b] k_{eff} value obtained with measured nuclide concentrations.
[c] The difference between the k_{eff} values obtained with calculated and measured nuclide concentrations.

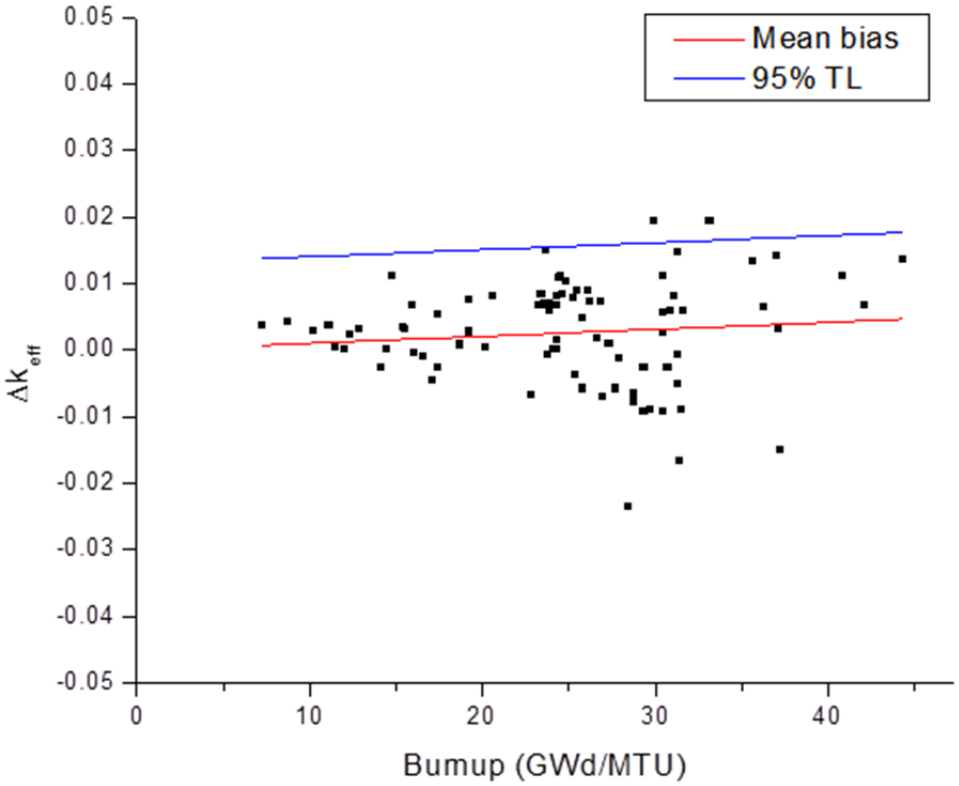

Figure 6.3 Linear regression analysis of the Δk_{eff} results illustrating the bias and the margin for uncertainty represented by the one-sided tolerance limit at a 95% probability, 95% confidence level [95% tolerance limit (TL)] for the unpoisoned SFP storage rack

The following points summarize the main considerations when using the direct-difference analysis approach:

1. The analysis should account for the effect of nuclides not measured in samples either through the use of appropriate surrogate data or some other means to demonstrate that potential bias in code calculations for nuclides without extensive measurements has been taken into account.

2. Surrogate data for nuclides with very few measurements may require additional margins of uncertainty. In cases where extrapolation beyond the range of the measured data is required, the surrogate data should include additional uncertainty associated with the extrapolation to the criticality safety application. The use of sensitivity and uncertainty methods in the analysis of nuclide uncertainty trends provides a means to technically support extrapolating data to the range of the application.

3. Statistical analysis of the Δk_{eff} distribution should consider the similarity between the nuclide concentrations of the measured fuel samples and the nuclide concentration of the application model. For example, uncertainties derived from measured fuel samples with a high burnup (e.g., low k_{eff}) may not be appropriate for an application model using fuel assemblies with low burnup (e.g., k_{eff} = 0.99). Applicability may be established with an appropriately determined trending parameter (e.g., fuel burnup or burnup divided by enrichment).

4. Measured and calculated nuclide concentrations used in the application model should have a consistent decay time. The relative worth of the different nuclides changes as a function of the decay time and must be accounted for to provide an accurate estimate of the k_{eff} bias and bias uncertainty. Adjusting measured nuclide concentrations to the time of application may be performed accurately through use of the nuclide decay half-lives. For nuclides with decay precursors, the production from decay parents must be evaluated or, in cases where a decay precursor was not measured, accounted for with conservative methods.

7. BIAS AND BIAS UNCERTAINTY IN k_{eff} RESULTS

This section presents reference values of estimated bias and bias uncertainty in k_{eff} associated with bias and bias uncertainty in the calculated nuclide concentrations for representative safety analysis models (see Sect. 5). The values presented are specific to SCALE 6.1 and the ENDF/B-VII nuclear data (see Sect. 4). The results were obtained with the Monte Carlo uncertainty sampling method described in Sect. 6.1 and the PWR and BWR isotopic bias and bias uncertainty values presented in Table 6.1 and Table 6.2, respectively. The k_{eff} bias [i.e., the term β_i in Eq. (1)] and k_{eff} bias uncertainty [i.e., the term Δk_i in Eq. (1)] were determined as a function of assembly average burnup. The k_{eff} bias uncertainty values correspond to a 95% probability, 95% confidence level. Depletion validation results for the representative PWR and BWR safety analysis models are presented in Sects. 7.1 and 7.2, respectively. Results based on parametric variations for the representative PWR SFP storage rack model are presented in Sect. 7.3.

7.1 PWR SNF ANALYSIS MODELS

Table 7.1 presents the k_{eff} bias and k_{eff} bias uncertainty values as a function of assembly average burnup for the representative PWR SFP storage rack model (see Sect. 5.2) using either actinide or actinide and fission product nuclides (refer to Table 3.1 for the list of burnup credit nuclides). The k_{eff} bias uncertainty values are illustrated as a function of assembly average burnup in the bar graph shown in Figure 7.1. For the actinide and fission product compositions, the assembly average burnup corresponding to a maximum fuel initial enrichment of 5 wt % ^{235}U was 44.33 GWd/MTU; hence, the graph shows k_{eff} bias uncertainty values for actinide and fission product compositions up to an assembly average burnup of 44.33 GWd/MTU. Table 7.2 presents the k_{eff} bias and k_{eff} bias uncertainty values for the unpoisoned PWR storage rack model (see Sect. 5.2) using actinide and fission product nuclide compositions. The unpoisoned rack model was used to determine k_{eff} bias and bias uncertainty values for assembly average burnup values greater than 44.33 GWd/MTU because this model is more reactive than the representative rack model (e.g., the ^{235}U-to-^{239}Pu atom density ratio values for the reference and the unpoisoned rack models with a 40-GWd/MTU average assembly burnup are 2.37 and 0.90, respectively). The PWR SFP storage rack models include an 18-zone axial burnup profile. Nuclide compositions for PWR SFP storage rack calculations were determined for a 3-day cooling time and for selected assembly average burnup values within the burnup range 5 to 60 GWd/MTU so that the k_{eff} value is 0.99.

Table 7.3 presents the k_{eff} bias and k_{eff} bias uncertainty values as a function of assembly average burnup for the representative PWR SNF cask model (see Sect. 5.3) using either actinide or actinide and fission product nuclide compositions. The k_{eff} bias uncertainty values are illustrated as a function of assembly average burnup in the bar graph shown in Figure 7.2. The cask models include an 18-zone axial burnup profile. Nuclide compositions for cask calculations were determined for a 5-year cooling time and for selected assembly average burnup values within the burnup range 5 to 60 GWd/MTU so that the k_{eff} value is 0.94. For the actinide and fission product compositions, the assembly average burnup corresponding to a maximum fuel initial enrichment of 5 wt % ^{235}U was 45 GWd/MTU; hence, the graph shows k_{eff} bias uncertainty values for actinide and fission product compositions up to an assembly average burnup of 45 GWd/MTU.

The relative importance of the burnup credit nuclides to fuel reactivity is similar for the representative SFP storage rack and SNF cask models, as shown in Figures A.1 and A.2, respectively. The neutronic similarity of the two different nuclear systems leads to similar results for k_{eff} bias and k_{eff} bias uncertainty, as shown in Table 7.1 and Table 7.2. Based on the demonstration of neutronic similarity of the two systems, the k_{eff} bias and bias uncertainty values obtained for the unpoisoned rack model (see Table 7.2) are aplicable to cask configurations using assembly average burnup values within the range 45 to 60 GWd/MTU.

Table 7.1 k_{eff} bias and k_{eff} bias uncertainty for the representative PWR SFP storage rack model

	Actinide nuclides			Actinide and fission product nuclides		
Burnup [a] (GWd/MTU)	Initial wt % ^{235}U [b]	k_{eff} bias [c]	k_{eff} bias uncertainty [d]	Initial wt % ^{235}U [b]	k_{eff} bias [c]	k_{eff} bias uncertainty [d]
5	2.08	0.0043	0.0154	2.28	0.0038	0.0148
10	2.23	0.0040	0.0152	2.49	0.0034	0.0150
18	2.63	0.0050	0.0150	3.12	0.0031	0.0145
25	2.93	0.0050	0.0145	3.55	0.0034	0.0154
30	3.21	0.0052	0.0145	4.00	0.0028	0.0148
40	3.68	0.0064	0.0167	4.70	0.0034	0.0168
44.33	–	–	–	5.00	0.0045	0.0189
50	4.14	0.0083	0.0194	–	–	–
60	4.65	0.0109	0.0251	–	–	–

[a]Assembly average burnup.
[b]Fuel initial enrichment value is so that the k_{eff} value for the assembly average burnup is 0.99.
[c]Positive k_{eff} bias values are typically not credited in criticality safety analyses.
[d]Uncertainty in k_{eff} at a 95% probability, 95% confidence level.

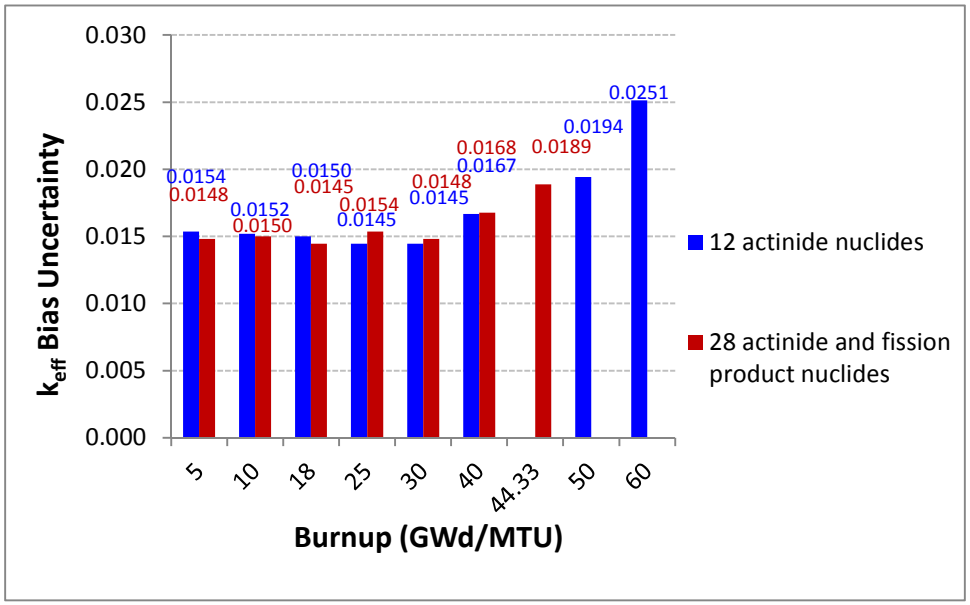

Figure 7.1 k_{eff} bias uncertainty for the representative PWR SFP storage rack model. Uncertainty in k_{eff} is at a 95% probability, 95% confidence level.

Table 7.2 k_{eff} bias and k_{eff} bias uncertainty for the unpoisoned PWR SFP storage rack model using burnup credit actinide and fission product nuclides

Burnup [a] (GWd/MTU)	Initial wt % ^{235}U [b]	k_{eff} bias [c]	k_{eff} bias uncertainty [d]
25	1.95	0.0046	0.0190
40	2.69	0.0034	0.0188
50	3.14	0.0061	0.0219
60	3.62	0.0105	0.0300

[a]Assembly average burnup.
[b]Fuel initial enrichment value is so that the k_{eff} value for the assembly average burnup is 0.99.
[c]Positive k_{eff} bias values are typically not credited in criticality safety analyses.
[d]Uncertainty in k_{eff} at a 95% probability, 95% confidence level.

Table 7.3 k_{eff} bias and k_{eff} bias uncertainty for the representative PWR SNF cask model

	Actinide nuclides			Actinide and fission product nuclides		
Burnup [a] (GWd/MTU)	Initial wt % ^{235}U [b]	k_{eff} bias [c]	k_{eff} bias uncertainty [d]	Initial wt % ^{235}U [b]	k_{eff} bias [c]	k_{eff} bias uncertainty [d]
5	1.90	0.0042	0.0145	2.12	0.0040	0.0150
10	2.05	0.0040	0.0143	2.33	0.0039	0.0148
18	2.48	0.0036	0.0150	3.00	0.0037	0.0157
25	2.78	0.0047	0.0150	3.44	0.0023	0.0154
30	3.10	0.0052	0.0154	3.92	0.0031	0.0161
40	3.58	0.0059	0.0170	4.64	0.0035	0.0163
45	–	–	–	5.00	0.0050	0.0205
50	4.05	0.0073	0.0192	–	–	–
60	4.55	0.0112	0.0260	–	–	–

[a]Assembly average burnup.
[b]Fuel initial enrichment value is so that the k_{eff} value for the assembly average burnup is 0.94.
[c]Positive k_{eff} bias values are typically not credited in criticality safety analyses.
[d]Uncertainty in k_{eff} at a 95% probability, 95% confidence level.

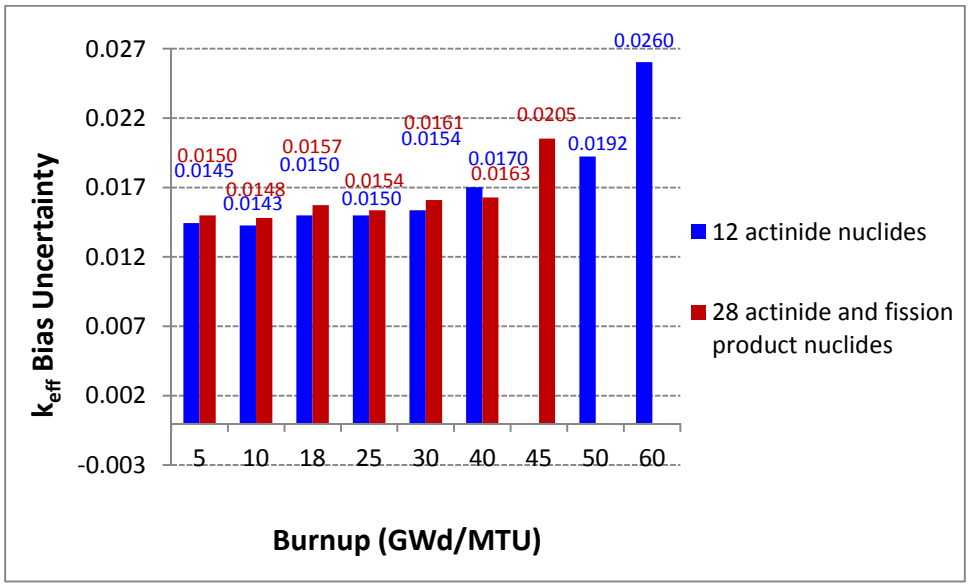

Figure 7.2 k_{eff} bias uncertainty for the PWR SNF cask model. Uncertainty in k_{eff} is at a 95% probability, 95% confidence level.

The calculation results for SCALE 6.1 and the ENDF/B-VII nuclear data indicate:

1. The calculated nuclide concentrations result in a slight overprediction of k_{eff}. The positive bias is significantly smaller than the uncertainty in the bias.
2. The k_{eff} bias uncertainty values for actinide compositions and the k_{eff} bias uncertainty values for actinide and fission product compositions are similar.
3. The k_{eff} bias and k_{eff} bias uncertainty values are fairly constant for the burnup range 5 to 30 GWd/MTU and gradually increase with increasing assembly average burnup values above 30 GWd/MTU.
4. For the representative SFP storage rack model, the values of estimated bias and bias uncertainty in k_{eff} due to biases and bias uncertainties in the calculated concentrations for the 28 burnup credit nuclides are approximately 0.016 and 0.019 for the assembly average burnup range 5 to 40 GWd/MTU and for a 44.33-GWd/MTU assembly average burnup, respectively.
5. For the representative PWR SNF cask model, the values of estimated bias and bias uncertainty in k_{eff} due to biases and bias uncertainties in the calculated concentrations for the 28 burnup credit nuclides are approximately 0.016 and 0.021 for the assembly average burnup range 5 to 40 GWd/MTU and for a 45-GWd/MTU assembly average burnup, respectively.
6. For the unpoisoned PWR SFP storage rack model, the values of estimated bias and bias uncertainty in k_{eff} due to biases and bias uncertainties in the calculated concentrations for the 28 burnup credit nuclides are approximately 0.019, 0.022, and 0.030 for the assembly average burnup range 25 to 40 GWd/MTU, for a 50-GWd/MTU assembly average burnup, and for a 60-GWd/MTU average assembly burnup, respectively. Based on demonstrated neutronic similarity between the fuel cask and storage rack models, these calculation results are also applicable to the cask configurations that use assembly average burnup values up to 60 GWd/MTU.

7.2 BWR SFP STORAGE RACK MODEL

The k_{eff} bias and k_{eff} bias uncertainty values for the BWR SFP storage rack model (see Sect. 5.6) are presented in Table 7.4. The nuclide concentrations in the model correspond to the fuel assembly at peak reactivity achieved at a burnup value of approximately 11 GWd/MTU. The calculated k_{eff} bias values for the actinide-only composition and for the actinide and fission product nuclide composition were 0.001 and 0.002, respectively. Typically, positive k_{eff} bias values are not credited in criticality safety analyses. The calculated k_{eff} bias uncertainty values were 0.029 and 0.032 for the actinide-only composition and for the actinide and fission product nuclide composition, respectively.

The BWR k_{eff} bias uncertainty is significantly larger than the k_{eff} bias uncertainty for PWR burnup credit applications and similar assembly average burnup because of the large variance of the M/C concentration ratio values in the small sample set of available BWR RCA data (see Sect. 3.3). For example, the bias uncertainty values associated with the calculated ^{235}U and ^{239}Pu concentrations are 0.0726 and 0.0561, respectively, based on the BWR fuel samples, and 0.0284 and 0.0453, respectively, based on the PWR fuel samples with burnup from 5 to 15 GWd/MTU. The large bias uncertainty values for the calculated ^{235}U and ^{239}Pu concentrations for BWR SNF are primarily the result of approximate moderator density values used in the depletion calculations for measured fuel samples with unavailable void fraction data.

Table 7.4 k_{eff} bias and k_{eff} bias uncertainty for the BWR SFP storage rack model

Fuel compositions [a]	k_{eff} bias [b]	k_{eff} bias uncertainty [c]
Actinide nuclides	0.0010	0.0287
Actinide and fission product nuclides	0.0017	0.0316

[a]Nuclide concentrations correspond to fuel peak reactivity achieved during irradiation.
[b]Positive k_{eff} bias is typically not credited in criticality safety analyses.
[c]Uncertainty in k_{eff} at a 95% probability, 95% confidence level.

7.3 PARAMETRIC ANALYSIS

An analysis was performed to determine the sensitivity of bias and bias uncertainty in k_{eff} to parameters important to PWR SFP criticality safety analyses, including fuel assembly design, fuel irradiation conditions, rack design, soluble boron concentration, fuel cooling time, axial representation of fuel burnup in the safety analysis model, and nuclear data. The reference case for the parametric analysis is the representative PWR SFP storage rack model loaded with the W 17×17 OFA described in Sect. 5.2. The parametric variations considered in the analysis are summarized in Table 7.5. Note that the reference case was developed with reactor operating parameters that increase fuel discharge reactivity (e.g., higher fuel and moderator temperatures, lower moderator density, and burnable absorber exposure) as described in Sect. 5.1. The SNF compositions used in the analysis include the burnup credit nuclides presented in Table 3.1. The sensitivity of bias and bias uncertainty in k_{eff} was evaluated as a function of assembly average burnup for the burnup values 10, 25, and 40 GWd/MTU.

For the soluble boron concentration cases, the reference case was modified to include the soluble boron concentration values shown in the table. The 1000 ppm soluble concentration case resulted in k_{eff} values much lower than 0.99 (i.e., 0.8425, 0.8617, and 0.8744 for assembly

average burnup values of 10, 25, and 40 GWd/MTU, respectively); the other soluble boron concentration variations resulted in a k_{eff} value of 0.94. For the other parametric variation cases, new nuclide concentrations were determined by STARBUCS (see Sect. 4) to yield a k_{eff} value of 0.99 for the burnup values of 10, 25, and 40 GWd/MTU. For the case using the Babcock and Wilcox (B&W) 15×15 fuel assembly in place of the W 17×17 assembly, conservative depletion parameters with respect to criticality, which are documented in Ref. 61, were used to develop ORGEN-ARP libraries for STARBUCS.

The calculated values for k_{eff} bias and k_{eff} bias uncertainty for the reference case and for the parametric variations considered are presented in Table 7.6 as a function of assembly average burnup. The k_{eff} bias uncertainty values are illustrated in the bar graphs shown in Figure 7.3 (a), (b), and (c) for the assembly average burnup values of 10, 25, and 40 GWd/MTU, respectively.

Table 7.5 Model parameters addressed in the sensitivity analysis

Model parameters	Reference case	Parameter varied [a]
Depletion condition	WABA rods	No WABA rods
Assembly type	W 17×17 OFA	B&W 15×15
Burnup axial representation	18-zone axial profile	Uniform
Cooling time	3 days	5 years 20 years 40 years
^{10}B areal density of the Boral panels	0.020 g/cm^2	0.022 g/cm^2 (10% increase from the reference value) 0.018 g/cm^2 (10% decrease from the reference value) 0 g/cm^2
Pitch size of rack cell	9.110 in. (23.1394 cm)	Reference value + 0.5 in. (1.27 cm)
Soluble boron concentration in pool water	0 ppm	1000 ppm (10, 25, and 40 GWd/MTU assembly burnup) Soluble boron concentrations yielding a target k_{eff} value of 0.94 (303, 348, and 393 ppm for assembly average burnup values of 10, 25, and 40 GWd/MTU, respectively)
Cross-section data	ENDF/B-VII, 238 energy groups	ENDF/B-V, 44 energy groups

[a]An individual calculation was performed for each parameter.

All the evaluated cases using the ENDF/B-VII nuclear data produced similar positive k_{eff} bias values. The average k_{eff} bias was approximately 0.0035, and the associated standard deviation was approximately 0.0007 (see Table 7.6), regardless of the assembly average burnup value. Positive k_{eff} bias is typically not credited in criticality safety analyses. The k_{eff} bias values in the case of the ENDF/B-V nuclear data were negative and varied with assembly average burnup from -0.0001 (10 GWd/MTU) to -0.0040 (40 GWd/MTU). Therefore, there are significant differences between the k_{eff} bias values based on the ENDF/B-VII and on the ENDF/B-V nuclear cross-section data libraries. As demonstrated in Sect. A.3 for the reference SFP storage rack model using a 40-GWd/MTU assembly average burnup, the nuclides with significantly different effects on k_{eff} bias between the ENDF/B-VII and ENDF/B-V nuclear data are ^{235}U, ^{239}Pu, ^{149}Sm, and ^{151}Sm. The calculated ^{235}U and ^{239}Pu concentrations for that application model using either

the ENDF/B-V or the ENDF/B-VII nuclear data result in an overprediction of k_{eff}. However, the k_{eff} overprediction based on the ENDF/B-VII nuclear data is larger. The calculated ^{149}Sm and ^{151}Sm concentrations based on the ENDF/B-V nuclear data result in an underprediction of k_{eff}; the calculated ^{149}Sm and ^{151}Sm concentrations based on the ENDF/B-VII nuclear data have a negligible effect on the k_{eff} bias. Therefore, the net k_{eff} bias resulting from the biases in the calculated concentrations for these nuclides varies depending on the nuclear data.

Overall, the k_{eff} bias uncertainty values exhibit a small variability as a function of sensitivity parameter and assembly average burnup throughout the burnup range 10 to 40 GWd/MTU. Based on the ENDF/B-VII calculations, the average values of k_{eff} bias uncertainty are 0.0152, 0.0160, and 0.0171 for the assembly average burnup values of 10, 25, and 40 GWd/MTU, respectively. The largest variations from the reference case were obtained for the unpoisoned (i.e., 0-g/cm^2 ^{10}B areal density in the Boral panels) PWR SFP analysis model.

Table 7.6 k_{eff} bias and k_{eff} bias uncertainty as a function of sensitivity parameter

Assembly burnup (GWd/MTU)	10		25		40 [c]	
Sensitivity parameter	k_{eff} bias [a]	k_{eff} bias uncertainty [b]	k_{eff} bias [a]	k_{eff} bias uncertainty [b]	k_{eff} bias [a]	k_{eff} bias uncertainty [b]
Reference	0.0034	0.0150	0.0034	0.0154	0.0034	0.0168
W 17×17: depletion w/o WABA	0.0043	0.0146	0.0028	0.0159	0.0027	0.0178
B&W 15×15	0.0037	0.0135	0.0028	0.0143	0.0031	0.0168
Axially uniform burnup	0.0029	0.0154	0.0029	0.0168	0.0022	0.0170
Cooling time: 5 years	0.0033	0.0152	0.0035	0.0152	0.0040	0.0167
Cooling time: 20 years	0.0043	0.0148	0.0034	0.0168	0.0032	0.0165
Cooling time: 40 years	0.0046	0.0152	0.0038	0.0161	0.0035	0.0174
^{10}B loading: +10%	0.0036	0.0159	0.0031	0.0161	0.0031	0.0170
^{10}B loading: -10%	0.0034	0.0154	0.0031	0.0150	0.0036	0.0168
^{10}B loading: 0% [d]	0.0030	0.0196	0.0046	0.0190	0.0053	0.0188
Rack cell pitch: +0.5 in.	0.0032	0.0139	0.0027	0.0148	0.0030	0.0168
Soluble boron: 1000 ppm	0.0042	0.0148	0.0042	0.0167	0.0044	0.0181
Soluble boron: 303, 348, 393 ppm	0.0041	0.0148	0.0035	0.0154	0.0036	0.0161
Average value [e]	0.0037	0.0152	0.0034	0.0160	0.0035	0.0171
Standard deviation [e]	0.0006	0.0014	0.0006	0.0012	0.0008	0.0007
Maximum value [e]	0.0046	0.0196	0.0046	0.0190	0.0053	0.0188
Minimum value [e]	0.0029	0.0135	0.0027	0.0143	0.0022	0.0161
ENDF/B-V [f]	-0.0001	0.0135	-0.0029	0.0139	-0.0040	0.0165

[a]Positive k_{eff} bias values are typically not credited in criticality safety analyses.
[b]k_{eff} bias uncertainty at a 95% probability, 95% confidence level.
[c]The burnup values corresponding to the 5 wt % ^{235}U initial enrichment limit were 39, 35, 33, 38, and 39.8 GWd/MTU for the 5-, 20-, and 40-year decay time, cell pitch, and uniform burnup profile cases, respectively.
[d]The initial enrichment for this case and a 10-GWd/MTU assembly average burnup was 1.34 wt % ^{235}U, which is an atypical fuel enrichment (see Figure 5.3).
[e]Bias and bias uncertainty values based on the results of all calculations using the ENDF/B-VII nuclear data.
[f]The values of bias and bias uncertainty in k_{eff} [(i.e., $\beta_i + \Delta k_i$ in Eq. (1)] are 0.0136, 0.0168, and 0.0205 for the assembly average burnup values of 10, 25, and 40 GWd/MTU, respectively.

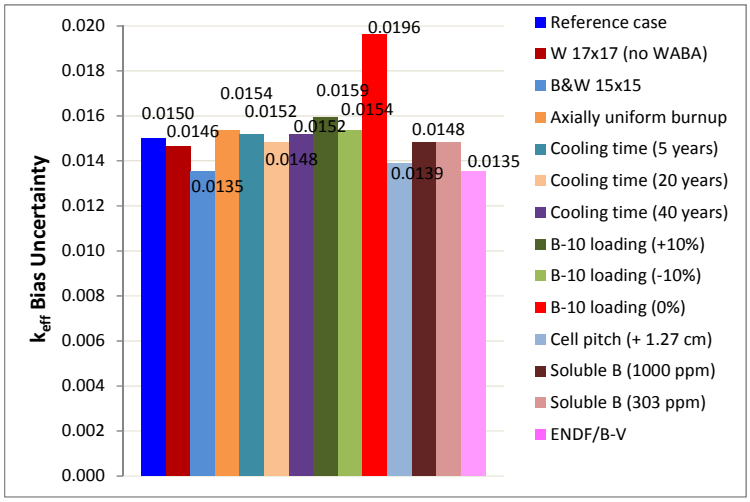

(a)

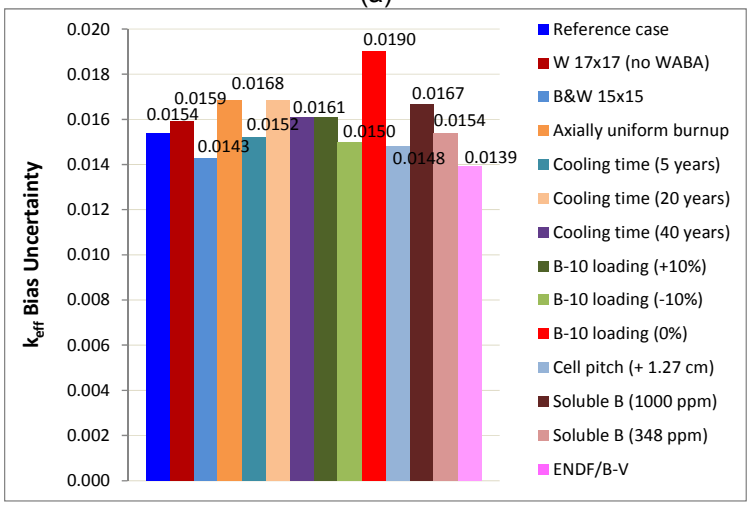

(b)

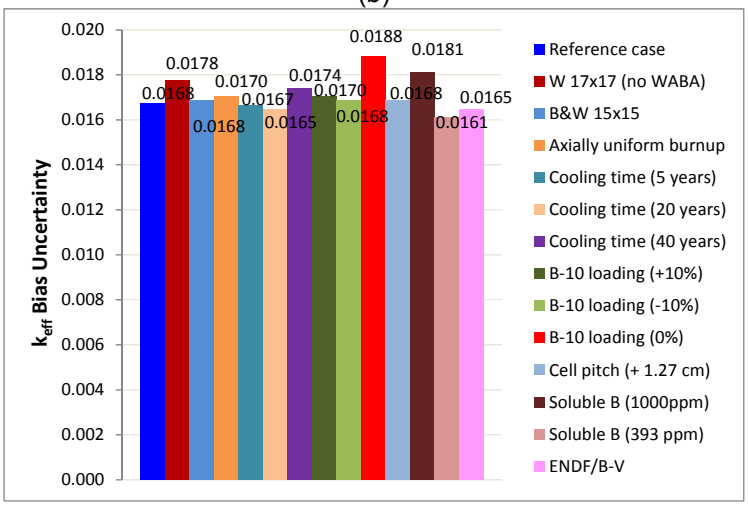

(c)

Figure 7.3 Variation of bias uncertainty in k_{eff} with parameters important to criticality analyses for (a) 10-, (b) 25-, and (c) 40-GWd/MTU assembly average burnup. Uncertainty in k_{eff} is at a 95% probability, 95% confidence level.

8. CONCLUSIONS

This report describes an approach for establishing depletion code bias and bias uncertainty in terms of a reactivity difference (i.e., Δk_{eff}) for burnup credit criticality safety analyses. The depletion validation approach is demonstrated with the SCALE 6.1 code system and the 238-group ENDF/B-VII cross-section library for representative SNF storage pool and cask configurations/conditions. A total of 28 actinide and fission product nuclides are considered in the fuel compositions. Depletion validation results are provided for PWR fuel assembly average burnup values up to 60 GWd/MTU and for a BWR fuel assembly at peak reactivity.

The validation approach described in this report is independent of the depletion and criticality computational methods being used and of the choice of the safety analysis models. The main characteristics of the depletion validation approach are as follows: (1) calculated nuclide concentrations are compared to available measurements of nuclide concentrations from destructive radiochemical assay to determine isotopic biases and bias uncertainties in the calculated nuclide concentrations, and (2) the isotopic biases and bias uncertainties are applied to the fuel compositions of representative safety analysis models to determine reference values for bias and bias uncertainty in k_{eff} by the use of the Monte Carlo uncertainty sampling method. The Monte Carlo uncertainty sampling method represents the effects of nuclide concentration uncertainty on k_{eff} values by sampling isotopic concentrations from uncertainty distributions developed from experimental data. The direct-difference method was used in a limited manner to provide a check of the validation results obtained from the Monte Carlo uncertainty sampling method. The direct-difference method applies measured nuclide concentrations directly in the safety analysis model to calculate a k_{eff} value, which then is compared with the k_{eff} value for the safety analysis model with calculated nuclide concentrations.

The validation results for the PWR safety analysis models obtained with SCALE 6.1 and the ENDF/B-VII nuclear data indicate that:

1. The calculated nuclide concentrations result in a slight overprediction of k_{eff}. The positive bias, which typically is not credited in criticality safety analyses, is significantly smaller than the uncertainty in the bias.
2. The k_{eff} bias and k_{eff} bias uncertainty values are fairly constant for the burnup range 5 to 40 GWd/MTU and gradually increase with increasing assembly average burnup values above 40 GWd/MTU.
3. For a representative SFP storage rack model, the values of estimated bias and bias uncertainty in k_{eff} due to biases and bias uncertainties in the calculated nuclide concentrations are approximately 0.016 and 0.019 for the assembly average burnup range 5 to 40 GWd/MTU and for a 44.33-GWd/MTU assembly average burnup, respectively.
4. Parametric variations from the representative SFP storage rack model have a relatively small impact on bias and bias uncertainty in k_{eff} for the burnup range 10 to 40 GWd/MTU. The estimated average value for k_{eff} bias is approximately 0.004 for this burnup range; the estimated average values for k_{eff} bias uncertainty are 0.015, 0.016, and 0.017 for the assembly average burnup values of 10, 25, and 40 GWd/MTU, respectively. The largest

k_{eff} bias uncertainty value was obtained for the unpoisoned SFP storage rack model (i.e., 0-g/cm^2 ^{10}B areal density in the Boral panels).

5. For the unpoisoned SFP storage rack model, the values of estimated bias and bias uncertainty in k_{eff} due to biases and bias uncertainties in the calculated nuclide concentrations are approximately 0.019, 0.022, and 0.030 for the assembly average burnup range 25 to 40 GWd/MTU, for a 50-GWd/MTU assembly average burnup, and for a 60-GWd/MTU average assembly burnup, respectively.
6. For a representative SNF cask model, the values of estimated bias and bias uncertainty in k_{eff} due to biases and bias uncertainties in the calculated nuclide concentrations are approximately 0.016 and 0.021 for the assembly average burnup range 5 to 40 GWd/MTU and for a 45-GWd/MTU assembly average burnup, respectively.
7. The uncertainties in the calculated ^{235}U and ^{239}Pu concentrations contribute approximately 90% to 95% of the k_{eff} bias uncertainty.
8. The k_{eff} bias uncertainty due to the depletion uncertainties in the calculated fission product concentrations is small (<3% of the k_{eff} bias uncertainty).

Bias and bias uncertainty in k_{eff} for the representative SFP storage rack model using 10-, 25-, and 40-GWd/MTU assembly average burnup values was also calculated with the SCALE 44-group library based on the ENDF/B-V nuclear data. The k_{eff} bias values obtained with the ENDF/B-V nuclear data are negative and vary with assembly average burnup from -0.0001 (10 GWd/MTU) to -0.004 (40 GWd/MTU). These values differ significantly from the k_{eff} bias value (~ 0.004) obtained with the ENDF/B-VII nuclear data primarily because different biases in the calculated ^{235}U, ^{239}Pu, ^{149}Sm, and ^{151}Sm concentrations were obtained from use of the two nuclear data libraries. The k_{eff} bias uncertainty values obtained with the ENDF/B-V nuclear data are approximately 0.014, 0.014, and 0.017 for the 10-, 25-, and 40-GWd/MTU assembly average burnup values, respectively, which are similar to the k_{eff} bias uncertainty values obtained with the ENDF/B-VII nuclear data.

The calculated k_{eff} bias and k_{eff} bias uncertainty values for BWR SNF are approximately 0.002 and 0.032, respectively. The BWR depletion validation was conducted for an assembly at peak reactivity with available RCA data for 32 BWR fuel samples obtained from discharged fuel of relatively old fuel designs and higher burnup. As additional RCA data for BWR SNF becomes available in the future, depletion code validations for BWR SNF should be performed to verify the validity of the k_{eff} bias and k_{eff} bias uncertainty values developed in this depletion validation study.

The bias and bias uncertainty values estimated from the direct-difference method for a single application model are comparable with, but smaller than, the values obtained by the Monte Carlo uncertainty sampling method. Although not definitive, the comparison provides increased confidence in the Monte Carlo approach for uncertainty propagation. For depletion code validations using the direct-difference method, recommendations are provided concerning use of surrogate (i.e., substitute) data for nuclides with very few measurement data and appropriate decay-time adjustments for measured nuclide concentrations.

9. REFERENCES

1. "Spent Fuel Project Office Interim Staff Guidance – 8, Rev. 2 – Burnup Credit in the Criticality Safety Analyses of PWR Spent Fuel in Transport and Storage Casks," U.S. Nuclear Regulatory Commission, September 27, 2002.

2. Memorandum from L. Kopp to T. Collins, "Guidance on the Regulatory Requirements for Criticality Analysis of Fuel Storage at Light-Water Reactor Power Plants," U.S. Nuclear Regulatory Commission, August 19, 1998.

3. J. M. Scaglione, D. E. Mueller, J. C. Wagner, and W. J. Marshall, *An Approach for Validating Actinide and Fission Product Burnup Credit Criticality Safety Analyses – Criticality (k_{eff}) Predictions*, NUREG/CR-7109 (ORNL/TM-2011/514), prepared for the U.S. Nuclear Regulatory Commission by Oak Ridge National Laboratory, Oak Ridge, Tennessee (2012).

4. I. C. Gauld, *Strategies for Application of Isotopic Uncertainties in Burnup Credit*, NUREG/CR-6811 (ORNL/TM-2001/257), prepared for the U.S. Nuclear Regulatory Commission by Oak Ridge National Laboratory, Oak Ridge, Tennessee (2003).

5. *Scale 6.1: A Comprehensive Modeling and Simulation Suite for Nuclear Safety Analysis and Design*. Available from Radiation Safety Information Computational Center at Oak Ridge National Laboratory as CCC-785.

6. M. B. Chadwick et al., "ENDF/B-VII.0: Next Generation Evaluated Nuclear Data Library for Nuclear Science and Technology," *Nucl. Data Sheets* **107**, 2931 (2006).

7. *Code of Federal Regulations*, Title 10, "Energy" (2011).

8. *Burnup Credit for LWR Fuel*, ANSI/ANS-8.27-2008, American Nuclear Society, La Grange Park, IL (2008).

9. NUREG/CR-6698, *Guide for Validation of Nuclear Criticality Safety Calculational Methodology*, U.S. Nuclear Regulatory Commission, Washington DC (2001).

10. *Workshop Proceedings – The Need for Post Irradiation Experiments to Validate Depletion Calculation Methodologies*, Prague, Czech Republic, May 11–12, 2006, Nuclear Energy Agency (2007) (NEA/NSC/DOC(2006)31).

11. *Advances in Applications of Burnup Credit to Enhance Spent Fuel Transportation, Storage, Reprocessing and Disposition*, Proceedings of a Technical Meeting held in London, August 29 – September 2, 2005, International Atomic Energy Agency (2007) (IAEA-TECDOC-1547).

12. Y. Rugama et al., Fuel Cycle Associated Activities of the OECD/NEA/NSC Working Party on Nuclear Criticality Safety, GLOBAL 2009, "The Nuclear Fuel Cycle: Sustainable Options & Industrial Perspectives," September 6–11, 2009, Paris, France.

13. *Spent Nuclear Fuel Assay Data for Isotopic Validation*, NEA/NSC/WPNCS/DOC(2011)5, Nuclear Energy Agency, Organisation for Economic Co-operation and Development (2011).

14. U. Hesse, *Verification of the OREST (HAMMER-ORIGEN) Depletion Program System Using Post-Irradiation Analyses of Fuel Assemblies 168, 170, 171, and 176 from the Obrigheim Reactor*, ORNL-TR-88/20 (GRS-A-962) Oak Ridge National Laboratory, Oak Ridge, Tennessee (1984).

15. G. Ilas, I. C. Gauld, and B. D. Murphy, *Analysis of Experimental Data for High Burnup PWR Spent Fuel Isotopic Validation—ARIANE and REBUS Programs (UO_2 Fuel)*, NUREG/CR-6969 (ORNL/TM-2008/072), prepared for the U.S. Nuclear Regulatory Commission by Oak Ridge National Laboratory, Oak Ridge, Tennessee (2010).

16. G. Ilas, I. C. Gauld, F. C. Difilippo, and M. B. Emmett, *Analysis of Experimental Data for High Burnup PWR Spent Fuel Isotopic Validation—Calvert Cliffs, Takahama, and Three Mile Island Reactors*, NUREG/CR-6968 (ORNL/TM-2008/071), prepared for the U.S. Nuclear Regulatory Commission by Oak Ridge National Laboratory, Oak Ridge, Tennessee (2010).

17. *ARIANE International Programme—Final Report*, ORNL/SUB/97-XSV750-1, Oak Ridge National Laboratory, Oak Ridge, Tennessee (2003).

18. D. Boulanger et al., "High Burnup PWR and BWR MOX Fuel Performance: A Review of BELGONUCLEAIRE Recent Experimental Programs," ANS International Meeting on LWR Fuel Performance, Orlando, FL, USA, September 19–22, 2004.

19. J. M. Alonso et al., "Spanish R&D Program on Spent Fuel Dry Storage," *Trans. International Meeting on LWR Fuel Performance, Top Fuel 2006*, Salamanca, Spain, October 22–26, 2006.

20. G. Radulescu, I. C. Gauld, and G. Ilas, *SCALE 5.1 Predictions of PWR Spent Nuclear Fuel Isotopic Compositions*, ORNL/TM-2010/44, Oak Ridge National Laboratory, Oak Ridge, Tennessee (2010).

21. U. Mertyurek, M. W. Francis, and I. C. Gauld, *SCALE 5 Analysis of BWR Spent Nuclear Fuel Isotopic Compositions for Safety Studies*, ORNL/TM-2010/286, Oak Ridge National Laboratory, Oak Ridge, Tennessee (2010).

22. J. C. Wagner and C. V. Parks, *Recommendations on the Credit for Cooling Time in PWR Burnup Credit Analyses*, NUREG/CR-6781 (ORNL/TM-2001/272), prepared for the U. S. Nuclear Regulatory Commission by Oak Ridge National Laboratory, Oak Ridge, Tennessee (2003).

23. M. D. DeHart, *Sensitivity and Parametric Evaluations of Significant Aspects of Burnup Credit for PWR Spent Fuel Packages*, ORNL/TM-12973, Oak Ridge National Laboratory, Oak Ridge, Tennessee (1996).

24. C. V. Parks, M. D. DeHart, and J. C. Wagner, *Review and Prioritization of Technical Issues Related to Burnup Credit for LWR Fuel*, NUREG/CR-6665 (ORNL/TM-1999/303), Oak Ridge National Laboratory, Oak Ridge, Tennessee (2000).

25. *Disposal Criticality Analysis Methodology Topical Report,* YMP/TR-004Q, Rev. 02, Yucca Mountain Site Characterization Project, Las Vegas, Nevada (2003).

26. C. Riffard, A. Santamarina, and J.-F. Thro, "Correction Factors Applied to Isotopic Concentrations in Burnup Credit Implementation of PWR LEU Applications with the Recent JEFF 3.1.1/SHEM Library," *Proceedings to International Conference on Nuclear Criticality (ICNC) 2011*, September 19–22, Edinburgh, United Kingdom (2011).

27. "Obrigheim," sections in *Nuclear Power Experience, Plant Description, and Histories*, Vol. PWR-1, pp. 1–10, Aug 1974, p. 1, Dec 1983, and p. 2, June 1985.

28. Y. Nakahara, Y. Suyama, and T. Suzaki, *Technical Development on Burnup Credit for Spent LWR Fuels*, JAERI-Tech 2000-071 (ORNL/TR-2001/01), English Translation, Oak Ridge National Laboratory, Oak Ridge, Tennessee (2002).

29. *Standard Review Plan for Spent Fuel Dry Cask Storage Systems at a General License Facility*, NUREG-1536, Revision 1, U.S. Nuclear Regulatory Commission, Washington, DC (2010).

30. S. M. Bowman, "SCALE 6: Comprehensive Nuclear Safety Analysis Code System," *Nucl. Technol*. **174**, 126 (2011).

31. A. C. Kahler and R. E. MacFarlane, ENDF/B-VII Data Testing with ICSBEP Benchmarks, *Proceedings of the International Conference on Nuclear Data for Science and Technology 2007*, Nice, France, April 22–27, 2007, Commissariat à l'Énergie Atomique, OECD Nuclear Energy Agency (2007).

32. J.-Ch. Sublet, JEFF-3.1, ENDF/B-VII and JENDL-3.3 Criticality Assemblies Benchmarking with the Monte Carlo Code TRIPOLI, *IEEE Trans. Nucl. Sci.* **55**(1), 604 (2008).

33. M. L. Williams and G. Ilas, ENDF/B-VII Nuclear Data Libraries for SCALE 6, *Advances in Nuclear Fuel Management IV (ANFM 2009),* Hilton Head Island, South Carolina, USA, April 12–15, 2009, on CD-ROM, American Nuclear Society, LaGrange Park, IL (2009).

34. M. L. Williams, "Resonance Self-Shielding Methodologies in SCALE 6," *Nucl. Technol*. **174**, 149 (2011).

35. S. Goluoglu et al., "Monte Carlo Criticality Methods and Analysis Capabilities in SCALE," *Nucl. Technol*. **174**, 214 (2011).

36. M. D. DeHart and S. M. Bowman, "Reactor Physics Methods and Analysis Capabilities in SCALE," *Nucl. Technol*. **174**, 196 (2011).

37. I. C. Gauld et al., "Isotopic Depletion and Decay Methods and Analysis Capabilities in SCALE," *Nucl. Technol*. **174**, 169 (2011).

38. G. Radulescu and I. C. Gauld, “Enhancements to the Burnup Credit Criticality Safety Analysis Sequence in SCALE,” *Proc. Topl. Mtg. Nuclear Criticality Safety Division: Realism, Robustness and the Nuclear Renaissance (NCSD 2009)*, Richland, Washington, September 13–17, 2009, American Nuclear Society (2009).

39. B. T. Rearden et al., “Sensitivity and Uncertainty Analysis Capabilities and Data in SCALE,” *Nucl. Technol*. **174**, 236 (2011).

40. J. C. Wagner and C. V. Parks, *Parametric Study of the Effect of Burnable Poison Rods for PWR Burnup Credit*, NUREG/CR-6761 (ORNL/TM-2000/373), prepared for the U.S. Nuclear Regulatory Commission by Oak Ridge National Laboratory, Oak Ridge, Tennessee (2002).

41. *Topical Report on Actinide-Only Burnup Credit for PWR Spent Nuclear Fuel Packages*, DOE/RW-0472, Rev. 2, U.S. Department of Energy (1998).

42. J. C. Wagner, M. D. DeHart, and C. V. Parks, *Recommendations for Addressing Axial Burnup in PWR Burnup Credit Analyses*, NUREG/CR-6801 (ORNL/TM-2001/273), prepared for the U.S. Nuclear Regulatory Commission by Oak Ridge National Laboratory, Oak Ridge, Tennessee (2003).

43. J. C. Wagner, *Computational Benchmark for Estimation of Reactivity Margin from Fission Products and Minor Actinides in PWR Burnup Credit*, NUREG/CR-6747 (ORNL/TM-2000/306), U.S. Nuclear Regulatory Commission, Oak Ridge National Laboratory, Oak Ridge, Tennessee (2001).

44. *Standard Review Plan for Transportation Packages for Spent Nuclear Fuel*, NUREG-1617, U.S. Nuclear Regulatory Commission, Washington, DC (2000).

45. *Standard Review Plan for Spent Fuel Dry Storage Facilities*, NUREG-1567, U.S. Nuclear Regulatory Commission, Washington, DC (2000).

46. *RW-859 Nuclear Fuel Data*, Energy Information Administration, Washington, DC (2004).

47. S. Cummings and S. Turner, “Design of Wet Storage Racks for Spent BWR Fuel,” *Proc. ANS Embedded Topical Meeting on Practical Implementation of Nuclear Criticality Safety* (p. 35608.pdf), Reno, Nevada, November 11–15, 2001, American Nuclear Society (2001).

48. M. D. DeHart, *A Stochastic Method for Estimating the Effect of Isotopic Uncertainties in Spent Nuclear Fuel*, ORNL/TM-2001/83, Oak Ridge National Laboratory, Oak Ridge, Tennessee (2001).

49. I. M. Sobol, *A Primer for the Monte Carlo Method*, CRC Press LLC, Boca Raton, Florida (1994).

50. *PREP/SPOP: Uncertainty and Sensitivity Analysis Mote Carlo Program and Input Preparation*, Available from Radiation Safety Information Computational Center at Oak Ridge National Laboratory as C00772.

51. M. Klein et al., “Influence of Nuclear Data Covariance on Reactor Core Calculations,” *Proceedings of the International Conference on Mathematics and Computational Methods Applied to Nuclear Science and Engineering (M&C 2011)*, Rio de Janeiro, RJ, Brazil, May 8–12, 2011, American Nuclear Society (2011).

52. W. A. Shewhart, *Economic Control of Quality of Manufactured Product*, D. Van Nostrand Company, New York (1931).

53. NIST/SEMATECH e-Handbook of Statistical Methods, available from http://www.itl.nist.gov/div898/handbook/, April 2010.

54. R. E. Odeh and D. B. Owen, *Tables for Normal Tolerance Limits, Sampling Plans, and Screening*, Marcel Dekker, Inc., New York and Basel (1980).

55. D. Sciff and R. B. D’Agostino, *Practical Engineering Statistics,* John Wiley & Sons, Inc., New York, New York (1996).

56. S. S. Shapiro and M. B. Wilk, “An analysis of variance test for normality,” *Biometrika* **52**, 591–611 (1965).

57. J. C. Neuber and A. Hoefer, “Data Evaluation Methods for Estimating the Variability in k_{eff} of a Nuclear Fuel System Due to the Variability of Parameters Characterizing the System,” *Proceedings of the 8th International Conference on Nuclear Criticality Safety (ICNC 2007)*, May 28–June 1, 2007, St. Petersburg, Russia (2007).

58. J. C. Neuber and A. Hoefer, “Statistical Evaluation of the Isotopic Bias in Burn-up Credit Criticality Analysis of Spent Nuclear Fuel Systems,” *Proceedings of the 8th International Conference on Nuclear Criticality Safety (ICNC 2007)*, May 28–June 1, 2007, St. Petersburg, Russia (2007).

59. G. Marsaglia and W. W. Tsang, “A Fast, Easily Implemented Method for Sampling from Decreasing or Symmetric Unimodal Density Functions,” *Siam J. Sci. Stat. Comput*. **5**, 349–359, June 1984.

60. I. C. Gauld and D. E. Mueller, *Evaluation of Cross-Section Sensitivities in Computing Burnup Credit Fission Product Concentrations*, ORNL/TM-2005/48, Oak Ridge National Laboratory, Oak Ridge, Tennessee (2005).

61. *Isotopic Generation and Confirmation of the PWR Application Model,* CAL-DSU-NU-000004 REV 00A, Bechtel SAIC Company, Las Vegas, Nevada (2003).

APPENDIX A. k_{eff} UNCERTAINTY ANALYSIS USING CROSS-SECTION SENSITIVITY/UNCERTAINTY ANALYSES

Sensitivity/uncertainty analysis is used to determine contributions made by individual nuclide concentration uncertainties to bias and bias uncertainty in k_{eff}. The cross-section sensitivity/uncertainty analysis uses first-order linear perturbation approximations to determine the effects of small perturbations (uncertainties) in nuclide concentrations on k_{eff}.

A sensitivity coefficient, defined as shown in Eq. (A-1) (Ref. 39), is a measure of the first-order effect of perturbations in the macroscopic cross section Σ_{tot}^{n} of a nuclide n upon k_{eff},

$$S_n = \frac{\delta k_{eff} / k_{eff}}{\delta \Sigma_{tot}^{n} / \Sigma_{tot}^{n}}. \tag{A-1}$$

Sensitivity coefficients specific to a nuclear system may be used to establish the relative importance of individual nuclides to fuel reactivity for that system. Uncertainties in calculated nuclide concentrations can be propagated to k_{eff} values through the use of sensitivity coefficients (Ref. 39). Equations (A-2) through (A-5) for k_{eff} bias and bias uncertainty calculations were derived from first-order (linear) approximation,

$$\Delta k_{eff_n} = k_{eff} \times S_n \times (1 - X_n^j), \tag{A-2}$$

$$\Delta k_{eff} = k_{eff} \times \sum_{n=1}^{N} S_n \times (1 - X_n^j), \tag{A-3}$$

$$k_{eff} \text{ bias} = k_{eff} \times \sum_{n=1}^{N} S_n \times (1 - \overline{X}_n), \tag{A-4}$$

$$k_{eff} \text{ bias uncertainty} = k_{eff} \times \sqrt{\sum_{n=1}^{N} \left(S_n \times \frac{\sigma_n}{\overline{X}_n} \right)^2}. \tag{A-5}$$

where

Δk_{eff_n}	=	k_{eff} bias due to the bias in the calculated nuclide concentration for nuclide n based on measurement data for fuel sample j;
k_{eff}	=	k_{eff} value using predicted nuclide concentrations;
S_n	=	sensitivity coefficient (see Eq. (A-1);
X_n^j	=	measured-to-calculated concentration ratio for nuclide n and fuel sample j;
Δk_{eff}	=	k_{eff} bias due to biases in the calculated nuclide concentrations based on measurement data for fuel sample j;
N	=	the number of burnup credit nuclides in fuel compositions (28 in this validation study);
$\overline{X}_n$	=	isotopic bias [see Eq. (3)];
σ_n	=	isotopic bias uncertainty [see Eq. (5)];
k_{eff} bias	=	k_{eff} bias due to biases in the calculated nuclide concentrations;
k_{eff} bias uncertainty	=	one-sigma k_{eff} bias uncertainty due to bias uncertainties in the calculated nuclide concentrations.

Eqs. (A-2) through (A-4) show that k_{eff} bias is a function of the sensitivity coefficients and biases in calculated nuclide concentrations; Eq. (A-5) shows that k_{eff} bias uncertainty is a function of

the square of the sensitivity coefficients and of the square of the uncertainties in calculated nuclide concentrations. Equations (A-1) through (A-5) were used to perform various analyses as described in Sections A.1 through A.4. Section A.1 illustrates the relative importance of individual burnup credit nuclides to fuel reactivity for the analysis models using sensitivity coefficients [see Eq. (A-1)], which were calculated with the TSUNAMI-3D sequence (see Sect. 4). Section A.2 presents an analysis in support of the data normality assumption used in the Monte Carlo uncertainty sampling method implementation (see Sect. 6.1). Individual nuclide contributions to k_{eff} bias and bias uncertainty for the representative analysis models are shown in Sect. A.3. An analysis illustrating the importance of decay time corrections for direct-difference calculations is presented in Sect. A.4.

A.1 Relative Importance of Individual Nuclides to Fuel Reactivity

The relative importance of the burnup credit nuclides to fuel reactivity for the representative PWR SFP storage rack and SNF cask analysis models is illustrated on a logarithmic scale in Figures A.1 and A.2, respectively, which use the absolute values of sensitivity coefficients [see Eq. (A-1)]. The absolute values of the sensitivity coefficients are shown for the 10- and 40-GWd/MTU assembly average burnup values. The nuclides are shown in order of decreasing nuclide importance to fuel reactivity for the 40-GWd/MTU burnup value. Sensitivity coefficients, which are illustrated in this section, were used to evaluate the contributions of individual nuclides to k_{eff} bias and bias uncertainty (see Sects. A.2 through A.4).

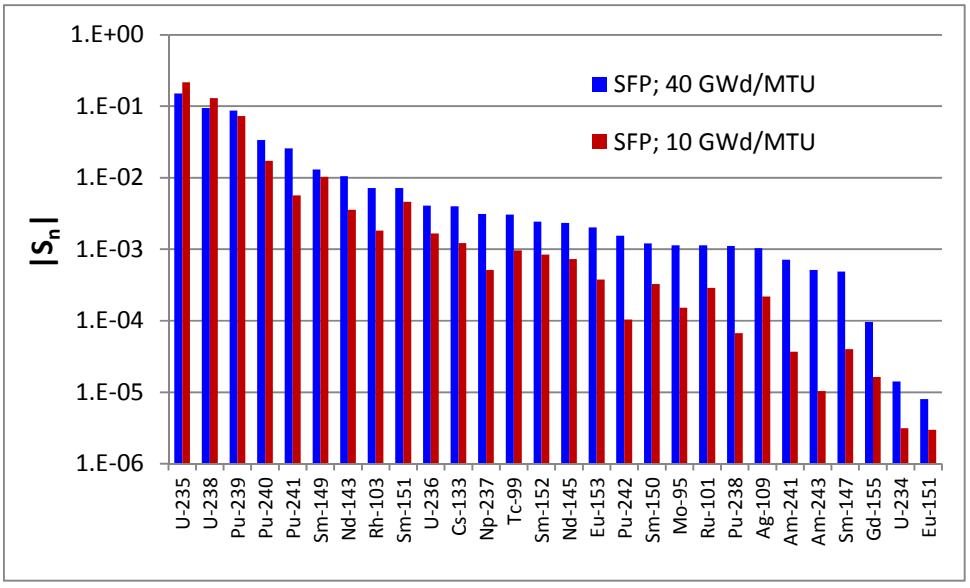

Figure A.1 Sensitivity coefficients (absolute values) shown on a logarithmic scale for burnup credit actinide and fission product nuclides in the representative PWR SFP rack model at 3-day cooling time

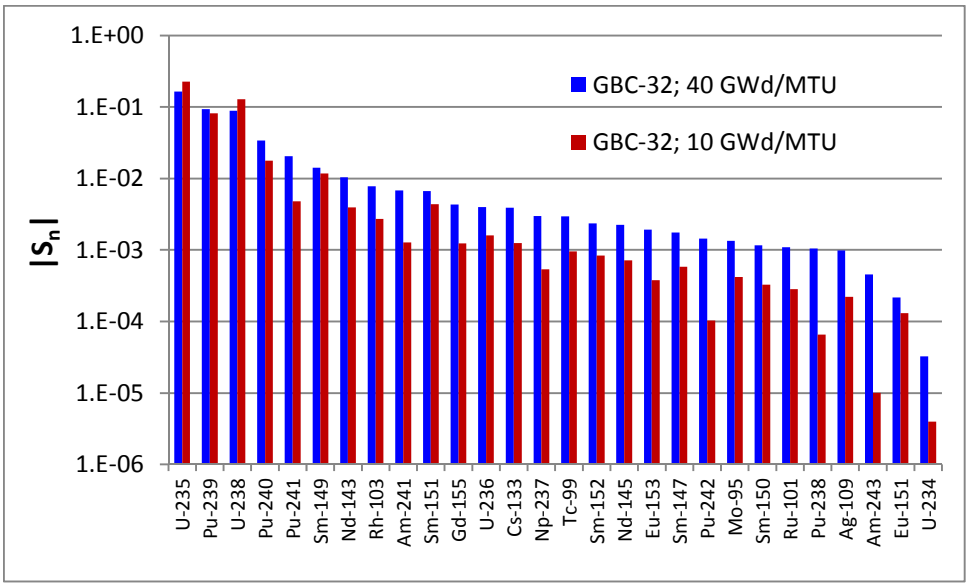

Figure A.2 Sensitivity coefficients (absolute values) shown on a logarithmic scale for burnup credit actinide and fission product nuclides in the PWR SNF cask (GBC-32) model at 5-year cooling time

A.2 Non-normal Distributions for Measured-to-Calculated Concentration Ratio

The M/C concentration ratio values for ^{235}U based on the PWR fuel samples within the burnup interval 15 to 40 GWd/MTU formed a skewed unimodal frequency distribution, as illustrated by the histogram shown in Figure A.3. In the Monte Carlo uncertainty sampling procedure, uncertainties in calculated ^{235}U concentrations were represented as a normal distribution with mean and standard deviation of 0.9907 and 0.0416, respectively. The impact on k_{eff} bias uncertainty of using the normal distribution in place of the actual distribution is evaluated on the basis of a sensitivity/uncertainty analysis for the representative SFP storage rack configuration and the 40-GWd/MTU assembly average burnup.

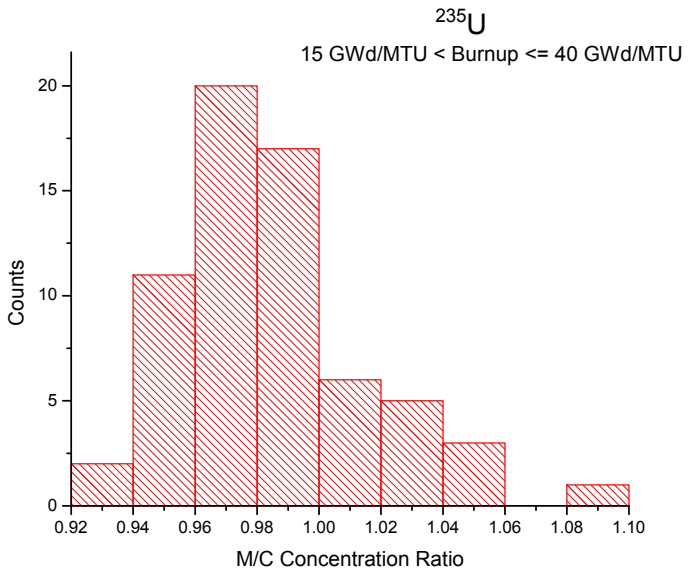

Figure A.3 Histogram of the M/C concentration ratio values for ^{235}U within the burnup interval 15 to 40 GWd/MTU

Table A.1 shows the M/C concentration ratio values for ^{235}U and the individual k_{eff} changes from the reference value of 0.99, $\Delta k_{eff_{235_U}}$ [see Eq. (A-2)], resulting from the bias in the calculated ^{235}U concentration, which were determined from measurement data within the burnup range 15 to 40 GWd/MTU. The $\Delta k_{eff_{235_U}}$ values did not approach a normal distribution, as illustrated in the histogram shown in Figure A.4. The 95/95 distribution-free tolerance limit for the $\Delta k_{eff_{235_U}}$ values was calculated as being 0.0125. Therefore, the k_{eff} bias uncertainty component due to the uncertainty in the predicted ^{235}U concentration is 0.0125. The total k_{eff} bias uncertainty can be calculated with all k_{eff} bias uncertainty components from individual nuclides, as shown in Eq. (A-5), where the $\Delta k_{eff_{235_U}}$ component is 0.0125. The k_{eff} bias uncertainty value thus calculated is 0.0152 compared to 0.0168 (see Table 7.1) based on calculations using the normal distribution model with mean and standard deviation of 0.9907 and 0.0416, respectively, for ^{235}U within the burnup range 15 to 40 GWd/MTU. For this case, a normal distribution can be used because the k_{eff} bias uncertainty value obtained with the normal distribution in place of the actual distribution is slightly conservative (i.e., it causes larger k_{eff} bias uncertainty).

Table A.1 k_{eff} bias due to the bias in calculated ^{235}U concentration based on measurement data from fuel samples within the burnup range 15 to 40 GWd/MTU

Reactor	Sample ID	X_{235_U} [a]	$\Delta k_{eff_{235_U}}$ [b]	Reactor	Sample ID	X_{235_U} [a]	$\Delta k_{eff_{235_U}}$ [b]
Trino Vercellese	509-032-E11-4	0.9702	0.0045	Turkey Point	D01.G10	0.9381	0.0094
Trino Vercellese	509-032-E11-7	0.9549	0.0068	Turkey Point	D01.G9	0.9826	0.0026
Trino Vercellese	509-032-H9-4	0.9920	0.0012	Turkey Point	D01.H9	0.9856	0.0022
Trino Vercellese	509-032-H9-7	1.0060	-0.0009	Turkey Point	D04.G10	0.9757	0.0037
Trino Vercellese	509-049-J8-7	0.9685	0.0048	Turkey Point	D04.G9	0.9497	0.0076
Trino Vercellese	509-069-E11-2	0.9758	0.0037	H.B. Robinson	B-05.N-9B-N	0.9994	0.0001
Trino Vercellese	509-069-E11-4	0.9561	0.0067	H.B. Robinson	B-05.N-9B-S	0.9946	0.0008
Trino Vercellese	509-069-E11-5	0.9926	0.0011	H.B. Robinson	B-05.N-9C-D	0.9773	0.0034
Trino Vercellese	509-069-E11-7	0.9778	0.0034	H.B. Robinson	B-05.N-9C-J	1.0567	-0.0086
Trino Vercellese	509-069-E11-8	0.9679	0.0049	Calvert Cliffs	BT03.NBD107-GG	1.0829	-0.0125
Trino Vercellese	509-069-E11-9	0.9815	0.0028	Calvert Cliffs	BT03.NBD107-MM	1.0409	-0.0062
Trino Vercellese	509-069-E5-4	0.9950	0.0008	Calvert Cliffs	D047.MKP109-CC	0.9976	0.0004
Trino Vercellese	509-069-E5-7	0.9761	0.0036	Calvert Cliffs	D047.MKP109-LL	1.0018	-0.0003
Trino Vercellese	509-069-E5-9	0.9913	0.0013	Calvert Cliffs	MLA098-BB	1.0005	-0.0001
Trino Vercellese	509-069-J9-4	0.9745	0.0039	Calvert Cliffs	MLA098-JJ	0.9943	0.0009
Trino Vercellese	509-069-J9-7	0.9803	0.0030	Calvert Cliffs	MLA098-P	0.9508	0.0075
Trino Vercellese	509-069-L5-4	1.0174	-0.0026	Takahama-3	NT3G23.SF95-2	0.9713	0.0044
Trino Vercellese	509-069-L5-7	0.9754	0.0037	Takahama-3	NT3G23.SF95-3	0.9643	0.0054
Trino Vercellese	509-069-L11-4	0.9903	0.0015	Takahama-3	NT3G23.SF95-4	0.9572	0.0065
Trino Vercellese	509-069-L11-7	0.9724	0.0042	Takahama-3	NT3G23.SF95-5	0.9759	0.0037
Obrigheim	BE124.E3P1	1.0148	-0.0022	Takahama-3	NT3G23.SF96-2	0.9728	0.0041
Obrigheim	BE124.E3P2	1.0601	-0.0091	Takahama-3	NT3G23.SF96-3	0.9535	0.0071
Obrigheim	BE124.E3P3	1.0693	-0.0105	Takahama-3	NT3G23.SF96-4	0.9433	0.0086
Obrigheim	BE124.E3P4	0.9954	0.0007	Takahama-3	NT3G23.SF96-5	0.9676	0.0049
Obrigheim	BE124.E3P5	1.0442	-0.0067	Takahama-3	NT3G24.SF97-2	0.9766	0.0035
Obrigheim	BE124.G7P1	1.0325	-0.0049	TMI-1	NJ070G.O12S4	0.9613	0.0059
Obrigheim	BE124.G7P2	1.0883	-0.0134	TMI-1	NJ070G.O12S5	0.9551	0.0068
Obrigheim	BE124.G7P3	0.9745	0.0039	TMI-1	NJ070G.O12S6	0.9804	0.0030
Obrigheim	BE124.G7P4	1.0779	-0.0118	TMI-1	NJ070G.O13S7	0.9599	0.0061
Obrigheim	BE124.G7P5	0.9876	0.0019	TMI-1	NJ070G.O13S8	0.9547	0.0069
Obrigheim	BE168	1.0331	-0.0050	TMI-1	NJ070G.O1S1	0.9560	0.0067
Obrigheim	BE170	1.0297	-0.0045	TMI-1	NJ070G.O1S2	0.9364	0.0096
Obrigheim	BE171	1.0324	-0.0049	TMI-1	NJ070G.O1S3	0.9647	0.0054
Obrigheim	BE172	1.0145	-0.0022	Gösgen	1701.GU4	0.9877	0.0019
Obrigheim	BE176	1.0215	-0.0033				

[a]Measured-to-calculated concentration ratio for ^{235}U in a fuel sample.
[b]k_{eff} bias due to bias in the calculated ^{235}U nuclide concentration based on ^{235}U measurement data for a fuel sample.

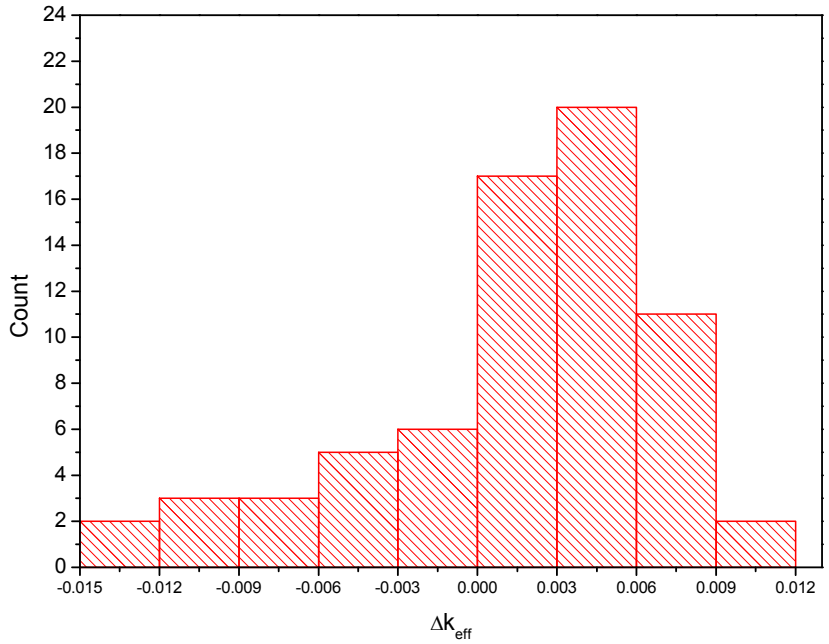

Figure A.4 Histogram plot for $\Delta k_{eff_{^{235}U}}$ values based on actual M/C concentration ratio values for ^{235}U within the burnup range 15 to 40 GWd/MTU. The $\Delta k_{eff_{^{235}U}}$ values used in the histogram were calculated with Eq. (A-2)**.**

A.3 Analysis of k_{eff} Bias and Bias Uncertainty Components

The contributions of individual burnup credit nuclides to k_{eff} bias and bias uncertainty were evaluated through sensitivity/uncertainty analyses. Figure A.5 through Figure A.8 show individual nuclide contributions to k_{eff} bias uncertainty for the reference PWR SFP storage rack and SNF cask models using 10- and 40- GWd/MTU assembly average burnup values. For these analysis models, the bias uncertainties in the calculated ^{235}U concentrations have a dominating effect on the k_{eff} bias uncertainty (~90%). The combined contributions from the bias uncertainties associated with the calculated ^{235}U and ^{239}Pu concentrations account for approximately 95%; the total contribution of bias uncertainties in calculated fission product concentrations is relatively small (<2%) for these representative analysis models.

Individual nuclide contributions to k_{eff} bias uncertainty for the unpoisoned SFP storage rack model and the 40-GWd/MTU assembly average burnup are illustrated in Figure A.9. For this model, ^{239}Pu has the largest contribution to k_{eff} bias uncertainty (~70%), ^{235}U contributes ~20% of k_{eff} bias uncertainty, and ^{241}Pu and ^{240}Pu contribute approximately 7% of the total k_{eff} bias uncertainty; the total contribution of bias uncertainties in the calculated fission product concentrations is relatively small (~3%).

In Figures A.5 through A.9, the ^{235}U and ^{239}Pu percentage values are shown on the left-hand side Y axis, whereas the percentage values for the other burnup credit nuclides are shown on the right-hand side Y axis.

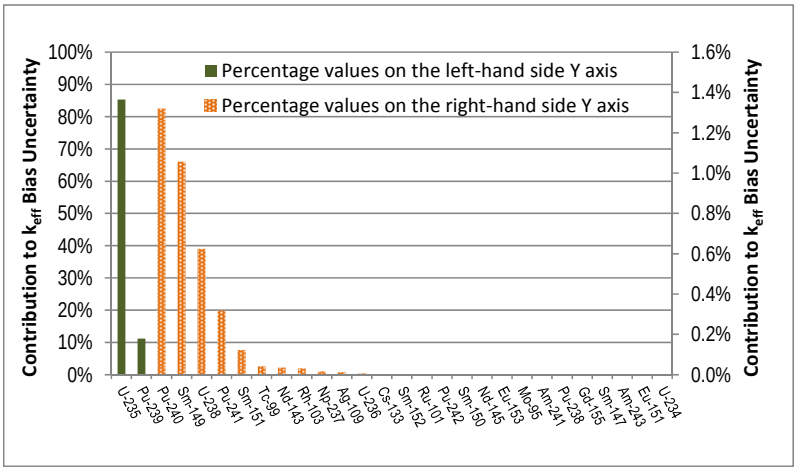

Figure A.5 Individual nuclide contributions to k_{eff} bias uncertainty for the representative PWR SFP storage rack model and 10-GWd/MTU assembly average burnup

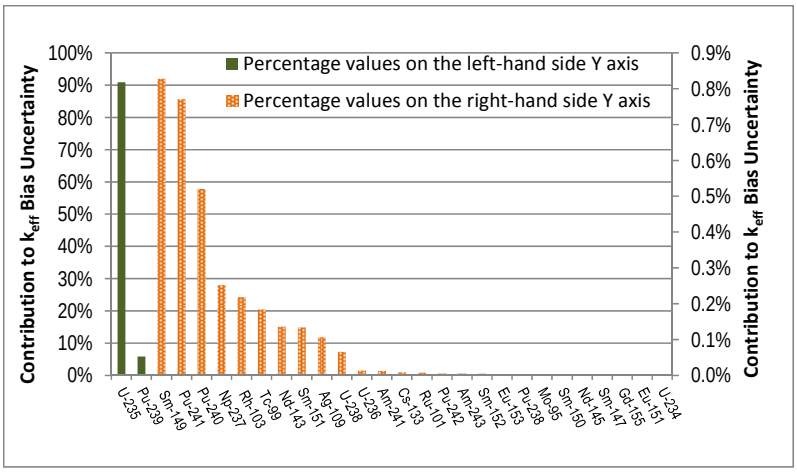

Figure A.6 Individual nuclide contributions to k_{eff} bias uncertainty for the representative PWR SFP storage rack model and 40-GWd/MTU assembly average burnup

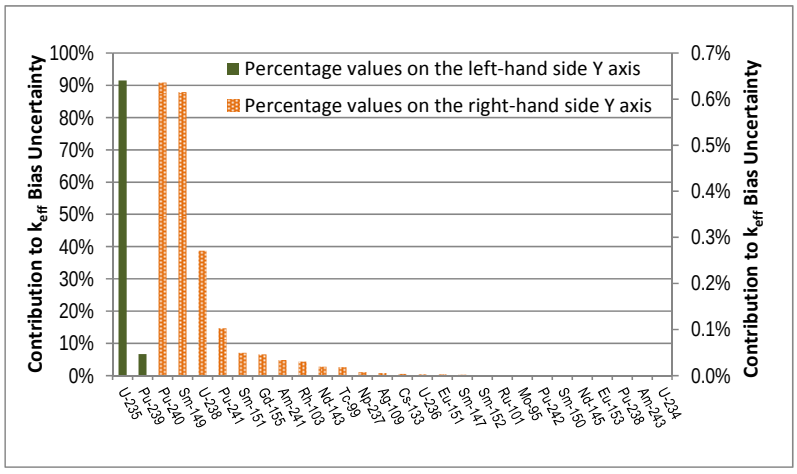

Figure A.7 Individual nuclide contributions to k_{eff} bias uncertainty for the PWR SNF cask model and 10-GWd/MTU assembly average burnup

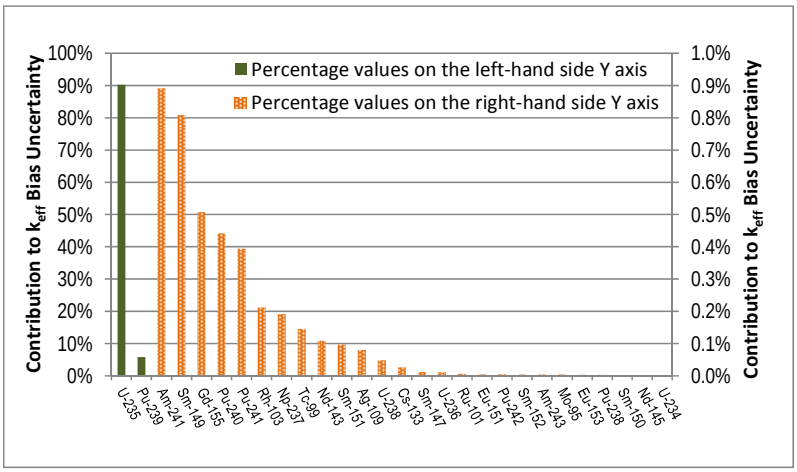

Figure A.8 Individual nuclide contributions to k_{eff} bias uncertainty for the PWR SNF cask model and 40-GWd/MTU assembly average burnup

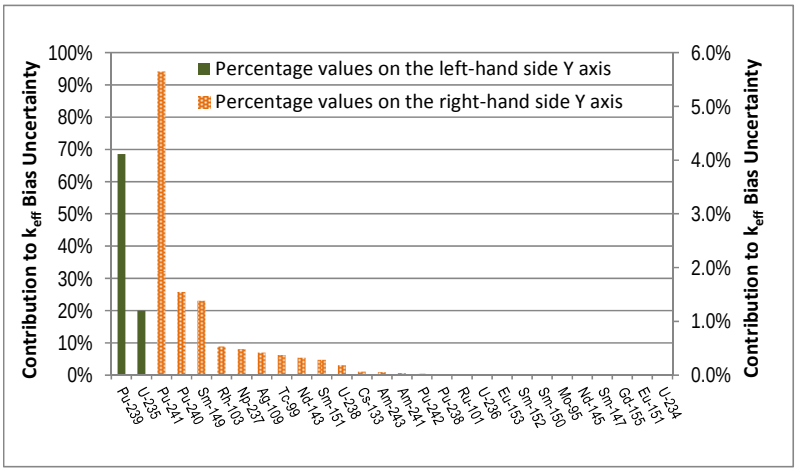

Figure A.9 Individual nuclide contributions to k_{eff} bias uncertainty for the unpoisoned PWR SFP storage rack model and 40-GWd/MTU assembly average burnup

The k_{eff} bias values obtained with the ENDF/B-VII and ENDF/B-V nuclear cross-section data were significantly different (see Sect. 7.3). For example, over the burnup range 10 to 40 GWd/MTU, the k_{eff} bias value based on the ENDF/B-VII nuclear data is approximately 0.0035, whereas k_{eff} bias values based the ENDF/B-V nuclear data vary from -0.0001 (10 GWd/MTU) to -0.0040 (40 GWd/MTU).

Individual nuclide k_{eff} bias components based on ENDF/B-VII and ENDF/B-V nuclear data are illustrated in Figure A.10 (a) and (b), respectively, for the reference SFP storage rack model and 40-GWd/MTU assembly average burnup. Nuclides with significantly different biases between the ENDF/B-VII and ENDF/B-V nuclear data are ^{235}U, ^{149}Sm, and ^{151}Sm. Both ENDF/B-V and ENDF/B-VII nuclear data overpredict ^{235}U and ^{239}Pu concentrations; however, the bias values based on the ENDF/B-VII data are greater than the bias values based on the ENDF/B-V data for these nuclides.

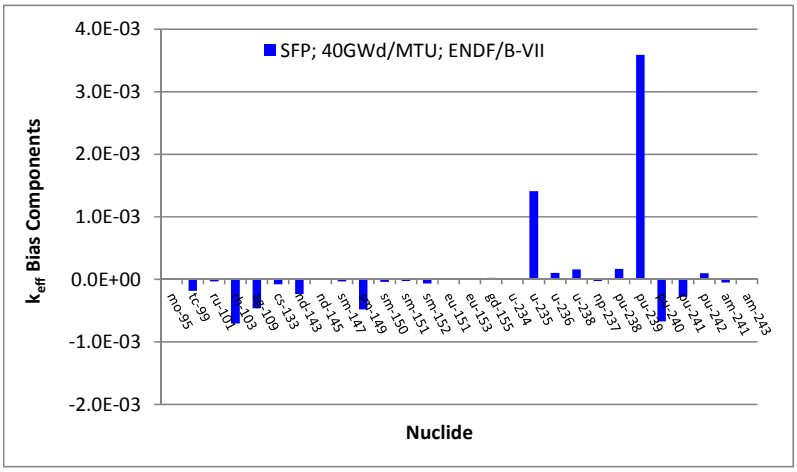

(a)

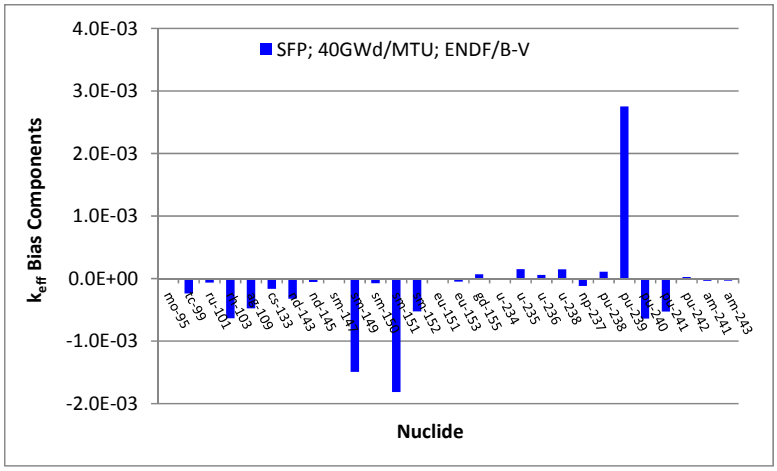

(b)

Figure A.10 Illustration of k_{eff} bias components using (a) ENDF/B-VII nuclear data; (b) ENDF/B-V nuclear data

A.4 Importance of Decay-Time Corrections for the Direct-Difference Method

The direct-difference method applies measured nuclide concentrations from representative fuel samples directly in safety application models for criticality calculations. Measured nuclide concentrations for burnup credit nuclides have been reported either at the time of fuel discharge or at the actual measurement time depending on the experimental programs (see Ref. 20). The measurement data reported for discharged compositions include decay time corrections for nuclides exhibiting concentration variation as a function of decay time (see Ref. 20). Therefore, a review of the measurement data and reported decay times should be performed to identify nuclides that require decay-time corrections because fuel sample nuclide concentrations for criticality calculations must correspond to the fuel cooling time considered in the safety analysis models.

The importance for direct-difference calculations to use fuel sample nuclide compositions corresponding to the cooling time considered in the safety analysis is discussed in the following sensitivity/uncertainty analysis example.

Measured and corresponding calculated nuclide concentrations for the Calvert Cliffs MKP109-P fuel sample were directly applied in the unpoisoned SFP storage rack model considering uniform axial burnup. The measured and calculated nuclide concentration values for the fuel sample correspond to the reported measurement time (e.g., 4,656 days after fuel discharge for ^{155}Gd). The purpose of these calculations is to determine the difference between the k_{eff} values using measured and calculated nuclide concentrations corresponding to the reported measurement time.

Nuclide concentration values were determined for the representative fuel assembly, W 17×17 (see Sect. 5.1), with a 50-GWd/MTU assembly average burnup, a uniform burnup profile, a 3-day cooling time, and a k_{eff} value of 0.99 in the unpoisoned SFP storage rack configuration. Measured-to-calculated concentration ratio values (i.e., isotopic uncertainties) based on Calvert Cliffs MKP109-P fuel sample measurements were applied as adjustment factors to the nuclide concentration values. The purpose of the calculations is to determine the effects of the isotopic uncertainty based on Calvert Cliffs MKP109-P fuel sample measurements on the k_{eff} for the analysis model. Note that the nuclide concentrations for the fuel sample and for the application model have very similar burnup-to-enrichment and ^{235}U-to-^{239}Pu atom density ratios, as seen in Table A.2.

Sensitivity coefficients, the Δk_{eff_n} bias due to individual isotopic biases [see Eq. (A-2)], and Δk_{eff} bias due to all isotopic biases [see Eq. (A-3)] were calculated for the unpoisoned SFP storage rack model using (1) fuel sample nuclide concentrations corresponding to the reported measurement time and (2) nuclide concentrations for the analysis model corresponding to the 3-day cooling time. Table A.2 presents the calculated values for those quantities as well as the M/C concentration ratio values based on the Calvert Cliffs MKP109-P fuel sample measurements. The Δk_{eff} value obtained with the direct-difference method for the Calvert Cliffs MKP109-P fuel sample was 0.0221 versus 0.0217 from Eq. (A-3), demonstrating the applicability of this equation for sensitivity/uncertainty analyses. The k_{eff} bias value obtained by applying Calvert Cliffs MKP109-P measurement uncertainty data for the application model is

only 0.009, which is significantly smaller than the k_{eff} bias value of ~0.022 from the direct-difference method using measurement-time nuclide compositions.

Table A.2 shows that the Δk_{eff_n} values due to individual isotopic biases for the fuel sample and for the analysis model are in fairly good agreement for all nuclides except for ^{155}Gd and ^{241}Am. For example, the bias associated with ^{155}Gd concentration causes a 0.0086 change in k_{eff}, if ^{155}Gd concentration corresponds to the reported measurement time, versus a 0.0001 change in k_{eff}, if this bias is applied to a 3-day cooling time nuclide concentration. This is because the ^{155}Gd is only present in negligible concentrations after 3 days of cooling, which demonstrates the impact of different nuclide worth effects if cooling time is not considered.

Table A.2 k_{eff} bias calculations using fuel sample and analysis model compositions

	Calvert Cliffs MKP109-P fuel sample			Unpoisoned SFP storage rack model		
Burnup (GWd/MTU)	44.3			50		
Initial wt % ^{235}U	3.04			3.56		
Burnup-to-initial enrichment ratio	14.6			14		
^{235}U-to-^{239}Pu atom density ratio	0.83			0.87		
k_{eff}	0.85			0.99		
Nuclide	S_n [a]	X_n [b]	Δk_{eff_n} [c]	S_n [a]	X_n [b]	Δk_{eff_n} [c]
^{95}Mo	-2.35E-03	1.0002	0.0000	-2.03E-03	1.0002	0.0000
^{99}Tc	-5.07E-03	0.8901	-0.0005	-5.24E-03	0.8901	-0.0006
^{101}Ru	-1.87E-03	0.9726	0.0000	-2.05E-03	0.9726	-0.0001
^{103}Rh	-1.40E-02	0.9021	-0.0012	-1.29E-02	0.9021	-0.0013
^{109}Ag	-2.49E-03	0.5546	-0.0009	-2.70E-03	0.5546	-0.0012
^{133}Cs	-6.62E-03	0.9914	0.0000	-6.65E-03	0.9914	-0.0001
^{143}Nd	-1.92E-02	0.9827	-0.0003	-1.85E-02	0.9827	-0.0003
^{145}Nd	-4.15E-03	1.0310	0.0001	-4.10E-03	1.0310	0.0001
^{147}Sm	-2.57E-03	1.1947	0.0004	-7.05E-04	1.1947	0.0001
^{149}Sm	-1.09E-02	0.9634	-0.0003	-1.70E-02	0.9634	-0.0006
^{150}Sm	-2.77E-03	0.9691	-0.0001	-2.83E-03	0.9691	-0.0001
^{151}Sm	-8.56E-03	0.9907	-0.0001	-1.09E-02	0.9907	-0.0001
^{152}Sm	-3.99E-03	1.0179	0.0001	-3.77E-03	1.0179	0.0001
^{151}Eu	-2.59E-04	1.4721	0.0001	-5.92E-06	1.4721	0.0000
^{153}Eu	-4.75E-03	1.0142	0.0001	-4.76E-03	1.0142	0.0001
^{155}Gd	-1.74E-02	1.5827	0.0086	-2.15E-04	1.5827	0.0001
^{234}U	-9.10E-04	0.9610	0.0000	-2.03E-05	0.9610	0.0000
^{235}U	1.09E-01	0.9673	0.0030	8.55E-02	0.9673	0.0028
^{236}U	-4.02E-03	0.9831	-0.0001	-4.39E-03	0.9831	-0.0001
^{238}U	-1.36E-01	1.0014	0.0002	-1.24E-01	1.0014	0.0002
^{237}Np	-5.80E-03	0.9737	-0.0001	-6.57E-03	0.9737	-0.0002
^{238}Pu	-5.10E-03	1.1155	0.0005	-4.93E-03	1.1155	0.0006
^{239}Pu	2.52E-01	0.9407	0.0126	1.81E-01	0.9407	0.0107
^{240}Pu	-5.96E-02	0.9712	-0.0015	-5.63E-02	0.9712	-0.0016
^{241}Pu	7.71E-02	1.0000	0.0000	8.08E-02	1.0000	0.0000
^{242}Pu	-4.47E-03	1.0826	0.0003	-4.86E-03	1.0826	0.0004
^{241}Am	-1.43E-02	1.0793	0.0010	-1.50E-03	1.0793	0.0001
^{243}Am	-2.44E-03	0.9216	-0.0002	-3.14E-03	0.9216	-0.0002
Δk_{eff}			0.0217			0.0089

[a]First-order effect of perturbations in the macroscopic cross section of a nuclide upon k_{eff} [see Eq. (A-1)].
[b]M/C concentration ratio for a nuclide based on measured data for the fuel sample.
[c]k_{eff} bias due to bias in the calculated nuclide concentration based on measured data for the fuel sample [Eq. (A-2)].

APPENDIX B. ISOTOPIC VALIDATION DATA CORRELATIONS

It was assumed that correlations (relationships) between validation data could be neglected in the implementation of the Monte Carlo uncertainty method so that sampling from probability distributions for nuclide composition uncertainties could be performed independently. To evaluate the potential impact of this assumption, an analysis was conducted to identify existing correlations that may impact the accuracy of the results obtained with the Monte Carlo uncertainty method. The degree of correlations (dependence) among nuclide composition uncertainties was determined on the basis of Pearson correlation coefficient (Ref. 53) calculations. Pearson correlation coefficient values closer to zero indicate that the variables are uncorrelated; values closer to either +1 or -1 indicate a strong linear dependence between variables. Positive values indicate positive correlations; negative values indicate negative correlation. A critical value, which depends on the degrees of freedom and statistical significance level, is used to identify statistically significant relationships between any pair of variables. A Pearson correlation coefficient greater than the critical value indicates a statistically significant relationship between the variables. For 26 degrees of freedom (2 less than the number of burnup credit nuclides considered) and 0.05 significance level, the critical value is approximately 0.36 (Ref. 53).

An example correlation matrix is shown in Table B.1 for the measured-to-calculated concentration ratio values used for depletion validation within the burnup range 40 to 60 GWd/MTU. This table shows the Pearson coefficients greater than the critical value of 0.36 above the main diagonal.

For the SFP storage rack and SNF cask models analyzed in this report, the uncertainties in the calculated ^{235}U and ^{239}Pu nuclide concentrations contribute approximately 90 to 95% of the k_{eff} bias uncertainty (see Sect. A.3). Based on correlation calculations, correlations between the isotopic validation data for ^{235}U and ^{239}Pu are insignificant at the 0.05 significance level throughout the burnup range 5 to 60 GWd/MTU. Statistically significant correlations were identified for the Pu isotopes; these correlations need to be considered in the uncertainty calculations for fuel assemblies with high burnup and relatively low initial enrichment for the burnup, such as the nuclide concentrations in the unpoisoned SFP storage rack model (see Sect. 5.2). For this SFP storage rack model and the 40-GWd/MTU burnup, the uncertainties in calculated ^{239}Pu, ^{241}Pu, and ^{240}Pu concentrations contribute approximately 70%, 5%, and 1.5%, respectively, to the k_{eff} bias uncertainty value (see Sect. A.3, Figure A.9). For this case, the total k_{eff} bias uncertainty is approximately 0.018; the k_{eff} bias uncertainty due to bias uncertainty in the calculated ^{241}Pu concentrations is approximately 0.001. Therefore, positive correlations between the isotopic validation data for ^{239}Pu and ^{241}Pu, if considered in the sampling procedure, would increase the small contribution (0.001) made by ^{241}Pu to k_{eff} bias uncertainty, and the net effect would be a relatively small contribution to the calculated k_{eff} bias uncertainty values based on independent sampling. Other neglected positive correlations would decrease the k_{eff} bias uncertainty if considered in the sampling procedure, such as the observed positive correlation between ^{239}Pu (fissile) and ^{240}Pu (absorber) uncertainties. Overall, the neglected correlations in the Monte Carlo uncertainty sampling would have the effect of a small increase in the calculated k_{eff} bias uncertainty comparable to the ^{241}Pu contribution to k_{eff} bias uncertainty. In this analysis, to account for additional uncertainty due to neglected positive correlations in the validation data for ^{239}Pu and ^{241}Pu, the contribution of ^{241}Pu concentration uncertainty to k_{eff} bias uncertainty (e.g., <1% and ~5% in the case of the representative models and the unpoisoned rack model, respectively) is doubled in the calculation of total k_{eff} bias uncertainty. For the reference PWR SFP and cask analysis models, existing correlations are considered to have negligible impact on the calculated k_{eff} bias uncertainty values because the k_{eff} bias uncertainty

is dominated by ^{235}U or ^{239}Pu concentration prediction uncertainties; all other nuclides have relatively small (<1.3%) or negligible contributions to k_{eff} bias uncertainty.

Table B.1 Correlations at the 0.5 significance level for the isotopic validation data applicable to the burnup range 40 to 60 GWd/MTU

	^{234}U	^{235}U	^{236}U	^{238}U	^{238}Pu	^{239}Pu	^{240}Pu	^{241}Pu	^{242}Pu	^{237}Np	^{241}Am	^{243}Am	^{95}Mo	^{99}Tc	^{101}Ru	^{103}Rh	^{109}Ag	^{133}Cs	^{143}Nd	^{145}Nd	^{147}Sm	^{149}Sm	^{150}Sm	^{151}Sm	^{152}Sm	^{151}Eu	^{153}Eu	^{155}Gd
^{234}U	1		-0.63	-0.46		-0.64	-0.82	-0.54									-0.53											
^{235}U		1						0.58				-0.71							0.76	0.57	0.50		0.51	0.69		-0.76		
^{236}U			1			0.67	0.74	0.63	0.46	0.49				-0.54					0.51	0.51	0.47							
^{238}U				1																		-0.46	-0.54	-0.49				
^{238}Pu					1									0.56									0.52					
^{239}Pu						1	0.84	0.70						-0.79					0.46		0.49					0.68		-0.53
^{240}Pu							1	0.58	0.51					-0.71												0.77		
^{241}Pu								1											0.87	0.79	0.74	0.38	0.72	0.61				
^{242}Pu									1																		0.64	
^{237}Np										1		0.57	0.55		0.62											0.62		
^{241}Am											1										-0.68	-0.50	-0.51	-0.58				
^{243}Am												1												-0.48		0.85		
^{95}Mo													1		0.75	0.59												
^{99}Tc														1														
^{101}Ru															1	0.79												
^{103}Rh																1												0.54
^{109}Ag																	1											
^{133}Cs																		1										
^{143}Nd																			1	0.76	0.44	0.53	0.36	0.42		-0.74		
^{145}Nd																				1		0.40		0.37				
^{147}Sm																					1		0.86	0.53	0.65	-0.78	0.72	-0.54
^{149}Sm																						1						
^{150}Sm																							1	0.56	0.66	-0.84	0.79	
^{151}Sm																								1	0.44	-0.48	0.62	
^{152}Sm																									1	-0.48	0.58	
^{151}Eu																										1	-0.71	
^{153}Eu																											1	-0.41
^{155}Gd																												1

Note: Matrix correlation identifying correlations that are significant at the 0.05 level; Pearson coefficient values and statistical significance obtained with OriginPro 8.1 (copyright OriginLab Corporation).

APPENDIX C. REFERENCE SPENT FUEL NUCLIDE CONCENTRATIONS

This appendix documents reference spent fuel nuclide concentrations that can be used in burnup credit calculations. These data are compiled from measurements of 100 PWR spent fuel samples that have been used in this report. The nuclide concentrations have been converted to a consistent format in units of mg/gU initial at the time of measurements (or the time reported by the laboratory). When laboratories have reported the results at the time of discharge, it is important to note that the results for ^{239}Pu include the contribution from short lived ^{239}Np. In several experiments the reported measurement dates vary for the different nuclides in the sample. This is the case for samples obtained from the GKN-II, Gösgen, Takahama (Sm isotopes), Calvert Cliffs (lanthanides), and Trino Vercellese (^{241}Am) reactors. The reference nuclide concentrations listed in this appendix have been adjusted by the authors to a common reference date for each sample using the analytical equations in Sect. 6.2 given for decay time corrections.

To enable users to derive nuclide concentrations for other decay times, the appendix includes the reference inventories for both the burnup credit nuclides (Table 3.1) and the major precursor nuclides. The additional precursor nuclides include ^{242}Cm, ^{244}Cm, ^{147}Pm, and ^{155}Eu. Any adjustments of the data to other decay times must be done within the time range where the given parent and daughter relationship remains valid.

For samples that did not include measurements of all burnup credit nuclides (and precursors), surrogate data based on calculated nuclide concentrations are provided. As discussed in Sect. 6.2, the surrogate data attempt to correct for bias in the calculated nuclide concentrations as based on measured nuclide contents obtained from other samples. The surrogate data therefore represent best-estimate calculated values and are largely independent of the code and nuclear data.

The reference data for the SNF compositions are listed in Table C.1. The table includes all 28 burnup credit nuclides plus four addition decay precursor nuclides that are not considered in burnup credit. Each sample is identified by the reactor, the assembly, and the sample identification. Also provided is the reference decay time for the nuclide concentration data. The concentrations of surrogate data developed from computations are identified with a negative sign.

Table C.1 Reference nuclide compositions (g/gU initial)

Nuclide	Calvert Cliffs BT03 NBD107-GG (5658 days)[a]	Calvert Cliffs BT03 NBD107-MM (2447 days)	Calvert Cliffs BT03 NBD107-Q (2447 days)	Calvert Cliffs D047 MKP109-CC (4653 days)	Calvert Cliffs D047 MKP109-LL (4171 days)	Calvert Cliffs D047 MKP109-P (4653 days)	Calvert Cliffs D101 MLA098-BB (2374 days)	Calvert Cliffs D101 MLA098-JJ (2374 days)	Calvert Cliffs D101 MLA098-P (2374 days)	GKN-II 419 M11 (2735 days)	Gösgen 1240 GU1 (1054 days)
U-234	1.590E-04	1.736E-04	8.497E-05	1.714E-04	1.871E-04	1.540E-04	1.373E-04	1.588E-04	1.361E-04	1.496E-04	1.201E-04
U-235	3.074E-03	4.379E-03	1.595E-03	5.865E-03	9.609E-03	4.016E-03	7.873E-03	1.163E-02	5.423E-03	5.130E-03	2.110E-03
U-236	3.437E-03	3.244E-03	3.449E-03	4.005E-03	3.562E-03	4.186E-03	3.392E-03	2.836E-03	3.698E-03	5.360E-03	4.830E-03
U-238	9.572E-01	9.581E-01	9.384E-01	9.446E-01	9.558E-01	9.358E-01	9.686E-01	9.700E-01	9.554E-01	9.220E-01	9.200E-01
Np-237	3.758E-04	2.967E-04	4.290E-04	4.134E-04	3.097E-04	5.434E-04	3.403E-04	1.984E-04	3.887E-04	6.090E-04	-7.229E-04
Pu-238	2.060E-04	1.618E-04	3.224E-04	2.022E-04	1.090E-04	2.871E-04	1.099E-04	5.502E-05	1.682E-04	4.281E-04	4.540E-04
Pu-239	4.349E-03	4.327E-03	4.272E-03	4.942E-03	4.836E-03	4.942E-03	4.824E-03	4.486E-03	4.750E-03	5.770E-03	4.890E-03
Pu-240	2.631E-03	2.345E-03	2.948E-03	2.538E-03	1.949E-03	2.883E-03	2.003E-03	1.410E-03	2.395E-03	3.220E-03	3.180E-03
Pu-241	6.008E-04	8.236E-04	1.005E-03	7.074E-04	5.691E-04	7.993E-04	7.739E-04	5.154E-04	9.217E-04	1.283E-03	1.440E-03
Pu-242	8.795E-04	6.197E-04	1.326E-03	6.535E-04	3.278E-04	9.530E-04	3.745E-04	1.581E-04	6.210E-04	1.170E-03	1.550E-03
Am-241	7.949E-04	3.901E-04	7.207E-04	7.000E-04	4.825E-04	7.833E-04	3.276E-04	2.205E-04	3.967E-04	5.218E-04	2.507E-04
Am-243	-1.790E-04	-1.076E-04	-2.958E-04	-1.328E-04	-4.993E-05	-2.054E-04	-5.854E-05	-1.676E-05	-1.199E-04	2.490E-04	4.030E-04
Cm-242[b]	-2.755E-09	-3.423E-09	-3.893E-09	-2.815E-09	-2.290E-09	-3.092E-09	-2.367E-09	-1.442E-09	-3.037E-09	4.608E-09	3.695E-07
Cm-244[b]	-3.609E-05	-2.405E-05	-1.235E-04	-2.794E-05	-7.425E-06	-6.010E-05	-1.102E-05	-2.019E-06	-3.054E-05	1.311E-04	2.451E-04
Mo-95	-8.066E-04	-7.035E-04	-9.541E-04	-8.192E-04	-6.339E-04	-9.421E-04	-6.184E-04	-4.536E-04	-7.424E-04	1.040E-03	1.230E-03
Tc-99	5.936E-04	5.101E-04	7.221E-04	8.149E-04	6.353E-04	8.944E-04	6.208E-04	4.684E-04	7.486E-04	1.250E-03	1.250E-03
Ru-101	-8.570E-04	-7.268E-04	-1.054E-03	-8.387E-04	-6.231E-04	-9.927E-04	-6.169E-04	-4.350E-04	-7.639E-04	9.680E-04	1.290E-03
Rh-103	6.800E-04	-4.164E-04	-5.462E-04	-4.703E-04	-3.658E-04	-5.367E-04	-3.703E-04	-2.675E-04	-4.465E-04	5.810E-04	6.130E-04
Ag-109	-5.789E-05	-4.590E-05	-7.609E-05	-5.065E-05	-3.260E-05	-6.461E-05	-3.495E-05	-2.057E-05	-4.798E-05	1.070E-04	7.510E-05
Cs-133	-1.214E-03	-1.059E-03	-1.429E-03	1.237E-03	9.643E-04	1.407E-03	-9.241E-04	-6.755E-04	-1.110E-03	1.600E-03	1.720E-03
Nd-143	7.189E-04	-6.561E-04	-7.367E-04	8.123E-04	6.954E-04	8.656E-04	-6.527E-04	-5.171E-04	-7.392E-04	1.070E-03	9.330E-04
Nd-145	7.246E-04	-6.202E-04	-8.170E-04	7.408E-04	5.786E-04	8.440E-04	-5.507E-04	-4.094E-04	-6.538E-04	9.970E-04	1.040E-03
Pm-147[b]	-2.545E-06	-2.413E-05	-2.804E-05	-6.208E-06	-7.653E-06	-6.583E-06	-3.058E-05	-2.470E-05	-3.390E-05	-2.974E-05	-1.077E-04
Sm-147	2.659E-04	-2.253E-04	-2.492E-04	2.704E-04	2.303E-04	3.081E-04	-1.984E-04	-1.619E-04	-2.173E-04	2.990E-04	2.220E-04
Sm-149	2.174E-06	-1.435E-06	-1.719E-06	-2.077E-06	-1.943E-06	-2.268E-06	-2.069E-06	-1.843E-06	-2.328E-06	2.390E-06	3.280E-06
Sm-150	3.000E-04	-2.485E-04	-3.726E-04	2.896E-04	2.089E-04	3.638E-04	-2.173E-04	-1.463E-04	-2.783E-04	4.780E-04	5.080E-04
Sm-151	7.970E-06	-7.261E-06	-8.883E-06	9.408E-06	7.521E-06	1.072E-05	-8.442E-06	-7.541E-06	-9.498E-06	1.430E-05	1.300E-05
Sm-152	1.210E-04	-1.087E-04	-1.377E-04	1.096E-04	8.968E-05	1.325E-04	-9.294E-05	-7.042E-05	-1.074E-04	1.470E-04	1.660E-04
Eu-151	-1.379E-06	-5.908E-07	-7.122E-07	-1.415E-06	-1.172E-06	-1.572E-06	-6.624E-07	-6.022E-07	-7.396E-07	-1.307E-06	-4.410E-07
Eu-153	1.483E-04	-1.131E-04	-1.721E-04	1.300E-04	8.516E-05	1.622E-04	-9.138E-05	-5.643E-05	-1.204E-04	1.920E-04	2.100E-04
Eu-155[b]	1.138E-06	-4.088E-06	-6.854E-06	1.385E-06	1.041E-06	1.815E-06	-3.316E-06	-1.861E-06	-4.670E-06	5.856E-06	1.130E-05
Gd-155	7.028E-06	-6.055E-06	-1.010E-05	7.408E-06	6.248E-06	9.959E-06	-4.678E-06	-2.644E-06	-6.570E-06	1.010E-05	5.644E-06

[a]Time after discharge.
[b]Decay precursor.

Table C.1 Reference nuclide concentrations (g/gU initial) (continued)

Nuclide	Gösgen 1701 GU3 (919 days)[a]	Gösgen 1701 GU4 (846 days)	HB Robinson B05 N9BN (3936 days)	HB Robinson B05 N9BS (3631 days)	HB Robinson B05 N9CD (3631 days)	HB Robinson B05 N9CJ (3631 days)	Obrigheim BE124 E3P1 (10 days)	Obrigheim BE124 E3P2 (10 days)	Obrigheim BE124 E3P3 (10 days)	Obrigheim BE124 E3P4 (10 days)	Obrigheim BE124 E3P5 (10 days)
U-234	1.435E-04	1.953E-04	1.556E-04	1.755E-04	1.253E-04	1.339E-04	-1.812E-04	-1.545E-04	-1.356E-04	-1.492E-04	-1.720E-04
U-235	6.050E-03	1.450E-02	8.181E-03	1.209E-02	5.514E-03	7.010E-03	1.275E-02	8.440E-03	6.090E-03	7.660E-03	1.185E-02
U-236	5.650E-03	4.590E-03	3.103E-03	2.487E-03	3.403E-03	3.204E-03	2.820E-03	3.770E-03	4.120E-03	3.870E-03	3.620E-03
U-238	9.270E-01	9.440E-01	9.613E-01	9.605E-01	9.549E-01	9.460E-01	9.571E-01	9.422E-01	9.430E-01	9.470E-01	9.534E-01
Np-237	8.110E-04	5.250E-04	2.953E-04	1.753E-04	3.778E-04	3.445E-04	-1.994E-04	-3.279E-04	-4.300E-04	-3.626E-04	-2.466E-04
Pu-238	3.715E-04	1.109E-04	7.894E-05	3.208E-05	1.479E-04	1.293E-04	4.100E-05	1.040E-04	1.650E-04	1.140E-04	6.200E-05
Pu-239	5.810E-03	5.160E-03	4.557E-03	4.132E-03	4.765E-03	5.162E-03	4.280E-03	4.620E-03	4.770E-03	4.925E-03	4.650E-03
Pu-240	2.840E-03	1.840E-03	1.890E-03	1.241E-03	2.404E-03	2.236E-03	1.360E-03	1.990E-03	2.410E-03	2.230E-03	1.620E-03
Pu-241	1.805E-03	9.811E-04	5.722E-04	3.447E-04	7.847E-04	7.733E-04	6.200E-04	1.020E-03	1.260E-03	1.185E-03	8.400E-04
Pu-242	1.020E-03	3.100E-04	3.208E-04	1.155E-04	6.001E-04	4.682E-04	1.390E-04	3.800E-04	6.290E-04	4.760E-04	2.110E-04
Am-241	2.261E-04	1.610E-04	-3.750E-04	-2.266E-04	-4.859E-04	-4.456E-04	-1.534E-05	-2.195E-05	-2.499E-05	-2.416E-05	-1.893E-05
Am-243	2.380E-04	4.380E-05	-4.432E-05	-1.061E-05	-1.155E-04	-8.332E-05	-1.719E-05	-6.743E-05	-1.381E-04	-8.561E-05	-3.026E-05
Cm-242[b]	1.367E-05	-2.858E-07	-1.019E-09	-6.030E-10	-1.557E-09	-1.489E-09	4.500E-06	-1.116E-05	1.479E-05	1.501E-05	7.100E-06
Cm-244[b]	1.386E-04	1.226E-05	-6.175E-06	-9.084E-07	-2.462E-05	-1.550E-05	2.040E-06	-1.675E-05	4.162E-05	2.349E-05	5.130E-06
Mo-95	1.180E-03	7.580E-04	-5.580E-04	-3.923E-04	-7.086E-04	-6.475E-04	-3.992E-04	-5.547E-04	-6.603E-04	-5.765E-04	-4.436E-04
Tc-99	1.120E-03	5.990E-04	5.360E-04	3.604E-04	6.691E-04	5.930E-04	-4.864E-04	-6.808E-04	-8.162E-04	-7.099E-04	-5.434E-04
Ru-101	1.210E-03	7.490E-04	-5.540E-04	-3.741E-04	-7.317E-04	-6.593E-04	-4.690E-04	-6.783E-04	-8.326E-04	-7.129E-04	-5.302E-04
Rh-103	5.400E-04	4.540E-04	-3.443E-04	-2.366E-04	-4.430E-04	-4.048E-04	-2.561E-04	-3.574E-04	-4.255E-04	-3.753E-04	-2.887E-04
Ag-109	1.190E-04	-3.224E-05	-3.153E-05	-1.750E-05	-4.760E-05	-4.114E-05	-2.088E-05	-3.722E-05	-5.110E-05	-4.091E-05	-2.603E-05
Cs-133	1.630E-03	1.080E-03	-8.375E-04	-5.862E-04	-1.064E-03	-9.738E-04	-7.272E-04	-1.010E-03	-1.200E-03	-1.051E-03	-8.099E-04
Nd-143	1.070E-03	8.620E-04	5.711E-04	4.429E-04	6.550E-04	6.592E-04	-5.477E-04	-6.922E-04	-7.723E-04	-7.200E-04	-5.988E-04
Nd-145	9.890E-04	6.760E-04	4.819E-04	3.445E-04	5.853E-04	5.573E-04	-4.451E-04	-6.070E-04	-7.131E-04	-6.297E-04	-4.923E-04
Pm-147[b]	-1.348E-04	-1.183E-04	-1.062E-05	-8.323E-06	-1.473E-05	-1.399E-05	-1.711E-04	-2.100E-04	-2.276E-04	-2.132E-04	-1.827E-04
Sm-147	1.960E-04	1.610E-04	-1.981E-04	-1.551E-04	-2.227E-04	-2.128E-04	-4.812E-05	-5.796E-05	-6.118E-05	-5.808E-05	-5.086E-05
Sm-149	3.360E-06	3.020E-06	-2.514E-06	-2.127E-06	-2.793E-06	-2.572E-06	-2.672E-06	-3.312E-06	-3.898E-06	-3.575E-06	-2.988E-06
Sm-150	4.460E-04	2.430E-04	-1.959E-04	-1.259E-04	-2.695E-04	-2.393E-04	-1.605E-04	-2.443E-04	-3.102E-04	-2.605E-04	-1.855E-04
Sm-151	1.470E-05	1.130E-05	-7.510E-06	-6.634E-06	-8.962E-06	-8.530E-06	-8.181E-06	-9.296E-06	-1.073E-05	-1.028E-05	-9.183E-06
Sm-152	1.340E-04	9.460E-05	-8.817E-05	-6.354E-05	-1.069E-04	-9.928E-05	-7.537E-05	-1.006E-04	-1.147E-04	-1.023E-04	-8.195E-05
Eu-151	-4.348E-07	-3.422E-07	-9.726E-07	-8.654E-07	-1.067E-06	-1.018E-06	-1.554E-08	-1.200E-08	-1.145E-08	-1.311E-08	-1.580E-08
Eu-153	1.840E-04	9.390E-05	-7.932E-05	-4.571E-05	-1.149E-04	-1.009E-04	-5.972E-05	-9.958E-05	-1.297E-04	-1.075E-04	-7.221E-05
Eu-155[b]	1.432E-05	4.405E-06	-1.536E-06	-8.306E-07	-2.680E-06	-2.288E-06	-5.164E-06	-9.433E-06	-1.300E-05	-1.031E-05	-6.392E-06
Gd-155	3.999E-06	2.635E-06	-5.186E-06	-2.812E-06	-7.737E-06	-6.613E-06	-4.599E-08	-6.728E-08	-8.600E-08	-7.579E-08	-5.582E-08

[a]Time after discharge.
[b]Decay precursor.

Table C.1 Reference nuclide concentrations (g/gU initial) (continued)

Nuclide	Obrigheim BE124 G7P1 (10 days)[a]	Obrigheim BE124 G7P2 (10 days)	Obrigheim BE124 G7P3 (10 days)	Obrigheim BE124 G7P4 (10 days)	Obrigheim BE124 G7P5 (10 days)	Obrigheim BE168 (10 days)	Obrigheim BE170 (10 days)	Obrigheim BE171 (10 days)	Obrigheim BE172 (10 days)	Obrigheim BE176 (10 days)	Takahama NT3G23 SF95-2 (10 days)
U-234	-1.894E-04	-1.635E-04	-1.479E-04	-1.571E-04	-1.623E-04	-1.617E-04	-1.683E-04	-1.636E-04	-1.657E-04	-1.633E-04	2.850E-04
U-235	1.521E-02	1.076E-02	7.555E-03	1.009E-02	1.009E-02	9.346E-03	1.043E-02	9.657E-03	9.830E-03	9.504E-03	1.927E-02
U-236	2.920E-03	3.850E-03	3.960E-03	4.050E-03	3.600E-03	3.785E-03	3.651E-03	3.738E-03	3.680E-03	3.751E-03	4.024E-03
U-238	9.580E-01	9.508E-01	9.464E-01	9.484E-01	9.502E-01	9.474E-01	9.494E-01	9.481E-01	9.491E-01	9.481E-01	9.424E-01
Np-237	-1.682E-04	-2.914E-04	-3.765E-04	-3.299E-04	-3.023E-04	-3.387E-04	-3.048E-04	-3.287E-04	-3.174E-04	-3.300E-04	-3.035E-04
Pu-238	3.100E-05	7.900E-05	1.415E-04	1.060E-04	7.900E-05	1.192E-04	8.875E-05	1.028E-04	9.392E-05	1.069E-04	7.102E-05
Pu-239	4.260E-03	4.700E-03	5.015E-03	5.080E-03	5.080E-03	5.008E-03	4.876E-03	4.923E-03	4.793E-03	4.928E-03	5.655E-03
Pu-240	1.160E-03	1.810E-03	2.280E-03	2.040E-03	1.950E-03	2.046E-03	1.881E-03	1.961E-03	1.895E-03	1.982E-03	1.539E-03
Pu-241	5.500E-04	9.400E-04	1.205E-03	1.110E-03	1.050E-03	1.123E-03	1.026E-03	1.076E-03	1.031E-03	1.093E-03	9.578E-04
Pu-242	9.900E-05	2.790E-04	4.890E-04	3.660E-04	3.200E-04	4.290E-04	3.445E-04	3.880E-04	3.720E-04	4.035E-04	1.844E-04
Am-241	-1.313E-05	-2.124E-05	-2.518E-05	-2.387E-05	-2.255E-05	-4.213E-05	-3.688E-05	-4.176E-05	-3.847E-05	-4.161E-05	2.344E-05
Am-243	-9.930E-06	-4.535E-05	-8.923E-05	-6.167E-05	-4.874E-05	-6.469E-05	-4.871E-05	-5.962E-05	-5.428E-05	-6.031E-05	2.289E-05
Cm-242[b]	2.940E-06	8.580E-06	1.479E-05	1.188E-05	-9.287E-06	2.135E-05	1.880E-05	2.010E-05	2.180E-05	2.020E-05	7.672E-06
Cm-244[b]	1.040E-06	9.490E-06	2.823E-05	1.652E-05	1.068E-05	1.755E-05	1.245E-05	1.590E-05	1.420E-05	1.675E-05	5.042E-06
Mo-95	-3.422E-04	-4.938E-04	-5.810E-04	-5.218E-04	-4.906E-04	-5.900E-04	-5.425E-04	-5.788E-04	-5.550E-04	-5.790E-04	-5.015E-04
Tc-99	-4.170E-04	-6.068E-04	-7.175E-04	-6.436E-04	-6.043E-04	-6.784E-04	-6.305E-04	-6.643E-04	-6.488E-04	-6.663E-04	-5.791E-04
Ru-101	-3.985E-04	-5.979E-04	-7.215E-04	-6.399E-04	-5.969E-04	-6.752E-04	-6.224E-04	-6.596E-04	-6.423E-04	-6.618E-04	-5.612E-04
Rh-103	-2.207E-04	-3.221E-04	-3.809E-04	-3.440E-04	-3.233E-04	-3.635E-04	-3.370E-04	-3.564E-04	-3.442E-04	-3.566E-04	-3.099E-04
Ag-109	-1.657E-05	-3.123E-05	-4.193E-05	-3.533E-05	-3.183E-05	-3.629E-05	-3.207E-05	-3.501E-05	-3.359E-05	-3.518E-05	-2.453E-05
Cs-133	-6.245E-04	-9.023E-04	-1.062E-03	-9.552E-04	-8.982E-04	-1.009E-03	-9.388E-04	-9.881E-04	-9.651E-04	-9.910E-04	-8.625E-04
Nd-143	-4.869E-04	-6.485E-04	-7.299E-04	-6.822E-04	-6.523E-04	-7.102E-04	-6.755E-04	-7.004E-04	-6.877E-04	-7.015E-04	7.149E-04
Nd-145	-3.841E-04	-5.450E-04	-6.350E-04	-5.745E-04	-5.420E-04	-6.074E-04	-5.678E-04	-5.959E-04	-5.830E-04	-5.975E-04	5.384E-04
Pm-147[b]	-1.524E-04	-1.961E-04	-2.146E-04	-2.016E-04	-1.942E-04	-1.822E-04	-1.780E-04	-1.796E-04	-1.776E-04	-1.797E-04	-1.937E-04
Sm-147	-4.281E-05	-5.405E-05	-5.789E-05	-5.485E-05	-5.315E-05	-8.641E-05	-7.990E-05	-8.582E-05	-8.487E-05	-8.636E-05	-5.667E-05
Sm-149	-2.586E-06	-3.194E-06	-3.675E-06	-3.483E-06	-3.346E-06	-2.931E-06	-2.915E-06	-2.884E-06	-2.980E-06	-2.907E-06	-3.863E-06
Sm-150	-1.342E-04	-2.127E-04	-2.648E-04	-2.313E-04	-2.136E-04	-2.395E-04	-2.187E-04	-2.332E-04	-2.248E-04	-2.336E-04	-1.969E-04
Sm-151	-8.274E-06	-9.466E-06	-1.063E-05	-1.049E-05	-1.023E-05	-9.853E-06	-9.614E-06	-9.765E-06	-9.670E-06	-9.771E-06	-1.361E-05
Sm-152	-6.463E-05	-8.995E-05	-1.022E-04	-9.290E-05	-8.819E-05	-9.930E-05	-9.342E-05	-9.762E-05	-9.555E-05	-9.785E-05	-8.020E-05
Eu-151	-1.918E-08	-1.448E-08	-1.374E-08	-1.550E-08	-1.619E-08	-1.724E-08	-1.742E-08	-1.774E-08	-1.634E-08	-1.740E-08	-3.832E-08
Eu-153	-4.812E-05	-8.514E-05	-1.095E-04	-9.429E-05	-8.603E-05	-9.929E-05	-8.906E-05	-9.624E-05	-9.277E-05	-9.668E-05	-7.489E-05
Eu-155[b]	-4.051E-06	-7.821E-06	-1.062E-05	-8.820E-06	-7.885E-06	-9.173E-06	-8.041E-06	-8.819E-06	-8.469E-06	-8.876E-06	-6.331E-06
Gd-155	-4.219E-08	-6.291E-08	-7.931E-08	-7.239E-08	-6.750E-08	-8.308E-08	-7.353E-08	-8.142E-08	-7.517E-08	-8.115E-08	-9.205E-08

[a]Time after discharge.
[b]Decay precursor.

Table C.1 Reference nuclide concentrations (g/gU initial) (continued)

Nuclide	Takahama NT3G23 SF95-3 (10 days)[a]	Takahama NT3G23 SF95-4 (10 days)	Takahama NT3G23 SF95-5 (10 days)	Takahama NT3G23 SF96-2 (10 days)	Takahama NT3G23 SF96-3 (10 days)	Takahama NT3G23 SF96-4 (10 days)	Takahama NT3G23 SF96-5 (10 days)	Takahama NT3G24 SF97-2 (1446 days)	Takahama NT3G24 SF97-3 (1446 days)	Takahama NT3G24 SF97-4 (1446 days)	Takahama NT3G24 SF97-5 (1446 days)
U-234	1.873E-04	1.870E-04	2.829E-04	1.522E-04	1.251E-04	1.250E-04	1.354E-04	2.386E-04	2.089E-04	1.971E-04	1.963E-04
U-235	1.326E-02	1.230E-02	1.544E-02	1.408E-02	8.638E-03	8.064E-03	9.937E-03	1.571E-02	1.030E-02	8.179E-03	7.932E-03
U-236	4.911E-03	4.999E-03	4.566E-03	2.411E-03	3.244E-03	3.302E-03	3.013E-03	4.560E-03	5.312E-03	5.528E-03	5.532E-03
U-238	9.338E-01	9.335E-01	9.388E-01	9.580E-01	9.476E-01	9.475E-01	9.522E-01	9.377E-01	9.282E-01	9.246E-01	9.247E-01
Np-237	-4.913E-04	-4.989E-04	-3.858E-04	1.323E-04	2.168E-04	2.252E-04	1.875E-04	4.037E-04	5.848E-04	6.607E-04	6.704E-04
Pu-238	1.539E-04	1.588E-04	1.020E-04	4.172E-05	1.206E-04	1.248E-04	7.978E-05	1.313E-04	2.680E-04	3.299E-04	3.275E-04
Pu-239	6.194E-03	6.005E-03	5.635E-03	5.459E-03	6.001E-03	5.819E-03	5.519E-03	5.927E-03	6.216E-03	6.036E-03	5.975E-03
Pu-240	2.186E-03	2.207E-03	1.821E-03	1.494E-03	2.303E-03	2.327E-03	1.964E-03	1.872E-03	2.478E-03	2.679E-03	2.659E-03
Pu-241	1.486E-03	1.466E-03	1.153E-03	8.684E-04	1.498E-03	1.480E-03	1.203E-03	1.019E-03	1.394E-03	1.461E-03	1.448E-03
Pu-242	4.516E-04	4.803E-04	2.976E-04	1.615E-04	5.103E-04	5.411E-04	3.551E-04	3.152E-04	6.517E-04	8.246E-04	8.341E-04
Am-241	3.310E-05	2.351E-05	2.840E-05	1.735E-05	2.845E-05	3.094E-05	2.149E-05	2.550E-04	3.429E-04	3.611E-04	3.584E-04
Am-243	8.047E-05	8.472E-05	4.400E-05	1.728E-05	8.872E-05	9.598E-05	5.078E-05	5.130E-05	1.409E-04	1.923E-04	1.934E-04
Cm-242[b]	1.964E-05	2.328E-05	1.006E-05	5.781E-06	1.628E-05	1.679E-05	1.115E-05	2.496E-08	4.260E-08	4.711E-08	4.403E-08
Cm-244[b]	2.562E-05	2.837E-05	1.064E-05	3.092E-06	2.862E-05	3.128E-05	1.280E-05	1.189E-05	4.895E-05	7.570E-05	7.582E-05
Mo-95	-6.978E-04	-7.226E-04	-6.159E-04	-3.065E-04	-5.085E-04	-5.214E-04	-4.447E-04	-7.203E-04	-9.467E-04	-1.040E-03	-1.046E-03
Tc-99	-8.081E-04	-8.356E-04	-7.105E-04	-3.930E-04	-6.511E-04	-6.664E-04	-5.679E-04	-7.067E-04	-9.319E-04	-1.023E-03	-1.028E-03
Ru-101	-8.084E-04	-8.373E-04	-6.983E-04	-3.854E-04	-6.635E-04	-6.793E-04	-5.691E-04	-6.953E-04	-9.472E-04	-1.053E-03	-1.058E-03
Rh-103	-4.289E-04	-4.402E-04	-3.753E-04	-2.363E-04	-3.831E-04	-3.890E-04	-3.337E-04	-4.046E-04	-5.286E-04	-5.731E-04	-5.731E-04
Ag-109	-4.250E-05	-4.411E-05	-3.310E-05	-2.225E-05	-4.411E-05	-4.499E-05	-3.572E-05	-3.327E-05	-5.278E-05	-6.090E-05	-6.073E-05
Cs-133	-1.193E-03	-1.233E-03	-1.054E-03	-5.911E-04	-9.716E-04	-9.942E-04	-8.501E-04	-1.051E-03	-1.373E-03	-1.501E-03	-1.510E-03
Nd-143	9.299E-04	9.373E-04	8.303E-04	4.778E-04	7.158E-04	7.184E-04	6.433E-04	8.307E-04	1.008E-03	1.048E-03	1.049E-03
Nd-145	7.392E-04	7.598E-04	6.518E-04	3.575E-04	5.766E-04	5.880E-04	5.095E-04	6.480E-04	8.387E-04	9.118E-04	9.179E-04
Pm-147[b]	-2.374E-04	-2.432E-04	-2.235E-04	-1.441E-04	-2.029E-04	-2.068E-04	-1.886E-04	-7.132E-05	-8.337E-05	-8.735E-05	-8.786E-05
Sm-147	-6.690E-05	-6.869E-05	-6.472E-05	-3.403E-05	-4.702E-05	-4.811E-05	-4.442E-05	2.050E-04	2.355E-04	2.468E-04	2.479E-04
Sm-149	-4.482E-06	-4.343E-06	-3.883E-06	-3.000E-06	-3.869E-06	-3.749E-06	-3.312E-06	3.976E-06	4.259E-06	3.943E-06	3.799E-06
Sm-150	-3.016E-04	-3.129E-04	-2.522E-04	-1.321E-04	-2.448E-04	-2.504E-04	-2.039E-04	2.499E-04	3.599E-04	4.074E-04	4.113E-04
Sm-151	-1.540E-05	-1.464E-05	-1.318E-05	-1.044E-05	-1.235E-05	-1.165E-05	-1.048E-05	1.351E-05	1.503E-05	1.491E-05	1.465E-05
Sm-152	-1.050E-04	-1.094E-04	-9.723E-05	-6.394E-05	-9.722E-05	-1.003E-04	-8.923E-05	9.546E-05	1.191E-04	1.298E-04	1.319E-04
Eu-151	-2.960E-08	-2.641E-08	-2.852E-08	-2.808E-08	-1.970E-08	-1.762E-08	-1.846E-08	-6.467E-07	-7.017E-07	-6.819E-07	-6.460E-07
Eu-153	-1.210E-04	-1.257E-04	-9.904E-05	-6.290E-05	-1.131E-04	-1.150E-04	-9.399E-05	-9.922E-05	-1.460E-04	-1.642E-04	-1.645E-04
Eu-155[b]	-1.168E-05	-1.225E-05	-8.994E-06	-5.351E-06	-1.098E-05	-1.123E-05	-8.767E-06	-4.979E-06	-8.301E-06	-9.682E-06	-9.696E-06
Gd-155	-1.293E-07	-1.246E-07	-1.003E-07	-8.541E-06	-7.718E-06	-7.085E-06	-6.989E-06	-3.528E-06	-5.830E-06	-6.771E-06	-6.771E-06

[a]Time after discharge.
[b]Decay precursor.

Table C.1 Reference nuclide concentrations (g/gU initial) (continued)

Nuclide	Takahama NT3G24 SF97-6 (1446 days)[a]	TMI-1 NJ05YU A1B (1711 days)	TMI-1 NJ05YU A2 (1103 days)	TMI-1 NJ05YU B1B (1711 days)	TMI-1 NJ05YU B2 (1103 days)	TMI-1 NJ05YU B3J (1711 days)	TMI-1 NJ05YU C1 (1103 days)	TMI-1 NJ05YU C2B (1711 days)	TMI-1 NJ05YU C3 (1103 days)	TMI-1 NJ05YU D1A2 (1711 days)	TMI-1 NJ05YU D1A4 (1711 days)
U-234	2.124E-04	2.054E-04	1.912E-04	1.877E-04	1.868E-04	1.834E-04	1.977E-04	1.808E-04	1.847E-04	1.927E-04	1.975E-04
U-235	1.016E-02	8.604E-03	6.319E-03	6.386E-03	6.205E-03	6.111E-03	6.588E-03	6.228E-03	6.251E-03	6.966E-03	7.485E-03
U-236	5.272E-03	5.111E-03	5.497E-03	5.402E-03	5.400E-03	5.456E-03	5.470E-03	5.185E-03	5.327E-03	5.452E-03	5.362E-03
U-238	9.310E-01	9.292E-01	9.239E-01	9.202E-01	9.247E-01	9.217E-01	9.240E-01	9.226E-01	9.233E-01	9.178E-01	9.229E-01
Np-237	5.573E-04	6.040E-04	6.938E-04	7.012E-04	6.917E-04	7.060E-04	7.041E-04	6.864E-04	6.823E-04	7.058E-04	6.848E-04
Pu-238	2.265E-04	4.033E-04	3.538E-04	4.316E-04	3.144E-04	3.982E-04	3.299E-04	4.585E-04	2.511E-04	3.809E-04	3.747E-04
Pu-239	5.676E-03	5.064E-03	5.340E-03	5.107E-03	5.289E-03	5.088E-03	5.405E-03	4.991E-03	5.512E-03	5.452E-03	5.399E-03
Pu-240	2.331E-03	2.342E-03	2.781E-03	2.632E-03	2.728E-03	2.654E-03	2.753E-03	2.546E-03	2.844E-03	2.708E-03	2.621E-03
Pu-241	1.233E-03	1.208E-03	1.358E-03	1.362E-03	1.387E-03	1.364E-03	1.423E-03	1.329E-03	1.403E-03	1.469E-03	1.430E-03
Pu-242	5.977E-04	6.792E-04	9.229E-04	9.570E-04	9.145E-04	1.106E-03	9.000E-04	9.318E-04	9.233E-04	9.637E-04	9.414E-04
Am-241	3.029E-04	3.466E-04	3.021E-04	2.880E-04	3.412E-04	5.060E-04	3.770E-04	5.074E-04	3.028E-04	3.350E-04	5.261E-04
Am-243	1.170E-04	1.245E-04	2.541E-04	2.043E-04	2.552E-04	2.111E-04	2.458E-04	1.956E-04	2.465E-04	2.056E-04	1.846E-04
Cm-242[b]	3.725E-08	-2.117E-08	-2.954E-07	-2.741E-08	-2.884E-07	-2.641E-08	-2.933E-07	-2.641E-08	-2.993E-07	-2.870E-08	-2.594E-08
Cm-244[b]	3.627E-05	-5.288E-05	-9.473E-05	-1.205E-04	-9.143E-05	-1.064E-04	-9.367E-05	-1.056E-04	-1.011E-04	-1.329E-04	-9.068E-05
Mo-95	-9.266E-04	1.041E-03	1.118E-03	1.150E-03	1.128E-03	1.124E-03	1.100E-03	1.098E-03	1.006E-03	1.111E-03	1.089E-03
Tc-99	-9.095E-04	1.422E-03	1.081E-03	1.316E-03	1.091E-03	1.244E-03	1.081E-03	1.356E-03	1.034E-03	1.138E-03	1.191E-03
Ru-101	-9.175E-04	1.115E-03	1.155E-03	1.187E-03	1.202E-03	1.171E-03	1.164E-03	1.172E-03	1.025E-03	1.129E-03	1.098E-03
Rh-103	-5.108E-04	5.956E-04	6.190E-04	6.267E-04	6.288E-04	6.203E-04	6.181E-04	6.145E-04	5.475E-04	6.168E-04	6.027E-04
Ag-109	-4.905E-05	5.111E-05	5.968E-05	4.399E-05	5.280E-05	7.788E-05	5.359E-05	6.532E-05	9.233E-05	4.607E-05	8.463E-05
Cs-133	-1.343E-03	-1.426E-03	-1.567E-03	-1.654E-03	-1.554E-03	-1.621E-03	-1.553E-03	-1.610E-03	-1.581E-03	-1.679E-03	-1.558E-03
Nd-143	9.736E-04	9.850E-04	9.516E-04	1.086E-03	9.987E-04	1.060E-03	9.794E-04	1.033E-03	9.510E-04	1.111E-03	1.080E-03
Nd-145	8.247E-04	8.521E-04	8.777E-04	9.847E-04	9.062E-04	9.770E-04	8.972E-04	9.411E-04	8.965E-04	1.000E-03	9.598E-04
Pm-147[b]	-8.329E-05	-6.966E-05	-1.113E-04	-7.263E-05	-1.104E-04	-7.257E-05	-1.102E-04	-7.191E-05	-1.109E-04	-7.312E-05	-7.135E-05
Sm-147	2.371E-04	2.258E-04	1.968E-04	2.549E-04	1.859E-04	2.479E-04	1.866E-04	2.288E-04	1.819E-04	2.515E-04	2.353E-04
Sm-149	3.843E-06	3.113E-06	3.816E-06	3.423E-06	3.264E-06	3.189E-06	3.188E-06	3.358E-06	2.899E-06	3.855E-06	3.599E-06
Sm-150	3.409E-04	3.577E-04	3.742E-04	4.675E-04	3.754E-04	4.525E-04	3.835E-04	4.189E-04	3.619E-04	4.525E-04	4.125E-04
Sm-151	1.294E-05	1.292E-05	1.256E-05	1.500E-05	1.341E-05	1.475E-05	1.247E-05	1.329E-05	1.256E-05	1.551E-05	1.412E-05
Sm-152	1.207E-04	1.217E-04	1.321E-04	1.436E-04	1.295E-04	1.419E-04	1.266E-04	1.301E-04	1.256E-04	1.423E-04	1.338E-04
Eu-151	-6.130E-07	-7.296E-07	-5.071E-07	-8.054E-07	-5.119E-07	-7.798E-07	-5.285E-07	-8.042E-07	-5.208E-07	-8.334E-07	-8.116E-07
Eu-153	-1.392E-04	1.468E-04	1.709E-04	1.859E-04	1.674E-04	1.834E-04	1.672E-04	1.725E-04	1.606E-04	1.891E-04	1.744E-04
Eu-155[b]	-7.776E-06	1.004E-05	1.284E-05	1.546E-05	1.313E-05	1.032E-05	1.432E-05	9.964E-06	1.274E-05	9.821E-06	1.264E-05
Gd-155	-5.444E-06	8.223E-06	6.060E-06	1.003E-05	6.547E-06	1.041E-05	6.357E-06	9.411E-06	6.666E-06	1.019E-05	1.394E-05

[a]Time after discharge.
[b]Decay precursor.

Table C.1 Reference nuclide concentrations (g/gU initial) (continued)

Nuclide	TMI-1 NJ05YU D2 (1103 days)[a]	TMI-1 NJ070G O12S4 (1298 days)	TMI-1 NJ070G O12S5 (1529 days)	TMI-1 NJ070G O12S6 (1298 days)	TMI-1 NJ070G O13S7 (1529 days)	TMI-1 NJ070G O13S8 (1529 days)	TMI-1 NJ070G O1S1 (1298 days)	TMI-1 NJ070G O1S2 (1529 days)	TMI-1 NJ070G O1S3 (1298 days)	Trino I 509-032 E11P1 (10 days)	Trino I 509-032 E11P4 (10 days)
U-234	1.923E-04	3.332E-04	3.126E-04	3.260E-04	3.427E-04	3.184E-04	3.263E-04	3.037E-04	3.134E-04	2.110E-04	2.312E-04
U-235	7.378E-03	2.356E-02	2.181E-02	2.388E-02	2.376E-02	2.191E-02	2.203E-02	1.916E-02	2.170E-02	2.329E-02	1.728E-02
U-236	5.334E-03	4.299E-03	4.615E-03	4.384E-03	4.216E-03	4.579E-03	4.529E-03	4.990E-03	4.668E-03	-1.554E-03	-2.676E-03
U-238	9.292E-01	9.386E-01	9.361E-01	9.367E-01	9.389E-01	9.363E-01	9.376E-01	9.345E-01	9.354E-01	9.624E-01	9.558E-01
Np-237	6.755E-04	3.032E-04	3.482E-04	3.278E-04	2.826E-04	3.474E-04	3.038E-04	3.953E-04	3.639E-04	-6.298E-05	-1.757E-04
Pu-238	3.252E-04	6.270E-05	8.799E-05	7.765E-05	6.019E-05	8.699E-05	7.192E-05	1.084E-04	9.354E-05	-5.814E-06	-3.304E-05
Pu-239	5.427E-03	5.435E-03	6.000E-03	6.182E-03	5.418E-03	5.880E-03	5.448E-03	5.588E-03	6.024E-03	3.483E-03	5.266E-03
Pu-240	2.667E-03	1.389E-03	1.647E-03	1.508E-03	1.371E-03	1.620E-03	1.519E-03	1.850E-03	1.712E-03	4.420E-04	1.118E-03
Pu-241	1.366E-03	6.890E-04	8.397E-04	7.999E-04	6.610E-04	8.230E-04	7.539E-04	9.149E-04	8.942E-04	1.710E-04	6.140E-04
Pu-242	7.945E-04	1.483E-04	2.059E-04	1.649E-04	1.446E-04	2.022E-04	1.800E-04	2.841E-04	2.208E-04	1.170E-05	8.425E-05
Am-241	3.457E-04	1.521E-04	2.078E-04	1.377E-04	1.624E-04	2.022E-04	1.144E-04	1.981E-04	1.712E-04	-3.545E-06	-1.446E-05
Am-243	1.923E-04	1.690E-05	2.771E-05	1.649E-05	1.606E-05	2.669E-05	1.500E-05	3.504E-05	2.563E-05	-3.999E-07	-8.362E-06
Cm-242[b]	-2.557E-07	1.849E-08	1.123E-08	1.873E-08	6.995E-09	1.170E-08	1.772E-08	1.635E-08	2.713E-08	-3.050E-07	-2.830E-06
Cm-244[b]	-6.015E-05	2.713E-06	5.158E-06	3.016E-06	2.460E-06	4.897E-06	2.494E-06	7.177E-06	4.976E-06	-2.337E-08	-1.141E-06
Mo-95	9.199E-04	-5.840E-04	-6.423E-04	-5.936E-04	-5.766E-04	-6.386E-04	-6.288E-04	-7.211E-04	-6.538E-04	-1.506E-04	-3.051E-04
Tc-99	9.757E-04	-5.642E-04	-6.219E-04	-5.746E-04	-5.571E-04	-6.184E-04	-6.075E-04	-6.986E-04	-6.332E-04	-1.815E-04	-3.722E-04
Ru-101	9.478E-04	-5.388E-04	-5.994E-04	-5.510E-04	-5.317E-04	-5.959E-04	-5.828E-04	-6.793E-04	-6.112E-04	-1.688E-04	-3.576E-04
Rh-103	5.157E-04	-3.211E-04	-3.569E-04	-3.296E-04	-3.171E-04	-3.551E-04	-3.466E-04	-4.024E-04	-3.647E-04	-9.609E-05	-2.032E-04
Ag-109	4.655E-05	-2.012E-05	-2.430E-05	-2.144E-05	-1.974E-05	-2.412E-05	-2.265E-05	-2.943E-05	-2.514E-05	-4.739E-06	-1.519E-05
Cs-133	-1.421E-03	-8.441E-04	-9.286E-04	-8.590E-04	-8.337E-04	-9.234E-04	-9.080E-04	-1.041E-03	-9.449E-04	-2.743E-04	-5.597E-04
Nd-143	9.134E-04	7.049E-04	7.638E-04	7.175E-04	6.958E-04	7.594E-04	7.454E-04	8.336E-04	7.745E-04	-2.353E-04	-4.516E-04
Nd-145	8.288E-04	5.247E-04	5.719E-04	5.283E-04	5.174E-04	5.693E-04	5.626E-04	6.420E-04	5.809E-04	-1.725E-04	-3.442E-04
Pm-147[b]	-1.071E-04	-8.540E-05	-7.556E-05	-8.473E-05	-7.164E-05	-7.528E-05	-9.014E-05	-8.168E-05	-9.072E-05	-7.746E-05	-1.399E-04
Sm-147	1.821E-04	1.699E-04	1.881E-04	1.677E-04	1.746E-04	1.863E-04	1.791E-04	2.056E-04	1.815E-04	-1.987E-05	-3.536E-05
Sm-149	3.094E-06	4.055E-06	4.156E-06	4.430E-06	3.972E-06	4.139E-06	4.051E-06	4.074E-06	4.415E-06	-2.248E-06	-2.907E-06
Sm-150	3.485E-04	1.981E-04	2.256E-04	2.033E-04	1.934E-04	2.228E-04	2.157E-04	2.598E-04	2.310E-04	-5.279E-05	-1.215E-04
Sm-151	1.264E-05	1.295E-05	1.413E-05	1.480E-05	1.268E-05	1.414E-05	1.275E-05	1.374E-05	1.431E-05	-7.796E-06	-1.016E-05
Sm-152	1.208E-04	8.091E-05	8.677E-05	7.877E-05	7.953E-05	8.605E-05	8.654E-05	9.999E-05	8.924E-05	-2.671E-05	-5.593E-05
Eu-151	-5.209E-07	4.027E-07	4.699E-07	4.580E-07	4.206E-07	4.672E-07	3.891E-07	4.430E-07	4.312E-07	-4.310E-08	-2.966E-08
Eu-153	1.561E-04	6.918E-05	8.097E-05	7.203E-05	6.695E-05	8.062E-05	7.548E-05	9.438E-05	8.231E-05	-1.478E-05	-4.351E-05
Eu-155[b]	1.227E-05	-3.267E-06	-3.590E-06	-3.440E-06	-2.915E-06	-3.555E-06	-3.721E-06	-4.443E-06	-4.100E-06	-1.425E-06	-3.597E-06
Gd-155	5.594E-06	1.905E-06	2.509E-06	2.182E-06	1.972E-06	2.528E-06	2.307E-06	2.888E-06	2.638E-06	-3.476E-08	-5.043E-08

[a]Time after discharge.
[b]Decay precursor.

Table C.1 Reference nuclide concentrations (g/gU initial) (continued)

Nuclide	Trino I 509-032 E11P7 (10 days)[a]	Trino I 509-032 E11P9 (10 days)	Trino I 509-032 H9P4 (10 days)	Trino I 509-032 H9P7 (10 days)	Trino I 509-032 H9P9 (10 days)	Trino I 509-049 J8P1 (10 days)	Trino I 509-049 J8P4 (10 days)	Trino I 509-049 J8P7 (10 days)	Trino I 509-049 J8P9 (10 days)	Trino I 509-049 L5P1 (10 days)	Trino I 509-049 L5P4 (10 days)
U-234	1.410E-04	-2.121E-04	-1.955E-04	1.502E-04	1.676E-04	1.367E-04	1.312E-04	-1.685E-04	-1.812E-04	1.291E-04	1.435E-04
U-235	1.661E-02	2.017E-02	1.672E-02	1.631E-02	1.889E-02	1.854E-02	1.390E-02	1.386E-02	1.663E-02	1.972E-02	1.503E-02
U-236	-2.734E-03	-2.190E-03	-2.807E-03	-2.904E-03	-2.298E-03	-1.680E-03	-2.416E-03	-2.461E-03	-1.999E-03	-1.555E-03	-2.366E-03
U-238	9.558E-01	9.595E-01	9.551E-01	9.548E-01	9.471E-01	9.654E-01	9.603E-01	9.595E-01	9.635E-01	9.658E-01	9.601E-01
Np-237	-1.802E-04	-1.153E-04	-1.845E-04	-1.961E-04	-1.198E-04	-7.793E-05	-1.583E-04	-1.615E-04	-1.048E-04	-7.101E-05	-1.592E-04
Pu-238	-3.455E-05	-1.611E-05	-3.601E-05	-3.982E-05	-1.727E-05	-8.971E-06	-2.989E-05	-3.088E-05	-1.478E-05	-7.622E-06	-3.005E-05
Pu-239	5.234E-03	4.418E-03	5.172E-03	5.234E-03	4.446E-03	3.606E-03	4.769E-03	4.926E-03	4.134E-03	3.608E-03	5.016E-03
Pu-240	1.137E-03	7.750E-04	1.211E-03	1.247E-03	8.340E-04	5.600E-04	1.160E-03	1.196E-03	8.020E-04	5.150E-04	1.121E-03
Pu-241	6.180E-04	3.690E-04	6.760E-04	6.940E-04	4.090E-04	2.280E-04	6.150E-04	6.370E-04	3.710E-04	2.040E-04	6.025E-04
Pu-242	9.252E-05	3.709E-05	1.047E-04	1.080E-04	-4.313E-05	1.887E-05	9.938E-05	1.036E-04	4.205E-05	1.532E-05	8.493E-05
Am-241	-1.486E-05	-8.487E-06	-1.545E-05	-1.632E-05	-9.102E-06	-5.749E-06	-1.430E-05	-1.449E-05	-8.535E-06	-4.868E-06	-1.418E-05
Am-243	-9.124E-06	-2.521E-06	-1.033E-05	-1.214E-05	-3.049E-06	-1.118E-06	-8.889E-06	-9.454E-06	-2.726E-06	-7.782E-07	-8.375E-06
Cm-242[b]	-3.009E-06	-1.187E-06	-3.296E-06	-3.674E-06	-1.369E-06	-6.598E-07	-2.952E-06	-3.073E-06	-1.261E-06	-5.015E-07	-2.816E-06
Cm-244[b]	-1.270E-06	-2.387E-07	-1.451E-06	-1.790E-06	-2.945E-07	-8.143E-08	-1.175E-06	-1.264E-06	-2.508E-07	-5.307E-08	-1.125E-06
Mo-95	-3.153E-04	-2.345E-04	-3.282E-04	-3.449E-04	-2.516E-04	-1.784E-04	-2.916E-04	-3.000E-04	-2.253E-04	-1.605E-04	-2.816E-04
Tc-99	-3.844E-04	-2.841E-04	-3.997E-04	-4.201E-04	-3.044E-04	-2.165E-04	-3.573E-04	-3.673E-04	-2.741E-04	-1.948E-04	-3.458E-04
Ru-101	-3.697E-04	-2.686E-04	-3.850E-04	-4.056E-04	-2.880E-04	-2.034E-04	-3.444E-04	-3.542E-04	-2.597E-04	-1.826E-04	-3.334E-04
Rh-103	-2.094E-04	-1.526E-04	-2.174E-04	-2.280E-04	-1.628E-04	-1.173E-04	-1.982E-04	-2.031E-04	-1.492E-04	-1.056E-04	-1.927E-04
Ag-109	-1.581E-05	-9.540E-06	-1.669E-05	-1.787E-05	-1.038E-05	-6.975E-06	-1.565E-05	-1.612E-05	-9.904E-06	-6.022E-06	-1.515E-05
Cs-133	-5.779E-04	-4.284E-04	-6.008E-04	-6.310E-04	-4.589E-04	-3.270E-04	-5.378E-04	-5.528E-04	-4.135E-04	-2.944E-04	-5.206E-04
Nd-143	-4.640E-04	-3.551E-04	-4.794E-04	-4.999E-04	-3.774E-04	-2.730E-04	-4.254E-04	-4.351E-04	-3.373E-04	-2.478E-04	-4.145E-04
Nd-145	-3.553E-04	-2.663E-04	-3.691E-04	-3.873E-04	-2.851E-04	-2.035E-04	-3.286E-04	-3.377E-04	-2.556E-04	-1.835E-04	-3.181E-04
Pm-147[b]	-1.438E-04	-1.137E-04	-1.484E-04	-1.542E-04	-1.208E-04	-8.941E-05	-1.338E-04	-1.370E-04	-1.092E-04	-8.146E-05	-1.300E-04
Sm-147	-3.633E-05	-2.900E-05	-3.756E-05	-3.898E-05	-3.086E-05	-2.294E-05	-3.399E-05	-3.482E-05	-2.797E-05	-2.089E-05	-3.286E-05
Sm-149	-2.876E-06	-2.502E-06	-2.850E-06	-2.877E-06	-2.440E-06	-2.056E-06	-2.514E-06	-2.488E-06	-2.153E-06	-2.073E-06	-2.603E-06
Sm-150	-1.260E-04	-8.787E-05	-1.317E-04	-1.396E-04	-9.471E-05	-6.517E-05	-1.171E-04	-1.207E-04	-8.515E-05	-5.803E-05	-1.133E-04
Sm-151	-9.959E-06	-8.767E-06	-9.869E-06	-9.813E-06	-8.522E-06	-7.362E-06	-8.788E-06	-8.601E-06	-7.581E-06	-7.377E-06	-9.156E-06
Sm-152	-5.799E-05	-4.336E-05	-6.053E-05	-6.351E-05	-4.693E-05	-3.369E-05	-5.573E-05	-5.748E-05	-4.334E-05	-2.987E-05	-5.343E-05
Eu-151	-2.799E-08	-3.299E-08	-2.638E-08	-2.479E-08	-2.967E-08	-3.211E-08	-2.381E-08	-2.248E-08	-2.637E-08	-3.538E-08	-2.603E-08
Eu-153	-4.535E-05	-2.845E-05	-4.760E-05	-5.108E-05	-3.091E-05	-1.983E-05	-4.236E-05	-4.380E-05	-2.783E-05	-1.726E-05	-4.105E-05
Eu-155[b]	-3.761E-06	-2.387E-06	-3.972E-06	-4.290E-06	-2.589E-06	-1.790E-06	-3.579E-06	-3.712E-06	-2.388E-06	-1.600E-06	-3.449E-06
Gd-155	-4.998E-08	-3.898E-08	-5.028E-08	-5.128E-08	-3.823E-08	-3.250E-08	-4.474E-08	-4.425E-08	-3.450E-08	-3.283E-08	-4.624E-08

[a]**Time after discharge.**
[b]**Decay precursor.**

Table C.1 Reference nuclide concentrations (g/gU initial) (continued)

Nuclide	Trino I 509-049 L5P9 (10 days)[a]	Trino I 509-104 M11P7 (10 days)	Trino II 509-069 E11P1 (10 days)	Trino II 509-069 E11P2 (10 days)	Trino II 509-069 E11P4 (10 days)	Trino II 509-069 E11P5 (10 days)	Trino II 509-069 E11P7 (10 days)	Trino II 509-069 E11P8 (10 days)	Trino II 509-069 E11P9 (10 days)	Trino II 509-069 E5P4 (10 days)	Trino II 509-069 E5P7 (10 days)
U-234	1.545E-04	-2.687E-04	-2.064E-04	-1.811E-04	-1.720E-04	-1.699E-04	-1.709E-04	-1.737E-04	-1.864E-04	-1.717E-04	-1.703E-04
U-235	1.745E-02	2.663E-02	1.946E-02	1.436E-02	1.248E-02	1.227E-02	1.235E-02	1.262E-02	1.497E-02	1.291E-02	1.221E-02
U-236	-1.879E-03	-2.503E-03	2.450E-03	3.315E-03	3.615E-03	3.620E-03	3.640E-03	3.590E-03	3.240E-03	3.530E-03	3.545E-03
U-238	9.639E-01	9.513E-01	9.591E-01	9.522E-01	9.498E-01	9.491E-01	9.496E-01	9.502E-01	9.542E-01	9.496E-01	9.487E-01
Np-237	-9.819E-05	-1.234E-04	-1.408E-04	-2.657E-04	-3.159E-04	-3.276E-04	-3.208E-04	-3.047E-04	-2.352E-04	-3.181E-04	-3.245E-04
Pu-238	-1.314E-05	-1.600E-05	2.500E-05	8.050E-05	1.090E-04	1.170E-04	1.170E-04	1.190E-04	6.800E-05	1.170E-04	1.155E-04
Pu-239	4.116E-03	4.586E-03	4.580E-03	5.755E-03	5.895E-03	6.010E-03	6.070E-03	5.910E-03	5.630E-03	5.950E-03	5.980E-03
Pu-240	7.325E-04	7.165E-04	8.400E-04	1.520E-03	1.755E-03	1.790E-03	1.825E-03	1.720E-03	1.410E-03	1.760E-03	1.785E-03
Pu-241	3.375E-04	3.475E-04	4.000E-04	8.850E-04	1.030E-03	1.040E-03	1.060E-03	1.030E-03	7.800E-04	1.050E-03	1.055E-03
Pu-242	3.373E-05	3.057E-05	4.600E-05	1.720E-04	2.435E-04	2.400E-04	2.575E-04	2.320E-04	1.470E-04	2.400E-04	2.540E-04
Am-241	-7.653E-06	-7.615E-06	3.053E-05	5.569E-05	7.018E-05	1.693E-04	1.588E-04	-7.372E-05	-5.837E-05	8.093E-05	1.025E-04
Am-243	-2.077E-06	-1.832E-06	-4.327E-06	2.395E-05	4.535E-05	5.495E-05	4.586E-05	4.372E-05	3.013E-05	-4.012E-05	4.617E-05
Cm-242[b]	-1.032E-06	-9.494E-07	5.188E-06	1.770E-05	2.436E-05	2.574E-05	2.665E-05	2.452E-05	1.739E-05	2.319E-05	2.513E-05
Cm-244[b]	-1.834E-07	-1.631E-07	-4.852E-07	4.677E-06	9.021E-06	9.918E-06	9.908E-06	7.590E-06	3.641E-06	8.964E-06	9.426E-06
Mo-95	-2.066E-04	-2.479E-04	-2.859E-04	-4.386E-04	-4.974E-04	-5.126E-04	-5.096E-04	-4.933E-04	-4.149E-04	-5.002E-04	-5.141E-04
Tc-99	-2.515E-04	-2.944E-04	-3.136E-04	-4.856E-04	-5.520E-04	-5.690E-04	-5.651E-04	-5.465E-04	-4.577E-04	-5.552E-04	-5.703E-04
Ru-101	-2.378E-04	-2.801E-04	-2.993E-04	-4.774E-04	-5.483E-04	-5.665E-04	-5.619E-04	-5.415E-04	-4.467E-04	-5.517E-04	-5.674E-04
Rh-103	-1.373E-04	-1.565E-04	-1.767E-04	-2.771E-04	-3.147E-04	-3.240E-04	-3.211E-04	-3.103E-04	-2.591E-04	-3.165E-04	-3.240E-04
Ag-109	-8.831E-06	-8.596E-06	-1.151E-05	-2.339E-05	-2.859E-05	-2.990E-05	-2.935E-05	-2.773E-05	-2.072E-05	-2.884E-05	-2.977E-05
Cs-133	-3.795E-04	-4.494E-04	-4.742E-04	-7.303E-04	-8.280E-04	-8.530E-04	-8.475E-04	-8.203E-04	-6.893E-04	-8.328E-04	-8.551E-04
Nd-143	-3.125E-04	-3.806E-04	-3.924E-04	-5.739E-04	-6.372E-04	-6.524E-04	-6.476E-04	-6.300E-04	-5.441E-04	-6.401E-04	-6.522E-04
Nd-145	-2.349E-04	-2.821E-04	-2.931E-04	-4.441E-04	-5.012E-04	-5.158E-04	-5.128E-04	-4.971E-04	-4.208E-04	-5.039E-04	-5.172E-04
Pm-147[b]	-1.013E-04	-1.211E-04	-7.947E-05	-1.134E-04	-1.251E-04	-1.280E-04	-1.276E-04	-1.245E-04	-1.087E-04	-1.257E-04	-1.285E-04
Sm-147	-2.590E-05	-3.084E-05	-7.251E-05	-9.869E-05	-1.068E-04	-1.089E-04	-1.089E-04	-1.070E-04	-9.602E-05	-1.072E-04	-1.095E-04
Sm-149	-2.180E-06	-3.019E-06	-2.352E-06	-2.719E-06	-2.821E-06	-2.826E-06	-2.762E-06	-2.704E-06	-2.511E-06	-2.822E-06	-2.766E-06
Sm-150	-7.712E-05	-9.085E-05	-9.584E-05	-1.605E-04	-1.874E-04	-1.944E-04	-1.923E-04	-1.843E-04	-1.485E-04	-1.887E-04	-1.944E-04
Sm-151	-7.750E-06	-1.044E-05	-9.552E-06	-1.148E-05	-1.198E-05	-1.199E-05	-1.167E-05	-1.139E-05	-1.047E-05	-1.199E-05	-1.170E-05
Sm-152	-4.015E-05	-4.372E-05	-4.705E-05	-6.994E-05	-7.799E-05	-8.012E-05	-8.007E-05	-7.806E-05	-6.734E-05	-7.843E-05	-8.072E-05
Eu-151	-2.969E-08	-4.447E-08	-8.589E-08	-5.323E-08	-4.530E-08	-4.308E-08	-4.189E-08	-4.283E-08	-5.178E-08	-4.493E-08	-4.141E-08
Eu-153	-2.453E-05	-2.826E-05	-3.396E-05	-6.597E-05	-7.941E-05	-8.279E-05	-8.164E-05	-7.762E-05	-5.950E-05	-8.004E-05	-8.269E-05
Eu-155[b]	-2.139E-06	-2.343E-06	-2.585E-06	-5.379E-06	-6.770E-06	-7.140E-06	-7.017E-06	-6.585E-06	-4.763E-06	-6.836E-06	-7.130E-06
Gd-155	-3.432E-08	-4.490E-08	-7.138E-08	-1.093E-07	-1.243E-07	-1.268E-07	-1.219E-07	-1.158E-07	-9.345E-08	-1.248E-07	-1.229E-07

[a]**Time after discharge.**
[b]**Decay precursor.**

Table C.1 Reference nuclide concentrations (g/gU initial) (continued)

Nuclide	Trino II 509-069 E5P9 (10 days)[a]	Trino II 509-069 J9P4 (10 days)	Trino II 509-069 J9P7 (10 days)	Trino II 509-069 L11P4 (10 days)	Trino II 509-069 L11P7 (10 days)	Trino II 509-069 L5P4 (10 days)	Trino II 509-069 L5P7 (10 days)	Turkey Point D01 G10 (927 days)	Turkey Point D01 G9 (927 days)	Turkey Point D01 H9 (927 days)
U-234	-1.866E-04	-1.694E-04	-1.689E-04	-1.715E-04	-1.708E-04	-1.703E-04	-1.710E-04	1.299E-04	1.299E-04	1.205E-04
U-235	1.514E-02	1.201E-02	1.175E-02	1.282E-02	1.225E-02	1.297E-02	1.231E-02	5.607E-03	5.793E-03	5.515E-03
U-236	3.270E-03	3.640E-03	3.690E-03	3.760E-03	3.465E-03	3.480E-03	3.570E-03	3.229E-03	3.228E-03	3.149E-03
U-238	9.536E-01	9.483E-01	9.489E-01	9.489E-01	9.486E-01	9.491E-01	9.476E-01	9.510E-01	9.506E-01	9.499E-01
Np-237	-2.344E-04	-3.266E-04	-3.281E-04	-3.191E-04	-3.214E-04	-3.256E-04	-3.203E-04	-3.557E-04	-3.574E-04	-3.665E-04
Pu-238	6.300E-05	1.200E-04	1.340E-04	1.060E-04	1.160E-04	1.100E-04	1.140E-04	1.370E-04	1.365E-04	1.436E-04
Pu-239	5.270E-03	5.820E-03	5.830E-03	6.060E-03	5.995E-03	6.060E-03	5.970E-03	4.875E-03	4.860E-03	4.966E-03
Pu-240	1.330E-03	1.810E-03	1.840E-03	1.790E-03	1.810E-03	1.770E-03	1.790E-03	2.311E-03	2.286E-03	2.312E-03
Pu-241	7.300E-04	1.070E-03	1.080E-03	1.050E-03	1.055E-03	1.060E-03	1.060E-03	1.076E-03	1.075E-03	1.113E-03
Pu-242	1.350E-04	2.700E-04	2.820E-04	2.470E-04	2.590E-04	2.440E-04	2.500E-04	5.286E-04	5.107E-04	5.517E-04
Am-241	5.431E-05	6.787E-05	-7.725E-05	-7.769E-05	6.116E-05	1.006E-04	1.565E-04	-1.643E-04	-1.658E-04	-1.688E-04
Am-243	-1.800E-05	-4.494E-05	5.015E-05	4.454E-05	4.249E-05	-4.271E-05	-4.137E-05	-1.029E-04	-1.056E-04	-1.141E-04
Cm-242[b]	1.394E-05	2.553E-05	2.848E-05	2.797E-05	2.467E-05	2.523E-05	2.482E-05	-3.371E-07	-3.430E-07	-3.594E-07
Cm-244[b]	2.544E-06	1.070E-05	9.672E-06	9.159E-06	9.739E-06	9.528E-06	8.790E-06	-2.852E-05	-2.951E-05	-3.252E-05
Mo-95	-4.142E-04	-5.199E-04	-5.288E-04	-5.014E-04	-5.107E-04	-5.088E-04	-5.099E-04	-6.872E-04	-6.911E-04	-7.074E-04
Tc-99	-4.569E-04	-5.766E-04	-5.860E-04	-5.565E-04	-5.664E-04	-5.649E-04	-5.654E-04	-6.919E-04	-6.956E-04	-7.119E-04
Ru-101	-4.458E-04	-5.742E-04	-5.838E-04	-5.531E-04	-5.632E-04	-5.622E-04	-5.621E-04	-7.047E-04	-7.093E-04	-7.285E-04
Rh-103	-2.586E-04	-3.274E-04	-3.314E-04	-3.173E-04	-3.218E-04	-3.220E-04	-3.212E-04	-4.207E-04	-4.230E-04	-4.327E-04
Ag-109	-2.065E-05	-3.033E-05	-3.077E-05	-2.894E-05	-2.944E-05	-2.965E-05	-2.935E-05	-4.425E-05	-4.474E-05	-4.637E-05
Cs-133	-6.880E-04	-8.644E-04	-8.784E-04	-8.347E-04	-8.494E-04	-8.470E-04	-8.480E-04	-1.031E-03	-1.036E-03	-1.060E-03
Nd-143	-5.432E-04	-6.573E-04	-6.636E-04	-6.413E-04	-6.486E-04	-6.491E-04	-6.476E-04	-6.911E-04	-6.932E-04	-7.014E-04
Nd-145	-4.201E-04	-5.226E-04	-5.310E-04	-5.050E-04	-5.139E-04	-5.121E-04	-5.131E-04	-6.065E-04	-6.094E-04	-6.230E-04
Pm-147[b]	-1.086E-04	-1.295E-04	-1.313E-04	-1.259E-04	-1.278E-04	-1.273E-04	-1.277E-04	-1.002E-04	-1.003E-04	-1.016E-04
Sm-147	-9.595E-05	-1.103E-04	-1.120E-04	-1.074E-04	-1.091E-04	-1.083E-04	-1.090E-04	-1.464E-04	-1.465E-04	-1.483E-04
Sm-149	-2.505E-06	-2.756E-06	-2.690E-06	-2.824E-06	-2.757E-06	-2.840E-06	-2.753E-06	-2.820E-06	-2.830E-06	-2.858E-06
Sm-150	-1.481E-04	-1.970E-04	-2.003E-04	-1.893E-04	-1.928E-04	-1.928E-04	-1.923E-04	-2.568E-04	-2.587E-04	-2.662E-04
Sm-151	-1.045E-05	-1.174E-05	-1.139E-05	-1.200E-05	-1.166E-05	-1.208E-05	-1.164E-05	-9.447E-06	-9.464E-06	-9.477E-06
Sm-152	-6.728E-05	-8.156E-05	-8.324E-05	-7.858E-05	-8.029E-05	-7.955E-05	-8.020E-05	-1.012E-04	-1.017E-04	-1.043E-04
Eu-151	-5.182E-08	-4.057E-08	-3.774E-08	-4.481E-08	-4.168E-08	-4.410E-08	-4.174E-08	-2.885E-07	-2.889E-07	-2.888E-07
Eu-153	-5.930E-05	-8.392E-05	-8.535E-05	-8.030E-05	-8.186E-05	-8.205E-05	-8.164E-05	-1.105E-04	-1.115E-04	-1.151E-04
Eu-155[b]	-2.139E-06	-2.343E-06	-2.585E-06	-5.379E-06	-6.770E-06	-7.140E-06	-7.017E-06	-6.585E-06	-4.763E-06	-6.836E-06
Gd-155	-9.305E-08	-1.241E-07	-1.206E-07	-1.251E-07	-1.218E-07	-1.273E-07	-1.215E-07	-3.005E-06	-3.037E-06	-3.149E-06

[a]Time after discharge.
[b]Decay precursor.

Table C.1 Reference nuclide concentrations (g/gU initial) (continued)

Nuclide	Turkey Point D04 G10 (927 days)[a]	Turkey Point D04 G9 (927 days)
U-234	1.298E-04	1.113E-04
U-235	5.593E-03	5.442E-03
U-236	3.226E-03	3.131E-03
U-238	9.502E-01	9.503E-01
Np-237	-3.662E-04	-3.645E-04
Pu-238	1.382E-04	1.392E-04
Pu-239	4.823E-03	4.977E-03
Pu-240	2.294E-03	2.337E-03
Pu-241	1.080E-03	1.132E-03
Pu-242	5.273E-04	5.467E-04
Am-241	-1.674E-04	-1.679E-04
Am-243	-1.112E-04	-1.113E-04
Cm-242[b]	-3.528E-07	-3.536E-07
Cm-244[b]	-3.189E-05	-3.181E-05
Mo-95	-7.022E-04	-7.012E-04
Tc-99	-7.073E-04	-7.060E-04
Ru-101	-7.227E-04	-7.214E-04
Rh-103	-4.298E-04	-4.291E-04
Ag-109	-4.584E-05	-4.582E-05
Cs-133	-1.053E-03	-1.051E-03
Nd-143	-7.002E-04	-6.993E-04
Nd-145	-6.187E-04	-6.177E-04
Pm-147[b]	-1.013E-04	-1.011E-04
Sm-147	-1.478E-04	-1.474E-04
Sm-149	-2.861E-06	-2.858E-06
Sm-150	-2.643E-04	-2.637E-04
Sm-151	-9.549E-06	-9.533E-06
Sm-152	-1.030E-04	-1.029E-04
Eu-151	-2.912E-07	-2.907E-07
Eu-153	-1.140E-04	-1.138E-04
Eu-155[b]	-7.130E-06	-7.770E-06
Gd-155	-3.121E-06	-3.115E-06

[a]Time after discharge.
[b]Decay precursor.

NRC FORM 335 (12-2010) NRCMD 3.7

U.S. NUCLEAR REGULATORY COMMISSION

BIBLIOGRAPHIC DATA SHEET

(See instructions on the reverse)

1. REPORT NUMBER (Assigned by NRC, Add Vol., Supp., Rev., and Addendum Numbers, if any.)

NUREG/CR-7108

2. TITLE AND SUBTITLE

An Approach for Validating Actinide and Fission Product Burnup Credit Criticality Safety Analyses – Isotopic Composition Predictions

3. DATE REPORT PUBLISHED

MONTH	YEAR
04	2012

4. FIN OR GRANT NUMBER

JCN V6005

5. AUTHOR(S)

G. Radulescu, I. C. Gauld, G. Ilas, and J. C. Wagner

6. TYPE OF REPORT

Technical

7. PERIOD COVERED *(Inclusive Dates)*

8. PERFORMING ORGANIZATION - NAME AND ADDRESS *(If NRC, provide Division, Office or Region, U.S. Nuclear Regulatory Commission, and mailing address; if contractor, provide name and mailing address.)*

Oak Ridge National Laboratory
Managed by UT-Battelle, LLC
Oak Ridge, TN 37831-6170

9. SPONSORING ORGANIZATION - NAME AND ADDRESS *(If NRC, type "Same as above"; if contractor, provide NRC Division, Office or Region, U.S. Nuclear Regulatory Commission, and mailing address.)*

Division of Systems Analysis, Office of Nuclear Regulatory Research
U.S. Nuclear Regulatory Commission
Washington, DC 20666-0002

10. SUPPLEMENTARY NOTES

D. Algama, NRC Project Manager

11. ABSTRACT *(200 words or less)*

Taking credit for the reduced reactivity potential of spent fuel in criticality analyses is referred to as burnup credit. Criticality safety evaluations employing burnup credit require validation of the depletion and criticality calculational methods with existing measurement data. To address the issues of burnup credit criticality validation, the U.S. Nuclear Regulatory Commission initiated a project with Oak Ridge National Laboratory to (1) develop and establish a validation approach for commercial spent nuclear fuel criticality safety evaluations based on best-available data and methods and (2) apply the approach on representative spent nuclear fuel storage and transport configurations and conditions to demonstrate its usage and applicability, as well as to provide reference bias and uncertainty results. This report describes an approach for establishing depletion code bias and uncertainty in terms of a reactivity difference.

12. KEY WORDS/DESCRIPTORS *(List words or phrases that will assist researchers in locating the report.)*

Burnup credit, depletion, validation, criticality safety, spent fuel, fission products

13. AVAILABILITY STATEMENT

unlimited

14. SECURITY CLASSIFICATION

(This Page)

unclassified

(This Report)

unclassified

15. NUMBER OF PAGES

16. PRICE

Federal Recycling Program

UNITED STATES
NUCLEAR REGULATORY COMMISSION
WASHINGTON, DC 20555-0001

OFFICIAL BUSINESS

NUREG/CR-7108

An Approach for Validating Actinide and Fission Product Burnup Credit Criticality Safety Analyses—Isotopic Composition Predictions

April 2012